

HSP90 INHIBITION IN THE SPINAL CORD: NOVEL STRATEGIES AND TARGETS FOR  
IMPROVING OPIOID TREATMENT

by

Christopher Scott Campbell

---

Copyright © Christopher Scott Campbell 2022

A Dissertation Submitted to the Faculty of the

GRADUATE INTERDISCIPLINARY PROGRAM OF NEUROSCIENCE

In Partial Fulfillment of the Requirements

For the Degree of

DOCTOR OF PHILOSOPHY

In the Graduate College

THE UNIVERSITY OF ARIZONA

2022

THE UNIVERSITY OF ARIZONA  
GRADUATE COLLEGE

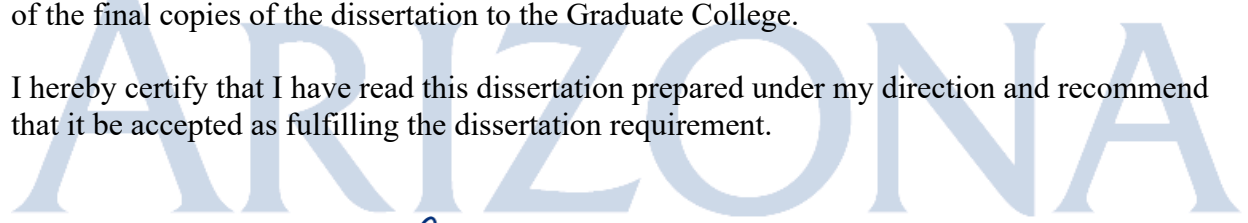
As members of the Dissertation Committee, we certify that we have read the dissertation prepared by: Christopher Campbell, titled: *Inhibition of Heat Shock Protein 90 in the Spinal Cord: Novel Strategies and Targets for Improving Opioid Treatment*

and recommend that it be accepted as fulfilling the dissertation requirement for the Degree of Doctor of Philosophy.

\_\_\_\_\_ *Ralph L. Fregosi* \_\_\_\_\_ Date: 11/21/22 \_\_\_\_\_  
 [Ralph Fregosi]  
 \_\_\_\_\_ *Konrad Zinsmaier* \_\_\_\_\_ Date: 11/21/22 \_\_\_\_\_  
 [Konrad Zinsmaier]  
 \_\_\_\_\_ *John Streicher* \_\_\_\_\_ Date: 11/21/22 \_\_\_\_\_  
 [John Streicher]  
 \_\_\_\_\_ *Andrew J. Fuglevand* \_\_\_\_\_ Date: 11/21/2022 \_\_\_\_\_  
 [Andrew J. Fuglevand]  
 \_\_\_\_\_ *Arthur C. Riegel* \_\_\_\_\_ Date: 11/21/22 \_\_\_\_\_  
 [Arthur Riegel]

Final approval and acceptance of this dissertation is contingent upon the candidate's submission of the final copies of the dissertation to the Graduate College.

I hereby certify that I have read this dissertation prepared under my direction and recommend that it be accepted as fulfilling the dissertation requirement.



\_\_\_\_\_ *Arthur C. Riegel* \_\_\_\_\_ Date: 11/21/22 \_\_\_\_\_  
 [Arthur Riegel]  
 Dissertation Committee Chair  
 [Department of Neuroscience]

## ACKNOWLEDGEMENTS

I would like to thank my PI, John Streicher, for allowing me to work in his lab, and mentoring me in the principles and details of physiology, pharmacology, neuroscience, and the philosophy and application of science. I am and will continue to be extremely grateful for the opportunity for such an education. Secondly, I would like to thank my thesis committee members for their support and evaluation of my contributions to the field of neuroscience. Specifically, I'd like to thank Dr. Zinsmaier and Fuglevand for their teaching of core systems and molecular neuroscience, Dr. Riegel for his mentorship during and after my rotation in his lab, and Dr. Fregosi for allowing me to learn electrophysiology in his laboratory. I'd also like to thank the others from my lab including Seph Palamino, Katherin Gabriel, Jesse Bowden, Jared Wahl, Partha Tanguturi, Attila Keresztes for their help, support, and friendship along this journey. I'd also like to thank David Duron and Kerry Chou for much of their work on the isoform-specific inhibitors. Lastly, I'd like to thank my family for their constant support and encouragement.

## DEDICATION

I dedicate this manuscript to Lisa, Erin, Brennan, and Bob Campbell.

## TABLE OF CONTENTS

• LIST OF FIGURES.....	7
• ABSTRACT.....	9
• CHAPTER 1: INTRODUCTION.....	11
○ THE PHYSIOLOGY AND PATHOPHYSIOLOGY OF PAIN.....	11
▪ <i>The Prevalence and Economic Burden Pain</i> .....	11
▪ <i>The Classification of Pain</i> .....	13
▪ <i>Non-Pharmacological Treatments for Pain</i> .....	15
▪ <i>The Anatomy and Physiology of Pain</i> .....	16
• <i>Dorsal Root Ganglia</i> .....	18
• <i>Spinal Cord</i> .....	19
• <i>Ascending Tracts</i> .....	20
• <i>Subcortical Regions of Pain Processing</i> .....	21
• <i>Cortical Regions of Pain Processing</i> .....	21
• <i>Descending Tracts</i> .....	22
○ THE PHARMACOLOGY OF ANALGESIA.....	25
▪ <i>The Endogenous Opioid System</i> .....	25
▪ <i>The Opioid System in Analgesia</i> .....	27
▪ <i>Supraspinal Nodes of Analgesia</i> .....	29
▪ <i>GABA Disinhibition of Opioid Analgesia</i> .....	31
▪ <i>Prescription Opioids and Their Abuses</i> .....	32
▪ <i>New Alternatives to Classical Opioids</i> .....	34
• CHAPTER 2: INHIBITING SPINAL CORD-SPECIFIC HSP90 ISOFORMS REVEALS A NOVEL STRATEGY TO IMPROVE THE THERAPEUTIC INDEX OF OPIOID TREATMENT .....	38
○ <i>Introduction</i> .....	38
○ <i>Methods and Materials</i> .....	39

○ <i>Results</i> .....	50
○ <i>Discussion</i> .....	59
● CHAPTER 3: INHIBITION OF HEAT SHOCK PROTEIN 90 IN THE SPINAL CORD AUGMENTS OPIOID ANALGESIA VIA DISABLING A GABAERGIC BRAKE....	64
○ <i>Introduction</i> .....	64
○ <i>Methods and Materials</i> .....	69
○ <i>Results</i> .....	74
○ <i>Discussion</i> .....	77
● CHAPTER 4: GENERAL DISCUSSION AND CONCLUSION.....	81
● FIGURES.....	86
● REFERENCES.....	123

## LIST OF FIGURES

1. Spinal Hsp90 Inhibition Increases Morphine Potency in Acute Heat-Induced Tail Flick.....	86
2. Spinal Hsp90 inhibition increases morphine potency in acute post-surgical paw incision pain.....	88
3. Spinal Hsp90 inhibition increases morphine potency in chronic HIV neuropathy pain...90	
4. Spinal Hsp90 inhibition reduces morphine anti-nociceptive tolerance and rescues established tolerance.....	92
5. Spinal Hsp90 inhibition does not alter morphine-induced constipation.....	94
6. Spinal Hsp90 inhibition does not alter reward learning.....	96
7. Identification of spinal-cord specific Hsp90 isoforms that regulate opioid anti-nociception.....	98
8. Systemic Grp94 inhibition enhances morphine anti-nociception.....	100
9. Systemic Grp94 inhibition enhances morphine anti-nociception in paw incision pain.....	102
10. Systemic Hsp90 $\beta$ inhibition enhances morphine anti-nociception.....	104
11. Systemic Hsp90 $\beta$ inhibition enhances morphine anti-nociception in paw incision pain.....	106
12. Systemic Grp94 and Hsp90 $\beta$ inhibition rescues established tolerance without worsening opioid-induced respiratory depression.....	108
13. Systemic Hsp90 $\alpha$ inhibition blocks opioid anti-nociception.....	110

14. Model of Hsp90 isoform inhibition in the brain vs. spinal cord.....	111
15. Enhanced morphine anti-nociception after Grp94 inhibitor treatment dissipates by 48 hours post-treatment.....	113
16. The Grp94 and Hsp90 $\beta$ inhibitors KUNG65 and KUNB106 do not bind to the opioid receptors.....	114
17. Mass spectrometry analysis of protein quantification following intrathecal 17-AAG administration.....	116
18. Intrathecal Administration of Nipecotic Acid Blocks the Effect of 17-AAG on Morphine Analgesia.....	117
19. Hsp90 inhibition mediates augmentation of opioid induced analgesia via GABAR signaling in a sex-dependent manner.....	118
20. Hsp90 inhibition mediates augmentation of opioid induced analgesia via GABA-B Receptor signaling in a sex-dependent manner.....	120
21. CRISPR/Cas9 Slc6a13 Knockout in the spinal cord mimics the effects of intrathecal 17-AAG administration.....	122

## ABSTRACT

Pain is defined as an unpleasant sensory and affective experience typically associated with tissue damage. As such, it is often prevented, avoided, or attenuated when possible. Acute pain signals organisms to avoid noxious stimuli, but chronic pain is maladaptive and may still be experienced long after the harmful stimuli are no longer present. In the treatment of both acute and chronic pain, opioids are often and widely prescribed, as they can be highly potent and efficacious. Opioids inhibit neuronal signaling that transmits nociceptive information from peripheral nerve endings to the central nervous system (CNS). Importantly, opioids also produce a wide range of side effects, including constipation, reward, tolerance, addiction, respiratory depression, and death. Considering the increase in the prevalence of opioid-related deaths and opioid use disorder diagnoses in the U.S. today, seeking safer alternatives or co-therapeutics to treat acute and chronic pain is a worthwhile venture. Recent studies from our lab and others have shown that non-selectively inhibiting heat shock protein 90 (Hsp90) in the spinal cord augments the potency of systemically administered opioids in mouse models of acute and chronic pain. Because varied isoforms of Hsp90 are expressed differentially in diverse tissues, the resultant effects of nonselective Hsp90 inhibition vary by route of administration and the compartments and cell types in which they act. Nonspecific inhibition of Hsp90 in the brain blocks opioid-induced antinociception but, when delivered intrathecally, systemic opioid potency is increased. This led our lab to believe that the actions of specific Hsp90 isoforms play different roles in modulating opioid signaling cascades in a context-specific manner. Thus, with the treatment of isoform-specific small molecule Hsp90 inhibitors, isoforms expressed specifically in the spinal cord, but

not the brain, could be targeted and subsequent enhancement of opioid antinociception occurred even when they were delivered systemically. These isoform-specific small molecule inhibitors of Hsp90 show high affinity, potency, solubility, and distribution, and when co-administered with morphine, a reduced or unchanged side-effect profile compared to morphine alone. The mechanisms by which these outcomes occur are incompletely understood. However, much light has been shed on the mechanisms involved in this phenomenon. Using a proteomic approach we found that, 24hrs after spinal administration of the nonselective Hsp90 inhibitor, sodium-and-chloride dependent GABA reuptake transporter 2 (GAT-2) expression was upregulated. Upon further analysis, the pharmacological blockade of this protein attenuated the enhancement of opioid analgesia from Hsp90 inhibition in the spinal cord. To target GAT-2 more specifically, GAT-2 was knocked out via CRISPR/Cas9 in the spinal cord. After which, again the effect of Hsp90 inhibition on morphine was absent. Further, to distinguish between GABA-A and GABA-B mediated mechanisms, GABA agonists and antagonists were administered intrathecally and showed sex-specific differences in the role of GABAergic transmission in influencing Hsp90-modulated opioid antinociception. These data suggest that, in part, that GABA signaling in the spinal cord exerts a mediating role in the enhancement of opioid analgesia resulting from Hsp90 inhibition. The details of the underlying circuitry engaged in this mechanism are explicated in further detail later in this paper. In summary, isoform-selective Hsp90 inhibitors have been revealed to be promising co-therapeutics to offset or abolish the harmful side effects of commonly prescribed opioids, and the mechanism by which they produce these effects is likely by disabling a tonically inhibitory GABAergic projection that inhibits opioidergic interneurons in the dorsal horn of the spinal cord.

## CHAPTER 1: INTRODUCTION

### THE PHYSIOLOGY AND PATHOPHYSIOLOGY OF PAIN

#### *The Prevalence and Economic Burden of Pain*

Pain is defined by the International Association for the Study of Pain (IASP) and the World Health Organization (WHO) as “an unpleasant sensory and affective experience associated with actual or potential tissue damage or described in terms of such damage” [1]. Medical conditions involving pain can negatively affect patients’ daily lives, including their relationships, daily activities, perceptions of general health, and interactions with others [2, 3]. Pain is also associated with depressive symptoms, and well-being is strongly and negatively related to the pain’s severity [2, 4]. Pain is one of the primary reasons why individuals seek medical help. Headaches, back pain, and osteoarthritis are three of the top ten reasons why patients seek care. More individuals are affected by pain than diabetes, heart disease, and cancer combined [242]. WHO’s Global Burden of Disease Study revealed that various pain conditions account for five of the top ten medical conditions that contribute to the greatest years lost to disability globally [5]. Pain permeates the globe and affects individuals psychologically, economically, and socially.

The prevalence of chronic pain conditions varies in a multitude of contingent ways, including by sex, age, socioeconomic, and individual lifestyle factors. For instance, many studies have shown that women appear to report greater and more frequent experiences of pain at higher

intensity, and for longer durations than men [6- 9]. Rates of chronic pain also increase with age. Between 83%-93% of the elderly living in residential care experience chronic pain conditions [10]. In nations with relatively large numbers of elderly citizens, the impacts of chronic pain conditions are likely to worsen with time. Regarding socioeconomic status, pain is less frequent in those with greater levels of education, higher income, and those that are employed [6]. Although various factors can predict the onset of a pain condition, like job security and satisfaction, sedentary lifestyle, social support, smoking, and obesity, the greatest single predictor is a previous episode of pain [6,11-13].

Chronic pain conditions evidently can also be devastating economically, both individually and societally. Patients with chronic pain often may be unable to perform tasks that healthy individuals can and may resort to outsourcing activities to professionals, such as housekeeping and yard work [14]. In the United Kingdom, the estimated cost per adolescent suffering from chronic pain is at about £8000 annually [15]. In another study investigating the financial and non-financial costs to adults with chronic pain in Australia, the estimates were between \$22,588-\$42,979 annually [12]. Individuals who suffer from chronic pain are estimated to lose between 8-10 workdays every six months [2]. The amalgamation of the economic burden at the individual level is strikingly evident at the macroeconomic scale. For instance, it is estimated that Australia loses approximately \$14.7 billion per year due to the number of citizens not participating in the workforce due to health issues, and nearly half of this burden is a consequence of arthritis and back pain [11]. The rates at which individuals with chronic pain visit physicians for medical care within one year are also increasing. One study reported that from 1992-2006, the rates of seeking medical attention increased from 73.1% to 84% [17]. Thus,

the impact of pain both on individuals and nations across the globe are continuing to worsen over time.

The cumulative economic burden resulting from chronic pain is greater than those of diabetes, cancer, and heart disease [20]. This includes estimated costs associated with loss of work, productivity, time family members and friends must spend caring for the suffering individuals, etc. In the United States, the total assessed costs were estimated in 2010 to be \$635 billion. In the EU the cost is estimated to be up to 3% of the total EU GDP, and in Australia, the estimate is approximately \$34.3 billion per year [18, 19]. In the US, there was an estimated 100 million adults with chronic pain, and the number is likely significantly higher today [19]. Needless to say, although pain may be an intrinsic part of the human experience, the duration and degree to which pain is experienced weighs heavily on people across the globe. Improving our ability to understand and treat acute and chronic pain conditions has the potential to drastically improve individuals' well-being and can restore their ability to participate in their society.

### *The Classification of Pain*

Acute pain is an important psychophysiological adaptation that confers a strong survival advantage to organisms that possess it. It acts both at the sensory and perceptual levels as a symbol (except in reflexes) representing to the nervous system that harmful and potentially lethal stimuli are present and should be avoided [21]. In fact, humans with pain insensitivities often experience early deaths, as many ailments that could be simply treated go on undiagnosed [22]. However, in the case of chronic pain, the sensation/perception persists beyond the point where

notifying the CNS of noxious stimuli would aid in the avoidance or alleviation of the harmful stimulus itself, and even well beyond the time expected for an injury to become healed [23].

Under the biopsychosocial model, chronic pain is conceptualized as a dynamic and multidimensional disease state which interacts with varied social, psychological, and biological factors [17]. This conceptualization highlights the fact that not only does chronic pain predispose individuals to anxiety, depression, sleep disorders, substance abuse disorders, and poor social interactions, but these factors can also predispose individuals to chronic pain [24-26].

Chronic pain is subdivided into three categories: neuropathic, nociceptive, and nociplastic [27]. Neuropathic pain accounts for between 15-25% of chronic pain and the most common manifestations are postherpetic neuralgia, diabetic neuropathy, and radiculopathy [28]. It is engendered via disease or tissue damage in the somatosensory nervous system [29]. Sensory abnormalities such as allodynia and numbness are common features of neuropathic pain. Nociceptive pain is instantiated by potentially damaging stimuli that activate nociceptive pathways in the nervous system, and most forms of spinal pain fall under this category [27]. Nociplastic pain is a result of the aberrant processing of pain signals in the CNS without any clear pathology evident in the somatosensory nervous system [30]. Commonly, alterations in the pain pathways, either by augmenting pain signaling or attenuating inhibitory projections, can elicit nociplastic pain [31]. One or more of these pain subtypes may co-occur within the same patient, and even within the same experience of pain. “Mixed” pain is becoming recognized as pain that may involve mechanisms related to more than one of the three categories of chronic pain, and it may account for nearly 50% of patients with chronic pain seeking care from primary care physicians [35,36].

### *Non-Pharmacological Treatments for Pain*

It may be the case that exercise confers the greatest pain relief out of all non-traditional treatment options. Exercise increases endorphins and improves sleep, both of which can strongly contribute to the attenuation of existing pain conditions. A study investigating the effects of exercise on pain revealed that it can contribute to improving the functionality of certain musculoskeletal movements and may decrease the experience of pain in patients with conditions across the pain spectrum [32]. However, the studies did not discriminate between different pain types or different exercise conditions. Future research may reveal specific beneficial relationships between certain forms of exercise and pain conditions. Several psychological interventions such as cognitive behavioral therapy (CBT) and mindfulness therapy have been shown to reduce pain compared to controls [33,34]. An analysis of 59 RCTs of CBT showed mild improvements in pain and disability but did not show differences at six-month follow-ups [33]. Mindfulness meditation practiced as either an adjuvant or monotherapy was reviewed in a meta-analysis of 30 randomized clinical trials and showed reductions in pain across studies, but even greater effects on anxiety and motor function than pain [34]. Other psychological interventions for pain such as Behavioral therapy, ACT, or Biofeedback showed very small effects across dozens of RCTs, most of which dissipated over time [37]. More direct, physical interventions such as massage [38], acupuncture [39], yoga [40], Tai Chi [41], or chiropractic adjustments [42, 43] show highly heterogenous effects, little or no effects, and pain subtype specificity. Many of the experiments conducted on these interventions have small sample sizes and poor controls (e.g., massage). Across many RCTs, some small effects can be determined, but generally, the evidence is mixed, and more evidence is needed to conclude that these treatment

options are efficacious compared to exercise or pharmacological alternatives [37]. Compared to classical opioid treatments, however, these alternative modes of treating pain often fall short and exhibit lower short and long-term efficacy.

### *The Anatomy and Physiology of Pain*

The anatomical and physiological substrates of pain are complex and dynamic. The sensory component of pain is termed “nociception” and begins in the free nerve endings expressed in the periphery. Nociception is the physiological activity in nociceptive pathways induced by noxious stimuli (e.g., mechanical, chemical, thermal), whereas pain refers to the phenomenological, subjective experience [44,45]. Myelinated A $\delta$  and unmyelinated C peripheral sensory afferents communicate electrochemical representations of nociceptive information about the stimuli to the CNS for further processing. The nociceptors expressed at the ends of these nerve fibers are specific for responding to putative harmful stimuli. Chemical, thermal, or mechanical stimuli are received by their respective sensory receptors, and the information is transduced into receptor potentials [46]. Chemical stimuli such as acetylcholine, serotonin (5-HT), and histamine bind to sensory receptors and alter membrane permeability or activate intracellular secondary messengers [44]. Mechanical stimuli directly produce alterations in the structure of sensory receptors, which change ionic permeability [44]. Thermal stimulation (hot or cold) induces conformational changes in TRP receptors which, in turn, produce alterations in ion permeability. If the sensory stimuli are potent enough, the electrical impulses are transmitted up the nerves to the cell bodies via saltatory (myelinated) or continuous (unmyelinated) conduction.

The pseudounipolar fibers project from cell bodies expressed in the dorsal root, trigeminal, or nodose ganglia of the brainstem and terminate in the dorsal horn (DH) where they synapse onto secondary neurons [45]. Nociceptive fibers are categorized into two types: A and C. A fibers are medium to large diameter, myelinated neurons, and C fibers are small unmyelinated neurons [46]. Consequently, pain signaling is bifurcated into fast and slow subtypes. The myelinated, large-diameter A $\delta$  fibers quickly transmit nociceptive information at rates of 6-30 m/sec [44]. Less rapidly, unmyelinated C fibers conduct pain from a range of 0.5-2 m/sec [46]. Thirdly, myelinated, large-diameter A $\beta$  fibers conduct tactile information including vibration, pressure, and touch, which are each transduced by specific sensory proteins at the nerve terminals (Meissner corpuscles, Pacinian corpuscles, Ruffini endings, etc.) [44]. Interestingly, even non-nociceptive or innocuous stimuli can activate the nociceptive fibers after repetitive injury. Enhancement of pain sensation and perception can present as hyperalgesia, allodynia, or sensitization. Hyperalgesia is the augmented experience or sensation of already noxious stimuli. Allodynia is the response to previously innocuous stimuli as though they were noxious. Sensitization in the context of pain refers to expanded receptive fields, altered excitability (e.g., lowered thresholds), or spontaneous firing of neurons that transduce/conduct nociceptive information, and express stronger responses to stimuli from alterations in synaptic strength [47]. Sensitization often occurs as a result of inflammatory signaling molecules such as serotonin (5-HT), bradykinin, prostaglandins, etc. [48]. Sensitization can affect both antinociceptive and pronociceptive circuits in the CNS, and long-term plastic changes can contribute to the chronification of pain [48]. Inflammation and nerve injury can produce alterations in GABA and opioid receptors expressed in nociceptive neurons [48]. The

upregulation of sodium channels resulting from injury may modulate the sensitivity of these receptors, changing the overall sensitivity of the neuron to both noxious and analgesic stimuli [44]. Two examples of plastic contributions to alterations in pain signaling are the upregulation of sodium channels near nerve terminals in C fibers, and the upregulation of substance P (SP) in A $\beta$  fibers resulting from inflammation [49,50]. Since sodium channel expression has been suggested to contribute to enhanced excitability, and A $\beta$  fibers synapse onto SP receptor-expressing secondary neurons in the SC, these lines of evidence suggest some means by which nociplastic sensitization may occur in the CNS.

### *Dorsal Root Ganglia*

The cell bodies of the peripheral nerves are localized in the ganglia just outside of the CNS. DRG neurons extend sensory neurites out into the periphery where they detect noxious and non-noxious stimuli and project into the spinal cord where they may synapse onto one or several neurons [51]. The DRG neurons are classified as peptidergic (CGRP, SP, and/or somatostatin-containing) and non-peptidergic neurons. Ion channels, neurotransmitters, neuropeptides, and receptors are manufactured in the cell bodies of DRG neurons and transported to terminals for appropriate neuronal signaling [51]. DRG neurons themselves do not directly communicate, but their activity can be indirectly modulated by post and preganglionic plastic changes [48,52]. For instance, after peripheral nerve injury, neurotrophin-mediated innervations from postganglionic axons can contact DRG neurons, providing signaling modulation [48]. Intracellular Ca<sup>2+</sup> and NMDAR expression can also be altered in a C-fiber input-dependent manner [49]. Both of these

sorts of alterations signaling protein expression in the DRG can produce concomitant alterations in anti- and pronociceptive signaling.

### *Spinal Cord*

From the DRG, sensory afferents project through the dorsal root entry zone (DREZ) into the dorsal horn [53-56]. Most axons synapse onto second-order neurons in the dorsal horn (DH) which then project to the opposite side of the SC and ascend through the spinal column [57]. The dorsal horn of the spinal cord is composed of six parallel layers of neurons and interneurons called Rexed laminae. Wide dynamic range (WDR) neurons and nociceptive-specific neurons are the two main types of cells comprising Rexed lamina I. The specifically tuned neurons respond to noxious stimuli and express receptors for 5-HT, enkephalin, CGRP, and SP [44]. Conversely, the WDR neurons display a large receptive field responsive to both noxious and innocuous stimuli and exhibit graded responses in proportion to input stimuli by firing at greater and greater frequencies in response [44, 58]. WDR neurons integrate a wide range of inputs and relay that information to higher-order centers for processing [45]. However, because of their integrative function, plastic changes induced by injury or inflammation may contribute to sensitization, and disproportionate excitability resulting from innocuous stimuli [48]. In lamina II, there are few projection neurons, and many sensory information-modulating neurons occurring from the high density of inhibitory GABAergic interneurons. These inhibitory interneurons (INNs) arborize to lamina I, II, III, and IV [44,59]. Lamina II primarily receives projections from A $\delta$  and C fiber projections. Loss of inhibitory tone (plastic changes in INNs) in lamina II is thought to engender disinhibition-induced chronic neuropathic pain. Laminae II and IV receive inputs from A $\beta$  and

A $\delta$  fibers, but after injury, A $\delta$  fibers may sprout into lamina I and II and produce chronic pain and allodynia [58,60]. Some preliminary information integration occurs between the early layers of the SC, wherein projections such as those from layer IV will project back to layer I, producing recursive feedback loops wherein bottom-up processing is gated by top-down recursive processes [44]. Both A $\delta$  and C fibers project to lamina V, where neurons then project rostrally up the spinothalamic tract (STT). Many WDR neurons in lamina V project to the reticular formation, medial thalamic nuclei, and periaqueductal gray (PAG) which form the mesial pathways which encode the affective components of pain [44,48]. Lamina X is a less well-characterized segment of the spinal cord, but it is thought to be involved in the central processing of visceral pain [44].

### *Ascending Tracts*

Nerves in the periphery communicate tactile and nociceptive information to the brain via the spinothalamic tract (STT). It is comprised of two sub-tracts, with ascending projections from superficial lamina (dorsolateral), and axons from deeper lamina (ventrolateral) [61]. Although there are some ipsilateral projections in the STT, most of its tracts project from the contralateral side [48]. The motivational and affective components of nociceptive traffic are relayed by the medial portion of the STT [62]. The reticular formation, thalamic nuclei, and hypothalamus receive inputs from the paleospinothalamic tract [44]. The reticular formation nuclei receive direct projections from neurons in lamina VI, VII, and VIII [63]. The reticular formation receives inputs from both A and C fibers, but the majority are A [63]. Response strength in the reticular formation is commensurate with the strength of nociceptive stimuli [63]. The pons

receives inputs from lamina I, VII, and VIII [63]. Both WDR and nociceptive-specific neurons encoding affective and motivational components of pain project from the marginal zone, lateral reticulated area, and nucleus proprius to the PAG, reticular formation, thalamus, and hypothalamus [64].

### *Subcortical Regions of Pain Processing*

The bifurcation between tactile/proprioceptive and noxious information processing in the spinal cord is largely maintained in the thalamus. The STT and trigeminal thalamic tract (TTT) project to the ventroposterior (VP) nucleus in the thalamus [64, 65]. DH and dorsal column glutamatergic projections terminate onto their targets in the VP [66]. There is somatotopic organization within the VP. Facial, limb, cutaneous extremities, and truncal somatotopic representations are present in the medial, lateral, ventral, and dorsal VP, respectively [65, 48]. Further distinctions are made within the VP between innocuous and noxious stimuli. The VP core responds to innocuous, and the posterior-inferior region responds to noxious stimuli [66]. After injury, alterations in the thalamic nuclei and their connections reveal their importance in neuropathic and other forms of chronic pain. For instance, after spinal cord injury, loss of excitatory STT, membrane hyperpolarization, and aberrant burst-firing properties are found in thalamic neurons, all of which are associated with certain forms of central neuropathic pain [61, 67, 68].

### *Cortical Regions of Pain Processing*

Nociceptive information projects widely throughout the cortex to many distinct areas, including the insula, amygdala, cingulate cortex, prefrontal cortex (PFC), orbitofrontal cortex (OFC), and SI and SII of the somatosensory cortex (SSC) [65]. Somatotopic organization of pain and anatomical representations are present in SI [69]. SI and SII receive direct and indirect synaptic input from the VPM and VPL, respectively, and exhibit graded responses commensurate with noxious stimulus intensity [65, 69]. Upon stimulation of C and A fibers, downstream SI and SII cortical areas are activated, primarily in layers III and IV of the cortices [70, 44]. SI, SII, project to the insula, which also exhibits a graded response to the strength of noxious stimuli, as well as the capacity to discriminate tactile-sensory information of pain from the nociceptive [65]. Additionally, the insula likely contributes to the encoding of affective and motivational components of pain, as lesions to the insula attenuate these responses [44]. Limbic structures, such as the perirhinal cortex and amygdala receive insular input and are associated with affective components of nociceptive processing. Similarly, the anterior cingulate cortex (ACC) is associated with affective-motivational properties of pain and is targeted by projections from the intralaminar and medial thalamic nuclei [65]. Increased ACC activity is present in patients with certain forms of chronic pain (e.g., chronic lower back pain) [69], whereas lesions to the ACC decrease affective-motivational responses to noxious stimuli [65]. The numerous cortical regions that receive projections from the insula are likely involved in meta-representational, higher-order processes that require consciousness in order to contribute to pain information processing [44].

### *Descending Tracts*

Pain processing in the CNS is complex, dynamic, and integrative. The nociceptive information arising from the periphery is heavily modulated at every higher hierarchically ordered node. Cortical processing of ascending nociceptive information can vary greatly with context, including behavioral, cognitive, cultural, and personal [71]. Descending projections from the higher nodes to lower can bidirectionally and drastically alter ascending nociceptive signaling. Pathways descending from the brain predominantly regulate pain signaling via synapses in the DH [71]. Two primary structures involved in the top-down regulation of pain processing are the rostroventral medulla (RVM) and the periaqueductal grey (PAG). These regions exert their effects at the level of the spinal cord DH by releasing monoamines such as dopamine (DA), norepinephrine (NE), and serotonin (5-HT) [72]. A set of relevant cell types have been revealed in the RVM-DH circuits that play a significant role in the central processing of pain: ON-cells and OFF-cells (citation). ON-cells express mu-opioid receptors (MOR), exhibit transient burst firing during noxious stimuli-induced pain and are inhibited by opioid administration [73]. Whereas OFF-cells express delta opioid receptors (DOR), and exhibit tonic firing but rapidly cease firing when noxious stimuli are applied [73]. These cells present in the RVM play opposing roles in the facilitation and inhibition of pain processing in the CNS. Dopaminergic projections from the hypothalamus and noradrenergic systems descending from the locus coeruleus (LC) also exhibit bidirectional modulation of nociceptive processing [74,75]. Dopamine release from these projections inhibits DH neurons in lamina I and elicit pro- or antinociceptive effects dependent on the dopamine receptor subtype enacted upon [75]. The circuitry involved in the processing of pain is complex. It involves both top-down and bottom-up pain and analgesic signaling, and the integration of both. Leveraging either system for

therapeutic purposes is the goal of many neuroscientific researchers investigating pain and analgesia, as well as industrial attempts at discovering and developing novel pharmacological therapeutics for the treatment of acute and chronic pain.

## THE PHARMACOLOGY OF ANALGESIA

### *The Endogenous Opioid System*

The endogenous opioid receptor family constitutes four unique genes (Oprm1, Oprd1, Oprk1, Oprl1) which each encode a seven-transmembrane spanning G protein-coupled receptor (GPCR) that have over 60% homology: the mu, delta, kappa, and nociceptin opioid receptors (MOR, DOR, KOR, NOR) [76-78]. The patterning of these receptors differs throughout the CNS, and their effects upon activation are diverse [79,80]. Detailed atomic-level structures of the opioid receptors in active and inactive conformations have been elucidated via X-ray crystallography. This has allowed computational pharmacologists to develop novel ligands (e.g., PZM21) that alter receptor conformations to engender different downstream signaling cascades than those of classical/endogenous opioids [81-85]. The four endogenous opioid ligand families are enkephalins, dynorphins,  $\beta$ -endorphins, and nociceptin/orphanin FQ [86]. The endogenous opioid receptor ligands are expressed widely in the CNS, particularly the nociceptive and antinociceptive pathways. Neurotransmission in the endogenous opioid system differs slightly from that of classical neurotransmitter systems. Whereas small molecule neurotransmission is tightly regulated spatially and temporally, peptidic signaling seems to depend on volumetric release and diffusion toward their cognate receptors [87,88]. Secondly, the majority of opioid receptors are localized extrasynaptically, “far” away from release sites compared to classical NT systems [89-91]. Additionally, the opioid peptides are packaged and secreted in large dense-core vesicles and require larger membrane depolarizations for release than that of monoamines packaged in smaller vesicles [86]. As the vesicles are transported down to axon terminals from

somas, the prepropeptides are enzymatically spliced to produce opioid receptor-specific ligands (e.g.,  $\beta$ -endorphin is spliced from proopiomelanocortin and preferentially binds to the MOR) [92,94]. This process of packaging larger proteins that are subsequently cleaved into smaller opioid ligands is common within this system, and allows for highly variable cellular signaling, as many of the products of cleavage have differential levels of specificity for one or more opioid receptors that they may act on. The opioid receptors are metabotropic  $G_{\alpha i}$  and  $G_{\alpha o}$  subtypes. When activated by agonist ligands, the  $\alpha$  and  $\beta\gamma$  subunits dissociate, and elicit activate different downstream second messenger cascades but are predominantly inhibitory [86]. However, it is important to note that agonist-independent opioid signaling has been revealed in chronic pain and stress conditions [94-96]. Although the mechanism is unclear, it is believed that the activation energy required for conformation changes to occur in the receptors is decreased and potentially related to alterations in receptor phosphorylation, accessory proteins, or receptor densities [85,97,98]. As with characteristic  $G_{\alpha i/o}$  signaling, adenylate cyclase is inhibited following ligand binding, which subsequently reduces cAMP production which decreases kinase activity (including PKA), putting a break on many transcriptional and translational processes. Opioid receptor signaling is predominantly inhibitory, but differences in signaling exist in receptors expressed presynaptically versus postsynaptically. Presynaptically, the  $\beta\gamma$  subunits may also interact with L-, P/Q-, and N-type voltage-gated calcium channels (VGCCs), by decreasing  $Ca^{2+}$  flux in presynaptic terminals, decreasing synaptic release at the cleft [99]. Pertinently, N-type calcium channels in the DRG may be co-internalized after long-duration exposure to opioid agonists, which attenuates NT release and nociceptive traffic from reaching higher-order nodes in the pain pathways [100]. Conversely, at postsynaptic terminals,  $\beta\gamma$  subunit signaling resulting

from opioid receptor activation can enhance G-protein gated inwardly rectifying potassium channels (GIRKs) [101]. Opening postsynaptic potassium channels allows further extrusion of the cation, hyperpolarizing the cell. Confirmatory studies have shown that genetic deletions of GIRK channels in mice attenuate opioid analgesia [102,103]. The cytoplasmic domains of opioid receptors are phosphorylated by GRKs (GPCR kinases) after ligand binding which leads to the subsequent recruitment of  $\beta$ -arrestin which initiates receptor internalization (leading to degradation or recycling), or desensitization [86]. However, even after internalization, GPCRs may still activate downstream second messenger molecules, eliciting physiological changes from within endosomal compartments [104,105]. Thus, the signaling of opioid receptors is not limited to cell surface reception of extracellular ligands.

### *The Opioid System in Analgesia*

The endogenous opioid receptors are expressed in nearly every nociception-related locus in the CNS. The somatosensory neurons in the CNS express all four opioid receptor subtypes [106-108]. Activation of opioid receptors expressed on somatosensory neurons decreases nociception when delivered intrathecally or intradermally [109-111]. Activation of endogenous opioid receptors attenuates glutamatergic and peptidergic release from somatosensory afferents in the CNS. Occasionally two or more of the receptor subtypes may be coexpressed by the same DRG neurons [86]. For instance, unmyelinated peptidergic nociceptors which express substance P and CGRP and are commonly involved in nociception, also express the MOPR and DOPR [112-114]. Recent development in single-cell RNA sequencing technology has elucidated that opioid receptor subtypes are differentially expressed across distinct classes of DRG neurons, and

differentially regulate distinct pain modalities [115-117]. For instance, Scherrer [118] et al. used transgenic lines of mice expressing fluorescently labeled DOR receptors to show that DOR and MOR are differentially expressed on distinct circuit subtypes and contribute differentially to mechanical and thermal nociception. Recent attempts to leverage our understanding of opioid circuitry have led to some advancements in developing safer alternatives to opioids. One example is the creation of peripherally restricted MOR agonists, which act on MORs expressed on the DRG, and elsewhere in the periphery, but fail to penetrate the BBB and mediate their deleterious side effects from within the CNS [119-121]. In another attempt, an opioid analgesic was created with a low acid dissociation constant, which allowed the molecule to only become active in sites with higher acidity/inflammation [122]. However, these compounds, as well as much evidence investigating the DRG contribution to pain and analgesia has revealed that the antinociceptive effects of systemic morphine are still potent in animal models with selective deletion of MOR in the DRG, indicating that MOR action within the CNS is of greater import [94, 123]. However, MOR activity in the DRG does contribute to tolerance and opioid-induced hyperalgesia, both of which are associated with chronic MOR agonist administration [94,124]. Thus, more specific targeting of compartment and circuit subtypes involved in pro- and antinociception may lead to the development of increasingly efficacious and decreasingly harmful treatments for pain. The second-order neurons in pain pathways express opioid receptors. Nociceptive dorsal horn neurons, especially excitatory projection neurons express MORs, which communicate information about painful stimuli through ascending tracts to the thalamus, PAG, and parabrachial nucleus [125,126]. There is mixed evidence as to whether DOR is restricted to primary afferent terminals or is expressed on various subtypes of spinal neurons

[127,128]. However, there is strong evidence that enkephalin and dynorphin are expressed specifically by distinct subtypes of dorsal horn interneurons and their expression is increased in order to modulate chronic pain after peripheral injury [129-131].

### *Supraspinal Nodes of Analgesia*

The descending pain modulatory system is highly involved in opioid-mediated regulation of nociception. Three of the main nodes within this system are the RVM, vlPAG, and spinal cord [132]. Administration of mu opioids into the RVM or PAG is sufficient to engender analgesia [133,134]. The vlPAG contains monosynaptic projections to the RVM, which, as mentioned above, are delineated as off, on, or neutral cells based on their firing properties during interactions with nociceptive stimuli [132,135-137]. RVM neuron subpopulations have been identified using novel genetic and molecular approaches to further elucidate the mechanisms by which mu opioid agonists produce their effects in this system. They can produce analgesia by directly inhibiting neurons, or by disinhibiting other inhibitory projections that may facilitate analgesia along the ascending or descending tracts [86]. Two important subpopulations within the RVM related to descending modulation of pain are the “off”, preproenkephalinergic (Penk) GABAergic neurons which project to the spinal cord, inhibit excitatory nociceptive circuits in the DH, and the MOR expressing projections that synapse onto Penk expressing DH neurons that inhibit mechanosensory neurons during mechanical nociception [138,139]. Cortical regions related to the central processing of pain seem to principally encode its affective components. For instance, clients given morphine mention experiencing the sensory components of pain but without the negative affective/aversive qualities [140]. This process is dose-dependent, in that, at

lower doses of opioids the affective component diminishes, and at higher doses, the sensory component follows [141-143]. The endogenous opioid system releases opioids during pain experiences as well as placebo-induced analgesia [144-147].

The aversiveness of pain is believed to be mediated by ACC opioid signaling, as MOR agonists delivered to the ACC relieve conditioned place aversion to painful stimuli in rodent models [148,149]. The relationship between the opioid system and reward circuitry is complex. Yet there is evidence that the relief of pain is intrinsically rewarding. This reward can be blocked by the administration of naloxone, a mu opioid receptor antagonist, into the ACC [150]. This effect is correlated with studies that show decreased dopaminergic release in the nucleus accumbens (NA) [151]. There are many instances of acute and chronic pain states affecting reward circuitry. For instance, opioid consumption in rodent models is increased following inflammatory pain, as the inflammatory state desensitizes MOR signaling in the VTA [152,153]. Additionally, NA dopamine release is decreased in states of neuropathic pain, an effect that is related to VTA microglial activation [154].

The amygdala is a CNS structure centrally involved in aversion and affect. GABAergic neurons in the amygdala express MORs in both the intercalated cell mass and the central nucleus, and when activated by mu opioid agonists, aversive responses to painful stimuli are decreased [155-157]. Information related to stress and anxiety initiating in the basolateral amygdala and locus coeruleus traveling to the nucleus of the stria terminalis is gated by the KOR system [158-160]. Across all major classes of drugs of abuse, the kappa-dynorphin system modulates stress, mood, aversion, and drug-seeking as it is expressed highly and integrally related to signaling nodes within the NA and amygdala, which mediate many of the

motivational/affective components of pain [161-168]. Thus, the endogenous opioid system is highly complex, involved in many nodes within the ascending and descending pain and analgesic tracts, as well as higher-order cortical regions that compute complex affective and motivational components of pain and analgesia.

### *GABA Disinhibition of Opioid Analgesia*

The aforementioned top-down system that modulates pain and analgesia includes the PAG, RVM, and dorsal horn is an integral and complex system within the CNS, comprised of many receptor and neuron subtypes. Activating this system at the level of the RVM or PAG produces analgesia [243]. This region is a major site of analgesic activity produced by opioids when consumed, as well as the structure in which stress-induced analgesia originates [244,245]. An early confounding finding by researchers investigating this circuitry found that both activating (via electrical stimulation or administration of excitatory amino acids) or inhibiting (via opioids) this circuit produced analgesia [246-248]. The supposition that followed was that inhibitory GABAergic interneurons tonically inhibited opioid neurons in the RVM and PAG, and when opioids were administered to the regions, the “brakes” were released, allowing opioid neurons to suppress ascending nociceptive traffic from reaching the brain and producing pain [243,249]. In studies using *ex vivo* electrophysiology to tease out these mechanisms, two subpopulations of cells termed “ON” and “OFF” cells were characterized in the RVM (as mentioned briefly earlier). Upon noxious stimulus application, ON cells show a distinctive increase in neuronal activity, whereas OFF cells exhibit decreased activity at the same time, just prior to a tail flick response [248]. When the PAG is chemically or electrically stimulated, the

projections that reach the RVM suppress ON cell activity, and enhance OFF cell activity, producing antinociception [246]. Local injections of opioids into the RVM or PAG can elicit these same effects [250-253]. Importantly, the OFF cells have been shown to project to the spinal cord and GABA<sub>A</sub> antagonist compounds decrease the inhibition of their firing preceding a nocifensive tail flick [249]. However, ON cells are understood to be local inhibitory GABAergic interneurons that decrease their firing before a tail flick. The role of opioids in these two subpopulations seems to be twofold: opioids activate descending OFF cell projections (eliciting antinociception), which inhibit nearby ON cells via lateral inhibition [254]. More specifically, opioids directly inhibit ON cells postsynaptically and presynaptically but do not directly affect the descending projections [255, 256-264]. This inhibition of ON cells elicits disinhibition of descending OFF cells, allowing for further antinociceptive signaling [261]. These top-down circuits are important in the study of pain and antinociception as they bidirectionally control the flow of pain-related information in the CNS and can be leveraged pharmacologically for therapeutic purposes.

### *Prescription Opioids and Their Abuses*

In 1995, the FDA approved oxycodone as a prescription opioid to treat acute and chronic pain, after which the market for opioid therapeutics dramatically increased [265-267]. Opioids became readily and widely available in different preparations (e.g., oral, intranasal, transdermal, etc.) [268]. Quickly following, the Federation of State Medical Boards released a set of guidelines in 1998, in an attempt to attenuate opioid abuse, but instead eventually paved the way for an increase in prescription and abuse rates [265,269]. Although some evidence suggested that

the rate of prescription opioid increases was not related to rates of abuse immediately in 1998, the direction of opioid prescriptions and opioid-related overdoses measurably changed following the 2001 Joint Commission on Accreditation of Healthcare Organizations, which emphasized the right to pain relief for patients suffering from acute and chronic forms of pain [270,271]. Opioid prescriptions in the US rose from 76 million in 1991 to 219 million in 2011, a near threefold increase [272,273]. In 2016, out of every 100 Americans, nearly 67 opioid prescriptions were written [274]. Prescription policies and practices vary by state, but overprescribing seemed to predominate in the Midwest and Appalachia [275,276]. One analysis of opioid prescriptions by county revealed that greater opioid proportions were present in populations with the following characteristics: a greater number of physicians per capita, greater poverty, lower educational attainment, lower insurance rates, and higher demographic representations of African American and non-Hispanic whites [277].

There is clear evidence now that indicates that the rates of opioid sales are strongly related to opioid abuse rates. In 2016, a study revealed that over 11 million Americans were actively abusing opioid prescriptions, over two million met the diagnostic criteria of opioid use disorder (OUD), and 42,000 died from opioid-related overdoses [278]. The US Department of Health and Human Services finally declared the opioid epidemic a public health emergency in late 2017 [279]. OUD, as defined by the DSM-5 is “a problematic pattern of opioid use leading to clinically significant impairment or distress” [280]. Individuals must meet two of the behavioral and/or psychological manifestations within a one-year period to meet the diagnostic criteria, such as strong cravings to use opioids, recurrent opioid use despite physical hazards associated with use, etc. [280]. Common symptoms associated with OUD include increasing

amounts of opioids consumed over time to achieve the desired effects (tolerance), negative physiological and psychological states after abstaining from use for a period of time (withdrawal), strong urges/desires to use opioids, and the inability to reduce or control the use of opioids [280,281].

Since 1999, opioid-related deaths have tripled [282]. These deaths account for nearly 115 deaths per day in the US, which is about one death every 13 minutes [282,283]. Between 2002 and 2015, there was nearly a threefold increase in overdose deaths from illicit and prescription opioids [282,283]. The totality of years of potential life lost in 2018 was estimated to be 830,652 years (excluding years over age 65) [284]. This tragic and devastating trend was primarily driven by opioid prescriptions until 2014 when illicit substances began to account for more of the opioid-related mortality [274,283]. Even as illicit substances begin to overtake prescription opioids in overdose deaths, the unfortunate fact remains that opioid-related overdose deaths continue to rapidly rise in the US, increasing from 47,600 in 2017 to 68,630 in 2020 [282,283]. In fact, 85% of the estimated \$504 billion economic burden related to the opioid crises is accounted for by fatality costs alone [285]. Needless to say, solutions to the opioid crisis are in dire need.

### *New Alternatives to Classical Opioids*

Most prescription opioid analgesics operate by activating the MOR along pain and analgesic pathways in the CNS. However, activation of these receptors also precipitates undesirable side effects such as constipation, respiratory depression, addiction, tolerance, withdrawal, and death. Attempts at improving upon opioid therapies have targeted this receptor

specifically over the past century [286]. However, novel approaches that attempt to leverage other receptor systems or secondary messenger molecules have begun to take shape over recent decades. Two predominant strategies to improve pain therapies include biased signaling molecules and multifunctional opioid compounds [286].

Multifunctional opioids leverage various opioid receptor subtype combinations in attempts to differentially modulate pain and side effect biology by activating or inactivating multiple opioid receptor systems simultaneously [286]. This is possible because opioid receptor compounds, although they all relate to nociception and analgesia, exhibit different phenotypes depending on the physiological context wherein they are activated. For instance, although MOR activation may produce respiratory depression and inhibition of gut motility (constipation), KOR activation produces antinociception and dysphoria, but without constipation or respiratory depression [286]. Thus, compounds such as U50,488H, a dual MOR/KOR agonist shows promise as they may produce greater levels of analgesia while reducing unwanted side effects [287]. Similar compounds, such as KOR/DOR dual agonists, MOR/DOR antagonists, and MOR/DOR dual agonists show promise as well but many of these multifunctional opioid ligands are still in the early stages of preclinical development.

Biased agonists have been developing, mostly in academic laboratories since 1999, when researchers revealed that genetically knocking down  $\beta$ -arrestin2 *in vivo* showed increased efficacy of morphine antinociception [288]. Since  $\beta$ -arrestin2 was known to mediate opioid receptor internalization and desensitization, the results were confirmatory. Surprisingly, however, the knockout mice also showed decreased tolerance to morphine, revealing a potential therapeutic strategy to improve opioids [289]. Unfortunately, with increased efficacy and

decreased desensitization resulting from  $\beta$ -arrestin2 knockout, the opioid-induced reward was also enhanced [290]. Following these and further studies investigating  $\beta$ -arrestin2 in opioid signaling, other laboratories began to develop compounds that produced different functional outcomes even when acting upon the same receptor subtypes [286]. Thus, functionally selective compounds began to be identified with the aim of activating opioid receptors but alternatively initiating intracellular cascades to produce more translationally relevant effects.

One understudied target in the context of opioid analgesics is Heat Shock Protein 90 (Hsp90). Hsp90 is a chaperone protein that is expressed in every cell type and plays numerous physiological roles, including protein folding, stabilization, protein localization, protein complex formation, and signal transduction regulation [286]. The inhibition of Hsp90 is suggested to be anti-inflammatory, as compounds that block Hsp90 activity attenuate the duration and onset of neuropathic pain [291]. In the context of opioid analgesia, however, Hsp90 has been shown to be upregulated after chronic opioid administration, and Hsp90 inhibition reduced opioid withdrawal severity [292]. Additionally, molecular markers of dependence and withdrawal were shown to be reduced after Hsp90 inhibition *in vitro* [293]. More evidence directly associating Hsp90 to opioid signaling in the CNS has been produced in recent years. For instance, Hsp90 in the brain has been shown to positively regulate opioid antinociception via ERK/MAPK signaling, and the inhibition of Hsp90 in the brain strongly attenuated systemic morphine-induced analgesia [294]. The effect of Hsp90 inhibition on opioid analgesia was consistent in the context of different models of pain [295,296]. Conversely, however, the inhibition of Hsp90 in the spinal cord increased opioid-induced antinociception [297]. This opposing effect of Hsp90 inhibition in the spinal cord was similarly consistent across different models of pain. More importantly, in

addition to improving the potency of morphine, side effects such as tolerance, constipation, and addiction were all either reduced or unchanged compared to controls [unpublished data]. These results taken together suggest that spinal cord Hsp90 inhibition provides a dose-reduction strategy, wherein patients may be co-administered lower doses of opioids along with Hsp90 inhibitors and achieve the same analgesic effects but have reduced risks of undesirable side effects. Further studies investigating the role of Hsp90 in opioid analgesia revealed that systemic administration of nonselective Hsp90 inhibitors showed similar effects as intracerebroventricular administration of Hsp90 inhibitors. This suggests that, when delivered systemically, the effects of Hsp90 inhibition in the brain predominates over that in the spinal cord. One way around this roadblock is to use small molecule inhibitors that selectively target Hsp90 isoforms that are expressed in the spinal cord, but not the brain. Additionally, co-chaperones of Hsp90 that contribute to Hsp90 signaling pathways in the spinal cord but not in the brain, may also be targeted and yield similar results. Our evidence collected over the past several years suggests that this Hsp90 isoform selective strategy is highly promising, and systemic administration of these compounds produces desirable effects, and reduced or unchanged side effects when co-delivered with opioids.

Given the complexity of the pain and analgesic molecular mechanisms and CNS circuitry, tackling the opioid epidemic appears to be a difficult, complex problem to solve even with the sociopolitical and economic considerations aside. Presently, two main routes to reducing the burden of the opiate crises seem apparent: replacing present opioid treatments with non-opioid alternatives (e.g., cannabinoids) or improving extant opioid treatments (via biased ligands or co-administered compounds). Our lab seeks to contribute to the latter path.

## CHAPTER 2

## INHIBITING SPINAL CORD-SPECIFIC HSP90 ISOFORMS REVEALS A NOVEL STRATEGY TO IMPROVE THE THERAPEUTIC INDEX OF OPIOID TREATMENT

*Introduction*

Opioid drugs like morphine are the gold standard for the treatment of moderate to severe chronic pain, but are limited by serious side effects, including tolerance, constipation, and reward/addiction liability [169, 170]. These limitations have spurred the search for alternate approaches to improve opioids, such as multifunctional ligands, or opioid agonists biased against the recruitment of  $\beta$ arrestin2 (recently reviewed in [171]). While none of these approaches has solved the opioid issue, they have revealed how manipulating the signal transduction cascades of the opioid receptors holds great promise in improving opioid outcomes (e.g., arrestin bias).

To this end, we've engaged in a long-term effort to investigate the role of Heat shock protein 90 (Hsp90) in regulating opioid signaling and anti-nociception. Hsp90 is a ubiquitous and highly expressed chaperone protein with a variety of roles, including nascent protein maturation, signaling kinase activation, and scaffolding signaling complex formation (reviewed in [172, 173]). Hsp90 has mostly been studied in the context of cancer. A few papers have shown that Hsp90 promotes inflammation during inflammatory and neuropathic pain [174-176], and another two papers have shown that Hsp90 could promote opioid dependence and withdrawal [177,178]. More recently, another paper has linked the Hsp90 $\beta$  isoform to opioid receptor signaling [179]. However, in general, the role of Hsp90 in the pain and opioid systems is mostly unstudied (reviewed in [180]).

In our work, we've uncovered a role for Hsp90 in opioid signaling and anti-nociception that differs between the brain and spinal cord. In brain, Hsp90 promotes ERK MAPK signaling via the Hsp90 $\alpha$  isoform and the co-chaperones Cdc37 and p23; Hsp90 inhibitor treatment in the brain thus reduces ERK MAPK signaling and opioid anti-nociception [182-184]. In contrast, Hsp90 represses opioid anti-nociception and signaling in the spinal cord, so that Hsp90 inhibitor treatment in the spinal cord promotes an ERK-RSK signaling cascade that results in enhanced opioid anti-nociception [185].

This enhanced anti-nociception led us to hypothesize that spinal Hsp90 inhibitor treatment could be used to improve the therapeutic index of opioids and enable a dose-reduction strategy. This is because many side effects are regulated outside the spinal cord, and would presumably not be impacted by spinal inhibition (e.g. reward in ventral tegmental area and striatum [186], constipation in the gut [187]). If anti-nociception were improved but side effects were either improved or not altered, then a lower dose of opioid could be given in combination with Hsp90 inhibitor treatment. This would hypothetically result in improved or maintained anti-nociception with decreased side effects (see [188] for a parallel approach). A novel dose-reduction strategy of this kind could be used to improve opioid therapy in chronic pain patients, decreasing the impact of the negative side effects of opioid therapy.

### *Materials and Methods*

#### ***Drugs and CRISPR constructs***

KU-32, KUNA115, KUNB106, and KUNG65 were synthesized, purified, and characterized as in our previously published work (KU-32 is Compound A4 in [189]; KUNA115

in [190]; KUNB106 in [191]; KUNG65 in [192]). Purity was confirmed by HPLC (>95%) and identity confirmed by HRMS and NMR. Inhibitors were stored under desiccation at -20°C, and stock solutions were prepared in DMSO, and also stored at -20°C. A matched Vehicle control for was included in every experiment; 0.02% DMSO in sterile USP water for the 0.01 nmol intrathecal injections and 10% DMSO, 10% Tween80, and 80% sterile USP saline for 1 mg/kg intravenous and 10 mg/kg oral injections. Morphine sulfate pentahydrate was obtained from the NIDA Drug Supply Program, stored at room temperature, and working solutions were made fresh prior to every experiment in sterile USP saline. USP saline injected controls were used for the reward and constipation assays below.

All-in-one CRISPR DNA constructs expressing Cas9 and a gRNA targeting Hsp90 $\alpha$  (MCP229411-CG01-3-B), Hsp90 $\beta$  (MCP227368-CG12-3-B), and Grp94 (MCP230394-CG12-3-B) were obtained from Genecopoeia (Rockville, MD). The DNA was amplified using standard molecular biology approaches, and complexed with TurboFect *in vivo* transfection reagent (Thermo Fisher, Waltham, MA) as described in our previous work [193] and by the manufacturer's protocol. The complexed DNA was injected into the mice by the intrathecal route (2  $\mu$ g DNA in 5  $\mu$ L) daily from days 1-3, with behavioral testing performed on day 10.

### ***Mice***

Male and female CD-1 mice in age-matched cohorts from 5–8 weeks of age were used for all behavioral experiments and were obtained from Charles River Laboratories (Wilmington, MA). CD-1 (a.k.a. ICR) mice are commonly used in opioid research as a line with a strong response to opioid drugs (*e.g.* [192], and our own previous Hsp90 research [181-184]). Mice

were recovered for a minimum of 5 days after shipment before being used in experiments. Mice were housed no more than 5 mice per cage and kept in an AAALAC-accredited vivarium at the University of Arizona under temperature control and 12-h light/dark cycles. All mice were provided with standard lab chow and water available *ad libitum*. The animals were monitored daily, including after surgical procedures, by trained veterinary staff. All experiments performed were in accordance with IACUC-approved protocols at the University of Arizona and by the guidelines of the NIH Guide for the Care and Use of Laboratory Animals. We also adhered to the guidelines of ARRIVE; no adverse events were noted for any of the animals.

### ***Behavioral experiments***

All animals were randomized to treatment groups by random assignment of mice in one cohort to cages, followed by random block assignment of cages to treatment group. Group sizes were based on previous published work from our lab using these assays [182, 184, 193, 194]. The mice were not habituated to handling. Prior to any behavioral experiment or testing, animals were brought to the testing room in their home cages for at least 1 h for acclimation. Testing always occurred within the same approximate time of day between experiments during the animal light (inactive) cycle, and environmental factors (noise, personnel, and scents) were minimized. All testing apparatus (cylinders, grid boxes, etc.) were cleaned between uses using 70% ethanol and allowed to dry. The experimenter was blinded to treatment group by another laboratory member delivering coded drug vials, which were then decoded after collection of all data. Naïve mice were used for every experiment, including each dose.

### ***Paw incision and mechanical allodynia***

Mechanical thresholds were determined prior to surgery using calibrated von Frey filaments (Ugo Basile, Varese, Italy) with the up-down method and four measurements after the first response per mouse as in [195] and our previously published work (e.g. [196]). The mice were housed in a homemade apparatus with Plexiglas walls and ceiling and a wire mesh floor (3-inch wide 4-inch long 3-inch high with 0.25-inch wire mesh). The surgery was then performed by anesthesia with ~2% isoflurane in standard air, preparation of the left plantar hind paw with iodine and 70% ethanol, and a 5-mm incision made through the skin and fascia with a no. 11 scalpel. The muscle was elevated with curved forceps leaving the origin and insertion intact, and the muscle was split lengthwise using the scalpel. The wound was then closed with 5-0 polyglycolic acid sutures. Mice were then injected with inhibitor or Vehicle control and left to recover for 24 h. Our intrathecal (i.t.) injection protocol is reported in [181]; briefly, the injection was made in awake and restrained animals with a 10  $\mu$ L Hamilton syringe and 30 g needle (5-7  $\mu$ L volume) between the L5-L6 vertebrae at a 45° angle, with placement validated by tail twitch. Since the injection was made through skin with no incision or other surgical intervention, repeated injection protocols were performed the same way. The next day, the mechanical threshold was again determined as described above. Mice were then injected with 0.32-5.6 mg/kg morphine by the subcutaneous (s.c.) route, and mechanical thresholds were determined over a 3-hour time course. No animals were excluded from these studies.

### ***Tail-flick assay***

Pre-injection tail-flick baselines were determined in a 52°C tail-flick assay with a 10-s cutoff time (method also reported in [181]). The mice were then injected with inhibitor or Vehicle control with a 24-hour treatment time. 24-hours post-injection baselines were determined. The mice were then injected s.c. with 1-10 mg/kg of morphine, and tail-flick latencies were determined over a 2-hour time course. For tolerance studies, baseline tail flick latencies were taken, and mice were then injected with inhibitor or Vehicle control with a 24-hour treatment time. 24 hours later mice were baselined again and then injected with 10 mg/kg s.c. morphine with one tail flick latency measured at 30 minutes post morphine. Mice were injected again with inhibitor or Vehicle and the process was repeated for an additional 7 days with twice daily morphine injection, and tail flick response measured after the morning injection. No animals were excluded from these studies.

### ***HIV peripheral neuropathy***

Mechanical threshold baselines were measured prior to any treatment on the left hind paw using von Frey filaments. HIV peripheral neuropathy was induced by intrathecal injection of gp120 IIIb protein (SPEED BioSystems, Gaithersburg, MD, Cat# YCP1549, 15 ng/μl in 0.1 M PBS and 0.1% BSA, 7-μl volume) using our previously established protocol [181] on days 1, 3, and 5. On day 20 a second mechanical threshold baseline was measured on the left hind paw using von Frey filaments and then KU-32 or Vehicle was injected i.t with a 24-h treatment time. A third mechanical threshold was then measured on day 21 and morphine (0.32-10 mg/kg s.c.)

was then injected, and mechanical thresholds were measured over a time course on the left hind paw. No animals were excluded from these studies.

### ***Conditioned place preference***

Conditioned place preference training, baseline runs, and post-training runs were all performed in Spatial Place Preference LE 896/898 rigs (Harvard Apparatus, Holliston, MA). Rigs were designed to consist of two chambers with one connecting chamber. Of the two conditioned chambers, one consisted of black and grey dotted walls with a textured floor. The other chamber consisted of black and grey striped walls with smooth floor. Chamber floors connected to a pressure sensor which transferred ongoing data to a computer running PPC WIN 2.0 software (Harvard Apparatus). Prior to preference training baselines were taken on day 0. Mice were placed in CPP chambers and allowed to roam freely for 15 minutes at ~7am. Chambers were cleaned thoroughly with VersaClean and allowed to dry in-between mice. Mice were then injected with i.t. KU-32 or Vehicle with a 24-hour treatment time. On day 1 mice were injected with i.t. KU-32 or Vehicle again and allowed to recover for 30 minutes. Mice were then injected s.c. with saline or morphine (3.2, 5.6, or 10mg/kg) at ~7am and placed in either stripe or dotted chambers. Half of each group paired morphine with the striped chamber and the other half to the dotted chamber in an unbiased design. At ~12pm mice were then given a second injection of either saline or morphine which was paired to the opposite chamber. This training process was repeated for 4 days total with morning and noon pairings alternating each day. On day 5 mice were placed in CPP chambers and allowed to roam freely for 15 minutes at ~7am. Raw data in

the form of seconds and percentage spent in each chamber was exported from PPC WIN 2.0 as an excel file and transferred to GraphPad Prism 9.3 (San Diego, CA) for further analysis.

### ***Opioid induced constipation***

Prior to the experiment mice were injected with either KU-32 or Vehicle i.t. and allowed to recover for 24 hours. Morphine (1, 3.2, or 10mg/kg s.c.) or saline was injected and followed by a 6-hour fecal production time course. During this time course the mice were housed in the von Frey boxes used to collect the paw incision and HIV neuropathy data above, which have a grate above a collection plate. The feces were counted and weighed in 1-hour bins and used to construct a cumulative plot. Morphine treated groups were normalized to saline groups and represented as a percentage at each timepoint.

### ***Respiratory depression***

Respiratory activity and subsequent morphine-induced depression was measured using whole body plethysmography in awake and freely moving mice using chambers from Data Sciences International (St. Paul, MN). Chambers were maintained at room temperature, with composition of the atmosphere set by mass flow controllers. Mice were injected with inhibitors or Vehicle control, followed by 24 hr treatment time, as for the above assays. The mice were then placed in the chambers for a 30-minute acclimation and baseline period, with respiratory measurements recorded for the last 7 minutes of the period. All mice were then treated with 7.5 mg/kg morphine i.v., immediately placed back in the chambers, and respiratory activity recorded for an additional hour.

### **In vitro ADME assays**

LogD Determination. Distribution coefficient (LogD) was determined by the method of Wilson et al. [197]. Briefly, 5  $\mu$ L volumes of test compounds diluted in DMSO were added to a mixture of equal volumes of 50 mM phosphate buffer and 1-octanol. The compounds were assayed using a 50 nM concentration in order to limit compound precipitation and to ensure that the assay values were maintained within the dynamic range of the LC-MS/MS instrumentation. Samples were vortex mixed at 800 rpm for 24 h. Subsequent to centrifugation at 14000 rpm for 30 min, 1  $\mu$ L of each layer was analyzed by LC-MS/MS. LogD was calculated using the peak areas obtained from each layer.

Aqueous Solubility. Aqueous solubility was determined using a miniaturized shake flask approach, under conditions of pH 6.8 and analyte concentration of 1.0 mM by the method of Zhou et al. [198]. Aqueous solutions of analyte were incubated at room temperature in the chamber of a Whatman (Piscataway, NJ) Mini-UniPrep syringeless filter for 24 h while shaking gently (600 rpm). Subsequent to incubation, filter plungers were pushed down to the bottom of the syringeless filter chamber assemblies, allowing filtrate to enter the plunger compartment. Following an additional 30 min incubation at room temperature, filtrates were diluted with 50:50 acetonitrile/water + 0.1% formic acid and analyzed by LC-MS/MS. Analyte concentrations were determined by the interpolation of peak area ratio from a calibration curve formed by matrix spiked with authentic reference material.

In Vitro Mouse Liver Microsomal Stability. Metabolic stability of lead compounds was assessed *in vitro* by the method of Di et al. [199]. Briefly, mouse liver microsomes (Corning Life Sciences, Woburn, MA) were isolated from CD-1 mice (male mice, 8–10 weeks of age). Assays

were conducted using 0.123 mg/mL protein concentration (total protein concentration in the microsomal solution) and 1.0  $\mu$ M drug concentration under incubation conditions of 37 °C. Metabolic stability was determined following 0, 5, 15, 30, and 60 min of incubation time. The samples were analyzed by reversed phase LC using a triple quadrupole mass spectrometer. Compound specific transitions of parent ion to product ion were monitored and percent remaining calculated based on peak area of 5–60 min time points (relative to time zero). Half-life calculations were determined using the formula  $t_{1/2} = -\ln(2)/k$ , where  $k$  ( $\text{min}^{-1}$ ) is the turnover rate constant (the slope) estimated from a log–linear regression of the percentage compound remaining versus time.

*In Vitro* Human Liver Microsomal Stability. Metabolic stability of the compounds in human liver microsomes was determined by the method described above using pooled human liver microsome preparations from 20 male donors (Corning Life Sciences, Woburn, MA). Assays were conducted as described above and the *in vitro* half-life of the compounds was calculated.

LC–MS/MS Analysis. LC–MS/MS analysis was conducted using an Agilent (Santa Clara, CA) 6460 triple quadrupole mass spectrometer coupled with an Agilent liquid chromatography (LC) system. The LC system consists of a binary pump, degasser, column heater, and autosampler. Chromatographic separation was performed on a Waters Atlantis T3 3 $\mu$ m 3.0 x 50 mm analytical column using a ballistic gradient of mobile phase consisting of 0.1% formic acid in water (A) and 0.1% formic acid in acetonitrile (B) at a flow rate of 0.75 mL/min. The mobile phase was heated to a temperature of 45 °C.

### ***In vivo pharmacokinetic study***

Mice were dosed with 10 mg/kg KUNG65 by the oral route, with groups over a 2 hr time course. The mice from each time point were sacrificed, and whole blood collected into EDTA tubes from a cardiac puncture. This was followed by saline perfusion to clear the vasculature, and the spinal cords were dissected and snap frozen in liquid nitrogen. The whole blood was separated, and the plasma stored in EDTA tubes; all samples were stored at -80°C prior to analysis. Compound exposure in plasma subsequent to *in vivo* dosing was determined by precipitation of protein with acetonitrile. Following centrifugation, the supernatant was injected for LC-MS/MS analysis, and plasma concentration determined via interpolation of peak areas from a standard curve prepared in plasma.

### ***Competition radioligand binding***

KUNB106 binding to the opioid receptors was performed substantially as in our previous work [200-204]. Human mu (#ES-542-C), delta (#RBHODM-K), and kappa (#ES-541-C) opioid-expressing CHO cell lines from PerkinElmer (Waltham, MA) were used. The cells were grown in in 1:1 DMEM/F12 medium with 10% heat-inactivated fetal bovine serum, 1X penicillin-streptomycin supplement, and 500 µg/mL G418 selection antibiotic. Cell pellets for experiments were collected using 5 mM EDTA in PBS and membrane protein extracted as described in our cited work. For the binding, 25-30 µg of membrane protein was combined with a fixed concentration (0.57-5.18 nM) of <sup>3</sup>H-diprenorphine (PerkinElmer) and concentration curves of KUNB106 or positive control (naloxone for mu and delta, U50,488 for kappa) in a 200 µL volume. The reactions were incubated for 1 hr at room temp, then collected onto 96 well

format GF/B filter plates using a Brandel Cell Harvester (Gaithersburg, MD). The radioactivity was read using a 96 well format MicroBeta2 scintillation counter (PerkinElmer). The resulting data was normalized to binding in the presence of Vehicle (100%) or 10  $\mu$ M naloxone/U50,488 (0%), and used to calculate the  $K_I$  based on the previously established  $K_D$  of  $^3\text{H}$ -diprenorphine in each cell line using GraphPad Prism 9.3 using a 1-site fit model.

### ***Statistical analysis***

All data were reported as the mean  $\pm$  SEM and normalized where appropriate as described above. The behavioral data from each individual dose was reported raw without maximum possible effect (MPE) or other normalization. Data for dose/response curves (except CPP) was normalized to %MPE using peak effect, except for constipation, which used Area Under the Curve [MPE = (Response-Baseline) / (Threshold – Baseline) \* 100]. The CPP dose/response curve was reported as the % Difference Score [Diff Score = % in Paired - % in Unpaired]. Technical replicates and further details are described in the Figure Legends. Potency ( $A_{50}$ ) values were calculated by linear regression using our previously reported method [181], with further details in the Figure Legends, and were reported with 95% confidence intervals. Statistical comparisons of individual dose/response curve time courses were performed using Repeated Measures 2-Way ANOVA with Sidak's (tail flick, paw incision, HIV neuropathy, tolerance rescue, constipation, respiratory depression) or Tukey's (tolerance, CPP) *post hoc* tests. The Geisser-Greenhouse correction was used to account for a potential lack of sphericity of the data, permitting valid Repeated Measures ANOVA. ANOVA *post hoc* tests were only performed when ANOVA F values indicated a significant difference, and there was homogeneity of

variance (permitting parametric analysis). In all cases, significance was defined as  $p < 0.05$ . The group sizes reported represent independent individual mice tested in each assay. All graphing and statistical analyses were performed using GraphPad Prism 9.3. Approximately equal numbers of male and female mice were used for each experiment. Comparison by 2 Way ANOVA using sex as a variable revealed no sex differences in this study, so all male and female mice were combined.

## *Results*

### ***Spinal Hsp90 inhibition enhances morphine anti-nociception in multiple pain models***

Based on our earlier work [184] we hypothesized that spinal cord Hsp90 inhibition would consistently enhance morphine anti-nociception over a full dose range in different acute and chronic pain models. We tested this using male and female CD-1 mice injected with 0.01 nmol of the non-isoform-selective Hsp90 inhibitor KU-32 or Vehicle control by the i.t. route with a default treatment time of 24 hours (time point based on our earlier work [181-184]). After the 24-hour treatment time, the mice were treated with a dose range of morphine and anti-nociception was measured.

We first tested acute thermal nociception in uninjured mice using the well-established tail flick model. KU-32 treatment caused a consistent and significant elevation in morphine anti-nociception over the dose range of 1-5.6 mg/kg (**Figure 1A-C**). The response was not different at 10 mg/kg; however, 10 mg/kg is a maximal dose in this assay, and responses were not recorded past the 10 second threshold (**Figure 1D**). Dose/response analysis revealed a potency of 3.0 (2.5 – 3.7; 95% confidence intervals reported in parentheses) mg/kg in Vehicle treated mice

and 1.6 (1.3 – 2.0) mg/kg in KU-32 treated mice, representing a 1.9-fold shift improvement in potency (**Figure 1E**).

This result was encouraging; however, tail flick is a spinal reflex in uninjured animals, and may not translate to clinical pain conditions. We thus used the post-surgical paw incision assay to model post-surgical pain, a common opioid indication [205]. Much as in heat-induced tail flick, KU-32 caused a significant and consistent elevation in morphine anti-nociception over the 0.32 – 5.6 mg/kg dose range (**Figure 2A-E**). Dose/response analysis showed an  $A_{50}$  potency value of 2.4 (2.0 – 2.8) mg/kg for Vehicle animals and 0.85 (0.64 – 1.1) mg/kg for KU-32 animals, representing a 2.8-fold improvement in potency (**Figure 2F**).

These results are again promising, but both pain states are acute and short in duration, and do not represent chronic pain, which is the most difficult to treat in the clinic. We thus used the HIV peripheral neuropathy model induced by gp120 protein injection, which is a sustained and long-lasting neuropathic pain model [205]. After 3 sustained weeks of chronic pain, the mice were treated with KU-32 or Vehicle control and tested as above. Again, KU-32 treatment caused a sustained and significant increase in morphine anti-nociception over the 0.32-10 mg/kg dose range (**Figure 3A-E**). Dose/response analysis showed a potency of 4.2 (3.7 – 4.8) mg/kg for Vehicle treatment and 1.2 (0.87 – 1.5) mg/kg for KU-32 treatment, an improvement of 3.5-fold (**Figure 3F**). Not only did KU-32 improve opioid anti-nociception in this chronic pain model, but it also had the largest fold-shift improvement of the 3 models tested. Importantly, KU-32 treatment did not cause baseline differences in any pain state measured.

### ***Spinal Hsp90 inhibition reduces morphine tolerance and rescues established tolerance***

The results above support our hypothesis that spinal Hsp90 inhibition could make opioids more potent. However, at the same time, if side effect potencies are enhanced, then the improvement does not result in an improved therapeutic index or improved opioid therapy. We thus tested the potency of morphine side effects with spinal Hsp90 inhibitor treatment, beginning with anti-nociceptive tolerance. Over a 7-day repeated treatment period, the anti-nociceptive efficacy of morphine steadily decreased in Vehicle treated mice, resulting in a complete loss of anti-nociceptive efficacy by day 7 for the entire 1-10 mg/kg dose range (**Figure 4A-C**). In contrast, KU-32 treatment caused a significant decrease in tolerance over the full 7-day treatment period and full dose range, so that at least some significant anti-nociceptive efficacy remained by day 7 at each dose with KU-32 treatment (**Figure 4A-C**). Notably, baseline responses were not altered by any treatment, demonstrating that KU-32 treatment is not altering baseline nociception (**Figure 4A-C**). To quantify this result, we compared day 1 vs. day 4 responses for each dose and treatment; day 4 was chosen because days 5-7 have no quantifiable Vehicle response for at least one dose each. Dose/response analysis of these data revealed a 21-fold tolerance shift from day 1 to day 4 for Vehicle-treated mice; this tolerance shift was reduced to 2.9-fold in KU-32 treated mice (**Figure 4D**).

This result suggests that morphine tolerance is blocked by KU-32 treatment; however, KU-32 treatment began before the tolerance regimen and continued during every morphine injection. We thus sought to determine if KU-32 treatment would reverse already-established tolerance. We thus subjected naïve mice to a tolerance regimen as above for 3 days; all mice showed normal morphine anti-nociception on day 1 and a near-complete tolerance by day 3

(**Figure 4E**). We then injected these mice with KU-32 or Vehicle, and 24 hours later, injected morphine again. The Vehicle-treated mice showed little anti-nociception, showing how their tolerance was maintained (**Figure 4F**). In sharp contrast, the KU-32 treated mice showed a full anti-nociceptive response to morphine, comparable to their day 1 response (**Figure 4F**). These results suggest that not only can spinal Hsp90 inhibition reduce the development of tolerance, but it can also restore responsiveness to already-tolerant mice.

### ***Spinal Hsp90 inhibition does not alter morphine-induced constipation and reward***

Based on our rationale described above, we continued to investigate clinically relevant opioid side effects. Opioid-induced constipation is a highly clinically significant side effect, that lowers medication compliance and patient quality of life [184]. After KU-32 or Vehicle treatment, we injected a dose-range of morphine and measured fecal output over a 6-hour time course. Compared to saline injected controls, morphine caused ~40% constipation at 1 mg/kg, that plateaued at ~70% constipation at 3.2-10 mg/kg (**Figure 5A-C**). Vehicle vs. KU-32 saline or morphine treatment curves were not significantly different at any dose or time point. After normalizing each treatment group to saline-injected controls, dose/response analysis revealed overlapping curves with a constipation potency of 0.67 (0.32 – 0.94) mg/kg for Vehicle and 0.97 (0.59 – 1.3) mg/kg for KU-32, further supporting the conclusion that KU-32 treatment did not alter morphine constipation (**Figure 5D**).

We next tested opioid-induced reward, which is the basis for opioid addiction, and has contributed to an opioid abuse and overdose crisis [185, 207]. We used the well-established conditioned place preference (CPP) assay, which demonstrates reward (or aversion) learning

[26]. Over the 3.2-10 mg/kg morphine dose range, we observed an increasing preference for the morphine-paired chamber by Vehicle-treated mice, that rose to the level of significance at 10 mg/kg of morphine (**Figure 6A-C**). KU-32 treatment did not differ significantly from Vehicle treatment at any dose, and also showed significant preference at 10 mg/kg of morphine (**Figure 6A-C**). Dose/response analysis showed overlapping curves and a potency of 5.1 (2.7 – 7.7) mg/kg for Vehicle and 5.3 ( $-\infty$  -  $+\infty$ ) mg/kg for KU-32, further supporting a lack of effect of KU-32 treatment on morphine-induced reward learning (**Figure 6D**).

### ***Identification of spinal cord specific Hsp90 isoforms***

The results above confirm our basic hypothesis that inhibition of Hsp90 in the spinal cord can improve the therapeutic index of opioids. However, all experiments above were performed with i.t. injection, which is of limited therapeutic relevance, and we already know that systemic delivery of non-selective Hsp90 inhibitors blocks opioid anti-nociception by inhibiting active Hsp90 in the brain [184]. We thus sought a way to block spinal Hsp90 in a clinically-relevant way. In our earlier work, we found that of the 4 Hsp90 isoforms, only Hsp90 $\alpha$  was active in regulating opioid signaling in the brain [182]. We thus hypothesized that if different Hsp90 isoforms were active in the spinal cord, these could be targeted by systemically delivered *selective* inhibitors to selectively block spinal cord Hsp90.

We thus treated mice with selective small molecule inhibitors and targeted CRISPR constructs for each Hsp90 isoform, all delivered by the i.t. route. We found that the Hsp90 $\alpha$ -selective inhibitor KUNA115 and Hsp90 $\alpha$ -targeted CRISPR enhanced morphine anti-nociception in the tail flick assay (**Figure 7A**). This result suggests that Hsp90 $\alpha$  regulates opioid

signaling in the brain *and* the spinal cord. However, unlike the brain, inhibitors and CRISPR targeted to Hsp90 $\beta$  and Grp94 also enhanced morphine pain relief (**Figure 7B-C**). This suggests that all 3 Hsp90 isoforms regulate opioid signaling in the spinal cord, while only Hsp90 $\alpha$  is active in the brain. If our hypothesis is correct, then systemic inhibition of Hsp90 $\beta$  and Grp94 should recapitulate the benefits of Hsp90 inhibition in the spinal cord by the i.t. route.

### ***Systemic Grp94 inhibition recapitulates the benefits of spinal Hsp90 inhibition***

To test this hypothesis, we used the selective Grp94 inhibitor KUNG65 ([191], **Figure 8A**). KUNG65 is a strongly selective Grp94 inhibitor, with a target  $K_D$  of 540 nM and at least 73-fold selectivity vs. the other Hsp90 isoforms (**Figure 8B**), making this molecule a good choice for this study. However, we are the first to use KUNG65 *in vivo*, and systemic delivery requires metabolic stability and the ability to cross the blood-brain barrier, which is unknown for this molecule. We thus tested *in vitro* ADME parameters of KUNG65, finding a LogD of 3.3, a solubility of 0.074  $\mu$ M, and a metabolic half-life of 144 and 32 minutes in human and mouse liver microsomes, respectively (**Figure 8C**). While the solubility is low, the other parameters were promising for *in vivo* delivery. We thus performed a pharmacokinetic study, giving KUNG65 at 10 mg/kg by the oral route, the most challenging route of administration. We found variable but measurable KUNG65 in the plasma, peaking at 79.7 nM in the plasma, and in the spinal cord, peaking at 5.2 nM (**Figure 8D**). While KUNG65 had relatively poor pharmacokinetic performance, preventing the calculation of clearance, half-life, etc., this result was sufficient to demonstrate that the drug could penetrate into the site of action in the spinal cord. We thus delivered KUNG65 at 1 mg/kg by the i.v. route (to enhance spinal cord

penetration) in a similar experimental design to the pain assays above, followed by a morphine dose-response in the tail flick assay. Much like our results with KU-32 above, we found that i.v. KUNG65 consistently elevated tail flick anti-nociception in response to morphine across the 1-5.6 mg/kg dose range (**Figure 8E**). We constructed a dose-response curve, finding an  $A_{50}$  of 3.6 (2.9 – 4.6) mg/kg in Vehicle treated mice, and 1.9 (1.4 – 2.3) mg/kg in the KUNG65 treated mice, a 1.9-fold shift improvement in morphine potency (**Figure 8F**). This 1.9-fold shift is identical to the fold shift found with i.t. KU-32 treatment in **Figure 1**, providing a strong initial confirmation of our hypothesis. To further evaluate the therapeutic potential of KUNG65, we tested tail flick anti-nociception 48 hours after treatment, instead of 24 hrs as above. This experiment found no effect of KUNG65 treatment, suggesting the effects of the drug persist for 24 but not 48 hrs (**Figure S1**). To rule out confounding effects at the opioid receptors, we also tested for the ability of KUNG65 to bind to any of the human opioid receptors, finding no binding up to a 10  $\mu$ M concentration (**Figure S2**).

Continuing our opioid anti-nociception analysis, we then tested i.v. KUNG65 in the post-surgical paw incision model. As expected, i.v. KUNG65 significantly elevated the morphine anti-nociceptive response across the 1 – 3.2 mg/kg dose range (**Figure 9A**). Dose-response analysis showed an  $A_{50}$  of 2.0 (1.4 – 3.0) mg/kg in Vehicle treated mice and 0.9 (0.5 – 1.2) mg/kg in the KUNG65 treated mice, a 2.2-fold shift improvement in morphine potency (**Figure 9B**). Again, these results support our hypothesis that systemic selective inhibition of Grp94 can mimic the effects of spinal cord Hsp90 inhibition.

### ***Systemic Hsp90 $\beta$ inhibition recapitulates the benefits of spinal Hsp90 inhibition***

We continued to test our hypothesis, this time using the Hsp90 $\beta$ -selective inhibitor KUNB106 ([190], **Figure 10A**). Similar to KUNG65 above, KUNB106 is a highly-selective Hsp90 $\beta$  inhibitor, with a target  $K_D$  of 91 nM and a minimum 275-fold selectivity vs. other isoforms (**Figure 10B**). *In vitro* ADME analysis showed a LogD of 2.26, a solubility of 0.014  $\mu$ M, and a human and mouse liver microsome half-life of 156 and 63 minutes, respectively (**Figure 10C**). These ADME results and profile are similar to KUNG65 above, so we proceeded directly to *in vivo* testing, using the same 1 mg/kg i.v. dose and route as for KUNG65. Again, KUNB106 caused an enhanced morphine tail flick anti-nociceptive response across the entire 1 – 5.6 mg/kg dose range (**Figure 10D**). Upon dose-response analysis, we found an  $A_{50}$  of 5.6 (4.4 –  $\infty$ ) mg/kg for Vehicle treated mice and 1.7 (1.1 – 2.3) mg/kg for KUNB106 treated mice, a 3.3-fold shift (**Figure 10E**). As a test for potential confounds, we tested for the ability of KUNB106 to bind to the opioid receptors, which could explain these results. We did not find any binding to any opioid receptor up to a 10  $\mu$ M concentration, suggesting our findings are on-target to Hsp90 $\beta$  inhibition (**Figure S2**).

Extending this analysis again to the post-surgical paw incision model, we found that KUNB106 elevated morphine anti-nociception across the 1 – 3.2 mg/kg dose range (**Figure 11A**). We found an  $A_{50}$  of 2.5 (2.0 –  $\infty$ ) mg/kg for Vehicle treated mice and 0.99 ( $\infty$  –  $\infty$ ) mg/kg for KUNB106 treated mice, a 2.5-fold shift (**Figure 11B**). Together these results support our hypothesis, in that systemic Hsp90 $\beta$  and Grp94 inhibitors both boosted morphine pain relief in a similar manner to direct spinal injection of a non-selective inhibitor like KU-32, suggesting that

they are targeting active Hsp90 isoforms in the spinal cord and avoiding active Hsp90 isoforms in the brain.

### ***Systemic Grp94 and Hsp90 $\beta$ inhibitors improve the therapeutic index of morphine***

The above results establish that systemic inhibition of Grp94 and Hsp90 $\beta$  boost pain relief much like we saw with direct spinal injection of Hsp90 inhibitor. However, these results do not show that systemic Grp94/Hsp90 $\beta$  inhibitors either improve or do not change side effects, which is necessary to fully show that these treatments boost the therapeutic index of morphine. We thus tested for the impact of KUNG65 and KUNB106 on tolerance and respiratory depression, a key side effect linked to opioid safety and overdose.

We first tested the Grp94 inhibitor KUNG65. We found that acute injection i.v. of 1 mg/kg KUNG65 could rescue established morphine tolerance (**Figure 12A**). This finding was very similar to the tolerance rescue observed with spinal injection of KU-32 in **Figure 4E-F** above and suggests that KUNG65 can prevent or rescue opioid tolerance. In respiratory depression, we found that KUNG65 had no effect on respiratory activity, either before or after morphine injection (**Figure 12B**). This was an important safety finding, suggesting that while these inhibitors can boost opioid pain relief, they will not boost side effects, thus they improve the therapeutic index of morphine. We found near-identical results for KUNB106, finding that KUNB106 injection rescued established tolerance (**Figure 12C**) while also having no effect on morphine-induced respiratory depression (**Figure 12D**). Together these results confirm that Hsp90 $\beta$  and Grp94 inhibitors do indeed boost the therapeutic index of morphine, enhancing pain relief while either improving or not changing side effects.

### ***Systemic Hsp90 $\alpha$ inhibitor blocks opioid anti-nociception***

Finally, we tested the last piece of our hypothesis by systemic i.v. injection of 1 mg/kg KUNA115, a selective Hsp90 $\alpha$  inhibitor. If our hypothesis is correct, then this drug should inhibit active Hsp90 in both the brain and spinal cord, leading to a loss of anti-nociception as we saw with systemic non-selective inhibitor. We used this drug in the post-surgical paw incision model and found that this treatment completely blocked anti-nociception in response to 3.2 mg/kg morphine (**Figure 13**). This last experiment ties together our model, finding that systemic Hsp90 $\beta$  and Grp94 inhibition recapitulates the beneficial effects of spinal cord inhibition, while Hsp90 $\alpha$  inhibition recapitulates the negative effects of brain inhibition.

### *Discussion*

We show here that Hsp90 inhibition in the spinal cord improves the therapeutic index of morphine, by increasing anti-nociceptive potency by 2-4 fold, reducing and rescuing tolerance, while not changing reward and constipation potency. We have further uncovered a novel strategy to avoid unwanted brain Hsp90 inhibition, which blocks opioid pain relief, by targeting spinal cord-specific Hsp90 isoforms. We found that Hsp90 $\beta$  and Grp94 alone regulate opioid signaling in the spinal cord, while Hsp90 $\alpha$  regulates both brain and spinal cord opioid signaling. Thus, by delivering isoform-selective Hsp90 $\beta$  and Grp94 inhibitors by a systemic and translationally relevant route, we could enhance opioid pain relief by a similar 2-3 fold while rescuing tolerance and not altering morphine-induced respiratory depression. By contrast, a systemic Hsp90 $\alpha$ -selective inhibitor recapitulated brain inhibition, resulting in a loss of opioid anti-nociception. Together these findings establish the potential for Hsp90 $\beta$  and Grp94 inhibitors as opioid co-

therapies, which would improve the therapeutic index of opioids, allowing for lower opioid doses with maintained analgesia and reduced side effects. Our model is summarized in **Figure 14**.

Selectively boosting anti-nociceptive potency/efficacy in order to enable a dose-reduction strategy has precedent in the literature. Examples include demonstrated synergy between the cannabinoid receptor type 2 and opioid receptor for anti-nociception, without synergizing the side effects of either [187]. Further examples include selective inhibition of G $\beta$  $\gamma$  signaling downstream of the mu opioid receptor, which similarly potentiates anti-nociception but not side effects [208], morphine and clonidine synergy [209], and using chemokine receptor antagonists to enable opioid dose-reduction [210]. These examples provide precedent and a reason to believe that dose-reduction with Hsp90 inhibitors would work. At the same time, to our knowledge, no such approaches are being used in the clinic, providing novelty and opportunity to use our findings.

Further factors argue for the clinical potential of our findings. Our earlier work suggests that other opioids, specifically oxycodone, are regulated similarly by Hsp90 inhibition as morphine, albeit in different pain models and inhibitor route [183]. This suggests that a broad spectrum of opioid drugs could be improved. We've also shown that these inhibitors have no impact on opioid-induced respiratory depression, which is a key safety concern (**Figure 12**). Our earlier work has shown that non-selective Hsp90 inhibitors given systemically mimic brain inhibition, resulting in a loss of opioid pain relief [184]; this means that our finding that isoform-selective inhibitors can be given systemically to recapitulate spinal inhibition is an important translational advance. Few patients are amenable to an intrathecal delivery route for chronic care,

meaning that an isoform-selective approach is necessary to achieve the benefits of spinal Hsp90 inhibition.

One potential concern in adopting these isoform-selective inhibitors for therapy is the potential for on-target side effects. Indeed, early generation non-selective inhibitors like 17-AAG did not make it through clinical trials due to liver toxicity [211]. However, later generation compounds like CNF2024 were far better tolerated, suggesting this toxicity could be off-target rather than Hsp90-mediated [211]. In any case, isoform-selective inhibitors as we propose here should be far better tolerated than non-selective inhibitors, since each isoform has a distinct cellular location and pool of client proteins. This is further supported by a recent report that Hsp90 $\alpha$  is the isoform responsible for the serious side effect of retinal degeneration associated with non-selective inhibitors [212]. Happily, our work suggests that Hsp90 $\alpha$  is the very isoform that should be avoided for opioid therapy. Together these findings suggest that isoform-selective Hsp90 inhibitors could be feasible for chronic patient therapy.

These observations also raise the question of by what mechanism are these effects taking place. Our earlier work described an ERK-RSK kinase cascade that is not normally active in spinal cord, but becomes “unchained” with Hsp90 inhibition and promotes enhanced anti-nociception [184]. This cascade is presumably responsible for the wider enhancement in anti-nociceptive potency we see here across multiple acute and chronic pain models. At the same time, reward is primarily modulated by a ventral tegmental area-striatal circuit [185] among other forebrain circuits, while constipation is primarily modulated by opioid receptors in the gut [186]; it thus makes sense why local spinal inhibition would not impact these regions and change the potency of those side effects. This leaves tolerance. Several studies have found that spinal

circuits modulate opioid tolerance through various mechanisms, suggesting that local spinal inhibition could alter tolerance [213, 214]. Spinal Hsp90 inhibition may favorably alter these mechanisms, blocking tolerance. Similarly, Hsp90 inhibition has been shown to be anti-inflammatory, and spinal neuroinflammation has been shown to contribute to opioid tolerance [175, 215]. Alternately, enhanced anti-nociceptive efficacy could lead to less tolerance over time simply because the efficacy was higher to begin with; in support of this hypothesis, high efficacy opioid agonists have been shown to produce slower/less tolerance than low efficacy agonists [216].

However, these hypotheses only address the slower tolerance seen over time with repeated treatment, they do not explain the tolerance rescue we observed. One potential clue for this rescue mechanism could be our earlier findings that both brain and spinal cord effects of Hsp90 inhibition on anti-nociception require rapid protein translation [182-184]. The translation inhibitor we used had no impact on anti-nociception in Vehicle-treated mice, suggesting that this mechanism is newly activated upon Hsp90 inhibitor treatment. The mechanisms we are uncovering could thus be parallel pathways to the normal/baseline anti-nociceptive signaling, which is further supported by our work on the spinal ERK-RSK cascade [182]. In the case of the tolerance rescue, we could be observing new pathways becoming turned on that have not developed tolerance as have the normal/baseline pathways. These new pathways could thus provide anti-nociceptive responsiveness even when other parts of the system remain tolerant. It's also unclear at this point whether the tolerance reduction and the tolerance rescue share the same or different mechanisms. Lastly, it is not at all clear why different Hsp90 isoforms are active in brain vs. spinal cord, and whether these isoforms differ in how they regulate opioid signaling.

These questions will provide new basic science directions to follow while at the same time these findings can be used to inform a new clinical opioid dose-reduction approach.

## CHAPTER 3

### INHIBITION OF HEAT SHOCK PROTEIN 90 IN THE SPINAL CORD AUGMENTS OPIOID ANALGESIA VIA DISABLING A GABAERGIC BRAKE

#### *Introduction*

There is a high prevalence of chronic pain (affecting over 20% of US Americans), and the commensurate economic loss is estimated at more than \$600 billion annually [218]. Chronic pain is the leading cause of disability and the highest contributor to global disease burden [228]. The leading pharmaceutical treatments for acute and chronic pain are opioid analgesics, yet these possess myriad detrimental side effects and are insufficient for most patients [218]. Individuals suffering from chronic pain can develop strong associations with the rewarding effects of opioids, creating dependence, addiction, and in some cases death [219]. Opioidergic receptor activation via agonist ligands can produce constipation by activating opioid receptors along the gastrointestinal tract, respiratory depression by inhibiting neurons in the pre-Bötzinger complex in the medulla, and addiction/reward by disinhibiting dopaminergic projections in the nucleus accumbens and VTA in the mesolimbic reward pathway. One strategy to improve treatment outcomes is to reduce opioid dosing by co-administering compounds that augment the analgesic effects of opioids but decrease the unwanted side effects.

Our previous research shows that spinal cord heat shock protein 90 (Hsp90) is implicated in opioid signaling and pain reduction [220,221]. By inhibiting Hsp90 in the spinal cord with 17-AAG, the potency of opioid-induced analgesia increases, while unwanted side effects decrease or remain unchanged [222]. Interestingly, if Hsp90 is pharmacologically inhibited in the brain,

opioid analgesia is strongly suppressed [220]. The effect of Hsp90 inhibition in the spinal cord can be blocked by pharmacological inhibition of ERK, RSK, or protein synthesis, suggesting that downstream effector molecules are upregulated downstream of this signal transduction pathway that leads to protein translation [220]. The proteins mediating the effects on opioid signaling after the translational step, downstream of Hsp90 inhibition, ERK, and RSK, are not known [220].

Seeking a mechanism for this effect, our lab used proteomic analyses to find that spinal administration of 17-AAG produced a substantial increase of GABA transporter 2 (GAT-2), a protein involved in the reuptake of the inhibitory neurotransmitter GABA (**Figure 17**) [220]. 17-AAG is an effective means to boost opioid antinociception; and further isoform-selective inhibitors above may be translationally beneficial. However, the exact mechanism by which Hsp90 inhibition increases opioid-induced analgesia and reduces side effects remains unclear. A better understanding of the mechanistic details of Hsp90 inhibition in spinal cord opioid and pain signaling may reveal new targets for pharmaceutical intervention and provide novel solutions to the opioid crisis. Our data suggest that, in mice, 17-AAG increases opioid analgesia by decreasing inhibitory GABAergic input to opioidergic interneurons that facilitate antinociception. Proteomic analyses reveal that administration of 17-AAG in the spinal cord upregulates the sodium and chloride dependent GABA reuptake transporter 2 (GAT-2; **Figure 17**). The pharmacological blockade of GAT-2 prevents the 17-AAG-induced increase in opioid analgesia in males and females (**Figure 18**). The downstream effects of GAT-2 upregulation resulting from Hsp90 inhibition in the spinal cord are less clear and include sex-specific differences. Recent investigations into the dynamics between opioid and GABAergic signaling in

ascending and descending nociceptive and analgesic circuitry may provide mechanistic insight into this phenomenon.

### *Spinal Cord Mechanisms of Pain*

Nociceptors in the skin and viscera transmit pain signaling to the brain by first producing and sending action potentials along primary afferents into the dorsal horn of the spinal cord. In the dorsal horn, the projections are organized according to the region of the body affected, and the sensory modality of the stimuli. The information transmitted to the dorsal horn is then processed by a complex network of excitatory and inhibitory interneurons before nociceptive traffic is communicated to projections that ascend to the brain. Neurokinin 1 receptors are localized in a majority (80%) of lamina I projection neurons and are activated by substance P – an undecapeptide ligand associated with inflammation and pain [224]. Latencies in tail flick responses in the hot water bath/tail flick assay have been shown to be reduced to baseline with the administration of NK1 receptor antagonists [222]. Additionally, morphine (a Mu opioid receptor agonist) blocks the relay of substance P induced facilitation of the tail flick reflex at the level of the spinal cord, indicating that the NK1 receptor-expressing neurons are involved in mediating the nociceptive traffic in the tail flick reflex and that opioid receptor activation can block these signals [223]. Understanding the interaction between MOR activity and Hsp90 inhibition in the spinal cord may elucidate novel targets for the development of pain therapeutics.

### *GABA and Opioids*

The interaction between GABAergic and opioidergic signaling in the spinal cord is complex, and not yet completely understood. In the spinal cord, morphine (a full Mu opioid receptor [MOR] agonist) precipitates analgesia by inhibiting neurons that send nociceptive signals along the ascending spinothalamic tract [224]. MOR-expressing interneurons in the spinal dorsal horn are predominantly localized on excitatory interneurons [226]. MOR activation in neurons can produce presynaptic [227-229] and postsynaptic [230-232] effects that largely engender a decrease in excitatory activity in the dorsal horn by producing hyperpolarizing currents in primary afferents, secondary afferents, and excitatory interneurons [226]. Activation of MOR produces a signaling cascade via the Gi/Go proteins [233]. Via this pathway, opioids activate inwardly rectifying GIRK channels and inhibit Ca<sup>2+</sup> channels, decreasing excitability through both mechanisms [234]. GABA receptors, however, facilitate inhibitory neurotransmission through other molecular signaling cascades. GABA-A receptors are ionotropic and, upon ligand binding, open and allow Cl<sup>-</sup> ions to flow in and hyperpolarize the cell [235]. Whereas, GABA-B receptors are metabotropic, and upon activation activate the Gi/Go pathway to inhibit inward Ca<sup>2+</sup> currents and activate outward K<sup>+</sup> currents [236]. In the spinal cord, GABAergic interneurons may exhibit one of three putative intrinsic firing patterns: tonic, initial burst, or phasic [240]. Importantly, over 90% of inhibitory GABAergic interneurons in the superficial dorsal horn exhibit a tonic firing pattern [237] – a subset of which, we believe, project onto PPE-expressing excitatory opioidergic interneurons. Thus, it may be the case that, since 17-AAG alone produces no analgesia in the tail-flick assay, the administration of a Mu opioid receptor agonist (e.g., DAMGO) may be necessary to observe the effect of reduced GABAergic tone on opioid-mediated analgesia.

### *GAT-2*

GAT-2 is a member of the solute carrier family (SLC6) which consists of sodium and chloride dependent transporters that modulate various physiological processes [297]. The four subfamilies within the SLC6 family contain GABA transporters, monoamine transporters, amino acid transporters, and “orphan” transporters [298,299]. Point mutations within genes encoding these proteins are related to a number of disorders including obesity, orthostatic hypotension, and obsessive-compulsive disorder [299]. Thus, many prescription drugs target these proteins to modulate their activity for therapeutic purposes. GABA is the most widely distributed inhibitory neurotransmitter in the nervous system and inhibits neurons postsynaptically by binding to its cognate receptors, which subsequently hyperpolarize neurons [300]. However, non-CNS actions of GABA have also been elucidated in the liver, kidney, stomach, intestine, testis, etc. [301]. The GABA subfamily of solute carriers consists of four transporters that decrease the available synaptic GABA by reuptaking it back into the cell body [300,302]. Very little is known about these transporters, and GAT-2 remains the least well-characterized [297]. GAT-1 and GAT-3 are highly expressed in the brain, but neither the cell type distribution nor expression levels of GAT-2 have been elucidated [303]. However, GAT-2 has been shown to reuptake GABA *in vitro* and *in vivo* [304-307] and shows affinity for taurine as well as GABA (although, shows much greater affinity for GABA) [307,308]. GABA is appropriately deemed the major inhibitory neurotransmitter within the nervous system. However, the functional circuitry wherein GABA neurons are distributed may decrease or increase the overall amount of neuronal communication and excitability. As reviewed earlier, inhibitory interneurons in the PAG-RVM-SC circuit, when inactivated by GABA receptor antagonists, decrease the tonic inhibition of downstream opioid

projections, which increases their output. Most recently, in a paper published in Nature this September, researchers revealed that axo-axonic GABA projections can target myelinated sensory neurons, and facilitate spike propagation, rather than inhibit [309]. Presumably, if these circuits play a role in the mechanism of Hsp90 inhibition on opioid analgesia, a decrease in available synaptic GABA in these contact sites as a result of GAT-2 upregulation would instead enhance antinociception rather than attenuate it. Thus, the functional role GABA plays within CNS circuitry is vastly complicated, and many circuits remain to be fully characterized.

Heat shock protein 90 (Hsp90) is a stress-inducible protein that acts primarily as a molecular chaperone, predominantly ensuring the proper folding of nascent polypeptides. Additionally, Hsp90 plays a role in maintaining, localizing, and trafficking kinases and other signaling molecules involved in intra and intercellular signaling transduction and communication (e.g., RSK, MAP/ERK) [296]. 17-allylamino-17-demethoxy-geldanamycin (17-AAG) binds to the ATP-binding region of Hsp90, inhibits Hsp90's ability to form multichaperone complexes, induces the degradation of its client proteins, thus altering downstream molecular signaling cascades. Intrathecal (IT) administration of the heat shock protein 90 inhibitor 17-AAG has been shown previously to potentiate the efficacy of morphine-induced antinociception while reducing or not changing opioid side effects, enabling a dose-reduction strategy. However, the signaling cascade and receptor-level mechanisms underlying the effects of 17-AAG remain to be entirely elucidated. In this study, we attempted to understand the cellular and circuit-level mechanisms of spinal cord Hsp90 inhibition in the context of morphine antinociception.

### *Materials and Methods*

### ***Drugs and CRISPR constructs***

17-AAG, Baclofen, Muscimol, CGP54626, and Bicuculline were stored under desiccation at -20°C, and stock solutions were prepared in DMSO, and also stored at -20°C. A matched Vehicle control for was included in every experiment; 0.02% DMSO in sterile USP water for the 0.01 nmol intrathecal injections and 10% DMSO, 10% Tween80, and 80% sterile USP saline for 1 mg/kg intravenous and 10 mg/kg oral injections. Morphine sulfate pentahydrate was obtained from the NIDA Drug Supply Program, stored at room temperature, and working solutions were made fresh prior to every experiment in sterile USP saline. USP saline injected controls were used for the reward and constipation assays below.

An all-in-one CRISPR DNA construct expressing Cas9 and a gRNA targeting GAT-2 (Slc6a13) were obtained from Genecopoeia (Rockville, MD). The DNA was amplified using standard molecular biology approaches, and complexed with TurboFect *in vivo* transfection reagent (Thermo Fisher, Waltham, MA) as described in our previous work [193] and by the manufacturer's protocol. The complexed DNA was injected into the mice by the intrathecal route (2 µg DNA in 5 µL) daily from days 1-3, with behavioral testing performed on day 10.

### ***Mice***

Male and female CD-1 mice in age-matched cohorts from 5–8 weeks of age were used for all behavioral experiments and were obtained from Charles River Laboratories (Wilmington, MA). CD-1 (a.k.a. ICR) mice are commonly used in opioid research as a line with a strong response to opioid drugs (*e.g.* [192], and our own previous Hsp90 research [181-184]). Mice were recovered for a minimum of 5 days after shipment before being used in experiments. Mice

were housed no more than 5 mice per cage and kept in an AAALAC-accredited vivarium at the University of Arizona under temperature control and 12-h light/dark cycles. All mice were provided with standard lab chow and water available *ad libitum*. The animals were monitored daily, including after surgical procedures, by trained veterinary staff. All experiments performed were in accordance with IACUC-approved protocols at the University of Arizona and by the guidelines of the NIH Guide for the Care and Use of Laboratory Animals. We also adhered to the guidelines of ARRIVE; no adverse events were noted for any of the animals.

### ***Behavioral experiments***

All animals were randomized to treatment groups by random assignment of mice in one cohort to cages, followed by random block assignment of cages to treatment group. Group sizes were based on previous published work from our lab using these assays [182, 184, 193, 194]. The mice were not habituated to handling. Prior to any behavioral experiment or testing, animals were brought to the testing room in their home cages for at least 1 h for acclimation. Testing always occurred within the same approximate time of day between experiments during the animal light (inactive) cycle, and environmental factors (noise, personnel, and scents) were minimized. All testing apparatus (cylinders, grid boxes, etc.) were cleaned between uses using 70% ethanol and allowed to dry. The experimenter was blinded to treatment group by another laboratory member delivering coded drug vials, which were then decoded after collection of all data. Naïve mice were used for every experiment, including each dose.

### ***Tail-flick assay***

Pre-injection tail-flick baselines were determined in a 52°C tail-flick assay with a 10-s cutoff time (method also reported in [181]). The mice were then injected with inhibitor or Vehicle control with a 24-hour treatment time. 24-hours post-injection baselines were determined. The mice were then injected s.c. with 1-10 mg/kg of morphine, and tail-flick latencies were determined over a 2-hour time course. For tolerance studies, baseline tail flick latencies were taken, and mice were then injected with inhibitor or Vehicle control with a 24-hour treatment time. 24 hours later mice were baselined again and then injected with 10 mg/kg s.c. morphine with one tail flick latency measured at 30 minutes post morphine. Mice were injected again with inhibitor or Vehicle and the process was repeated for an additional 7 days with twice daily morphine injection, and tail flick response measured after the morning injection. No animals were excluded from these studies.

### ***Intrathecal Injections***

Mice were acclimated in a lab setting for 30 minutes then placed under anesthesia (isoflurane, 5% induction, 2% maintenance). Once anesthetized, injections were made at the intervertebral space between L5-L6. A slight tail flick response was observed, indicating entry into the intradural space.

### ***Compounds***

Injection volumes consisted of 5uL of drug or vehicle. Compounds included .5nmoles 17-AAG (IT), .3umoles Nipectic Acid (IT), 20nmoles Muscimol (IT), 1.6nmoles Baclofen (IT), .01ug Bicuculline (IT), 10nmoles CGP54626 (IT), and 3.2mg/kg morphine (SC).

### ***General Experimental Design***

Male or female CD-1 mice were given 17-AAG intrathecally. 24 hours later, the mice were given the experimental compounds intrathecally followed twenty minutes later by subcutaneous administration of 3.2mg/kg morphine. Antinociception was measured using the tail flick/hot water bath assay over the course of 1.5-2 hours.

### ***Statistical analysis***

All data were reported as the mean  $\pm$  SEM and normalized where appropriate as described above. The behavioral data from each individual dose was reported raw without maximum possible effect (MPE) or other normalization. Technical replicates and further details are described in the Figure Legends. Statistical comparisons of individual dose/response curve time courses were performed using Repeated Measures 2-Way ANOVA with Sidak's *post hoc* tests. The Geisser-Greenhouse correction was used to account for a potential lack of sphericity of the data, permitting valid Repeated Measures ANOVA. ANOVA *post hoc* tests were only performed when ANOVA F values indicated a significant difference, and there was homogeneity of variance (permitting parametric analysis). In all cases, significance was defined as  $p < 0.05$ . The group sizes reported represent independent individual mice tested in each assay. All

graphing and statistical analyses were performed using GraphPad Prism 9.3. Approximately equal numbers of male and female mice were used for each experiment.

## *Results*

### ***Intrathecal Nipecotic Acid Blocks the 17-AAG Mediated Augment of Systemic Morphine Analgesia***

We first attempted to perturb the effect of 17-AAG on morphine analgesia pharmacologically. Based on the mass spectrometry data, it was unclear as to whether GAT-2 upregulation was directly involved in the signaling alterations in MOR activity, or an unrelated outcome of spinal 17-AAG administration. We hypothesized that GAT-2 was involved in mediating the enhancement of opioid antinociception induced by Hsp90 inhibition in the spinal cord. To elucidate this, we pharmacologically antagonized GAT-2 using nipecotic acid delivered to the spinal cord 2hr after 17-AAG administration and 10 minutes prior to systemic morphine delivery. Nipecotic acid is an antiepileptic drug that nonselectively and reversibly binds to the sodium and chloride dependent GABA reuptake transporter protein (Slc6a13). Surprisingly, we found that the nonselective GAT inhibitor, nipecotic acid, blocked the effect of 17-AAG (**Figure 18**). This suggested that downstream of Hsp90 inhibition, the upregulation of GAT-2 may be involved in mediating the enhancement of morphine potency in the spinal cord.

### ***CRISPR/Cas9 Mediated Knockdown of GAT-2 Shows Specific Involvement of GABA Reuptake in 17-AAG Mediated Enhanced Potency of Morphine***

Because nipecotic acid shows affinity for other GABA transporters within the same family, we utilized a custom CRISPR/Cas9 construct with three individual guides all targeting

regions of the Slc6a13 gene in order to specifically target and knock down GAT-2. CRISPR gRNA was grown and expanded in our lab and delivered using lipofection of 2 $\mu$ g intrathecally once daily for three days. On day nine, 17-AAG was administered intrathecally and tail flick assays were performed on day 10. We found a similar effect using the specific Slc6a13 knockout as we did with nipecotic acid. The knockout mice showed no enhancement of opioid analgesia compared to controls (**Figure 21**). This experiment revealed the specific involvement of GAT-2 in mediating the enhancement of opioid potency by 17-AAG. However, the GABAergic signaling mechanisms in the spinal cord are complex and a specific cell type or circuit was not apparent given the data. Whether downstream involvement of GABA<sub>A</sub> or GABA<sub>B</sub> receptors was unclear, which lead us to further attempt to characterize some of the interactions between GABA and morphine in the spinal cord.

### ***GABA-A and GABA-B Agonists Differentially Disrupt the Effect of 17-AAG in a Sex-Dependent Manner***

GABA is the predominating inhibitory neurotransmitter in the nervous system. It has three main families of receptor subtypes: GABA<sub>A</sub>, GABA<sub>B</sub>, and GABA<sub>C</sub>. GABA<sub>A</sub> receptors are ionotropic and conduct chloride anions upon ligand binding, producing hyperpolarization of neurons. GABA<sub>B</sub> receptors are G<sub>ai/o</sub> coupled metabotropic GPCRs. Since GABA reuptake transporters decrease synaptic levels of GABA, leading to disinhibition of downstream neurons, and GAT-2 is significantly upregulated after Hsp90 inhibition, we hypothesized the downstream effects of decreased GABA levels mediate an effect on post-synaptic GABA receptors. Thus, activation of GABA receptors in the circuitry wherein GAT-2 is upregulated after 17-AAG should block the effect of Hsp90 inhibition on morphine analgesia. In an attempt to characterize

the interplay between GABA receptor subtypes in the spinal cord on 17-AAG induced enhancement of morphine antinociception, we administered GABA<sub>A</sub> and GABA<sub>B</sub> agonists 24hrs after 17-AAG administration, and 10 minutes prior to morphine injections to inspect GABA receptor subtype differences in regulating the effects of Hsp90 inhibition. We found that both GABA<sub>A</sub> and GABA<sub>B</sub> agonists disrupted the effect of 17-AAG in male mice, but only the GABA<sub>A</sub> agonist Muscimol blocked the effect in females (**Figure 19**). This suggested that Hsp90 inhibition in the spinal cord is differentially modulated by GABA receptors in a sex-dependent manner.

#### ***GABA-A and GABA-B Antagonists Alter Opioid Signaling in the Spinal Cord in Male but Not Female Mice***

The previous results also suggested that GABA<sub>A</sub> and GABA<sub>B</sub> receptor distribution and function may be different between the sexes even outside of the context of Hsp90 inhibition. To test this, Muscimol and Baclofen were administered intrathecally 10 minutes before systemic morphine administration. To our surprise, both GABA<sub>A</sub> and GABA<sub>B</sub> antagonists enhanced the potency of morphine in naïve male mice, but neither had any effect on female mice. Sex differences in neurophysiology and pain sensation and perception are widely studied and many differences have been characterized (**Figure 20**). These results lend themselves to support our sex difference results in the context of Hsp90 inhibition in the spinal cord. To recapitulate, the effect of 17-AAG was disrupted by both GABA<sub>A</sub> and GABA<sub>B</sub> agonists, but only GABA<sub>A</sub> agonists affected female mice. Similarly, GABA<sub>A</sub> and GABA<sub>B</sub> antagonists affected opioid signaling in naïve male mice but did not affect female mice. Thus, there are intrinsic sex

differences in GABA circuit physiology in the context of opioid signaling, both with and without Hsp90 inhibition that remain to be fully elucidated.

### *Discussion*

The predominant pharmaceutical treatment for moderate to severe chronic pain is the administration of opioid analgesics, which are insufficient for most patients and possess myriad detrimental side effects [219]. Opioid drugs used in the treatment of pain are in desperate need of replacement due to their deleterious side effects. Individuals suffering from chronic pain can develop strong associations with the rewarding effects of opioids, creating dependence and addiction [220]. One strategy to avoid the side effects of opioids is the concomitant administration of painkillers with drugs that boost pain relief efficacy without boosting side effects, enabling a dose-reduction approach. This dose-reduction strategy augments the efficacy of the opioid while reducing unwanted side-effects such as addiction, tolerance, respiratory depression, and death. As mentioned above, we used mass spectrometry to find that spinal administration of 17-AAG causes an increase of GABA transporter 2 (GAT-2), a protein involved in the reuptake of the inhibitory neurotransmitter GABA (**Figure 17**). Interestingly, 17-AAG administration alone confers no measurable analgesia. To elucidate the role of GAT-2 in mediating the enhancement of morphine analgesia, 17-AAG treated male and female CD-1 mice were given a nonselective GAT inhibitor, Nipecotnic Acid (NA), in the tail flick pain assay. NA blocked the 17-AAG enhancement of morphine analgesia, suggesting that GAT-2 mediates 17-AAG's analgesic enhancement (**Figure 18**). Because NA nonspecifically targets other isoforms of GABA reuptake transporters, we used a custom CRISPR/Cas9 construct to specifically target

and knockdown (KD) the GAT-2 gene, *Slc6a13*. After treatment with the GAT-2 CRISPR or a negative control CRISPR construct, mice were then given 17-AAG or vehicle intrathecally. 24h later, all mice were given 3.2mg/kg morphine subcutaneously, and analgesia was measured in the tail flick/hot water bath assay. The experiment revealed that in GAT-2 KD mice, Hsp90 inhibition failed to increase the efficacy of morphine – confirming our pharmacological experiments with even more specificity (**Figure 19**).

These data taken together led us to hypothesize that an inhibitory interneuronal GABA circuit is present in the spinal cord which tonically reduces opioid analgesia and is disabled by Hsp90 inhibition and an increase in GAT-2 expression. The descending circuit described by Scherrer (2019) et al. is a likely candidate. To explore this further, mice were treated with spinally administered GABA receptor subtype (GABA-A or GABA-B) selective compounds prior to morphine administration (Baclofen or Muscimol). The GABA-A agonist reversed 17-AAG enhanced analgesia similar to NA, supporting our hypothesis. However, the GABA-B agonist reversed 17-AAG analgesia in males but not females, suggesting a sex-specific difference in GABA signaling in the spinal cord (**Figure 20**). We then tested naïve mice (no 17-AAG) with GABA-A or GABA-B antagonists alone before administering morphine (Bicuculline or CGP54626). Males showed enhanced morphine analgesia with either drug, supporting the GABA circuit hypothesis; however, neither drug had an impact on female mice, again suggesting mechanistic sex differences (**Figure 21**). Together, these findings show that a spinally administered Hsp90 inhibitor increases the pain-reducing effects of morphine by increasing the levels of GAT-2 in the spinal cord, likely decreasing GABA in synapses that inhibit circuitry conferring opioid analgesia.

We derive from these data that 17-AAG potentiation of opioid-induced antinociception is mediated by the sodium-and-chloride-dependent GABA transporter, GAT-2. Due to the inhibitory function of GABA, we further posit that GAT-2 decreases GABAergic signaling involved in an inhibitory brake on opioid antinociceptive circuitry. Immunohistochemistry can be performed in future experiments to characterize cells in the dorsal horn that exhibit the GAT-2 upregulation. This would provide us with the knowledge of what cell types upregulate GAT-2 expression after Hsp90 inhibition and how they relate to opioid and pain circuitry in the spinal cord. Additionally, conditional knockouts of GAT-2 in the identified cells in the dorsal horn may provide some cell-type insight into this circuitry.

It is our prediction that the circuit characterized by Scherer et al. (2018) is the circuit involved in these effects. However, it may be the case that the predicted neurons (Penk expressing GAD65+) in the dorsal horn are not the cell subtype wherein the alterations induced by Hsp90 inhibition are what confer the augmented opioid analgesia. If this is the case, additional cell subtypes in the dorsal horn can be visually and electrophysiologically characterized and therefore targeted and experimentally manipulated in future experiments. Another target to be investigated could be CGRP-expressing projection neurons, as they also transmit nociceptive signaling in the spinal cord to the brain. It is unlikely that no interneuronal cell type in the pain pathway reveals alterations after Hsp90 inhibition, given our behavioral pharmacology data. If this is the case, however, additional experimentation could be done in descending circuitry originating from the RVM that project to further downstream projections in the corticostriatal nociceptive pathway. These projections can be labeled, experimentally manipulated, and recorded from similarly, although an alternative transgenic model may be

necessary to do so. In any case, we have revealed a novel function of GAT-2 in the spinal cord as it relates to pain, analgesia, and Hsp90 inhibition.

## CHAPTER 4

### GENERAL DISCUSSION AND CONCLUSION

Pain continues to be an immense, worldwide problem that is predicted to worsen in the coming decades [242,5,10]. Opioids continue to be a useful but problematic treatment for acute and chronic pain states [274-278]. The combined estimated economic burden of pain conditions and opioid liabilities exceeds \$1 trillion, annually [20,285]. Fortunately, the promise of improving opioid therapies or generating alternatives to opioids has greatly increased in the past several decades [286]. Our previous research showed the promise of Hsp90 inhibition in the spinal cord in improving opioid therapy. However, due to the lack of specificity of 17-AAG and other nonselective Hsp90 inhibitors, routes of administration were limited, and off-target effects were likely. This led our lab to create Hsp90 isoform-selective inhibitors and to seek out further mechanistic understanding of how Hsp90 inhibition increases opioid potency. Our present research adds to this development with the Hsp90 isoform-selective inhibitors and the elucidation of a possibly novel circuit involved in their mechanisms.

#### *Isoform Selective Inhibitors*

These inhibitors confer enhanced opioid potency in several animal models of pain (e.g., acute thermal, post-operative, HIV-induced neuropathy) while reducing or unchanging opioid side effects. This allows for the possibility of human and animal patients to take lower doses of opioids while achieving the same relief or take higher doses of opioids and have a reduced risk

of side effects (e.g., constipation, reward, respiratory depression, tolerance). Overall, the specific Hsp90 inhibitors improve the therapeutic index of morphine. The characterization of these compounds shows that they exhibit high affinity for their targets, solubility, and bioavailability. Additionally, after investigating the mechanism by which Hsp90 inhibitors produce this effect, we found that the protein GAT-2 likely mediates this effect in the spinal cord by, hypothetically, decreasing synaptic GABA at tonically active GABAergic interneurons which project onto opioid neurons.

KU-32, the nonspecific Hsp90 inhibitor increased the potency of morphine by 1.9 fold in an acute thermal nociception assay, 2.8 fold in the post-surgical paw incision assay, and 3.5 fold in a model of HIV-induced peripheral neuropathy. Spinally administered KU-32 also rescued or attenuated the development of opioid tolerance in chronic opioid administration experiments and did not alter morphine-induced constipation or reward learning. The selective Hsp90 $\alpha$  inhibitor KUNA115, Hsp90 $\beta$  inhibitor KUNB106, and the Grp94 inhibitor KUNG65 all enhanced the potency of morphine in the thermal nociception assay when delivered intrathecally.

Confirmations of the role these proteins play in opioid antinociception were confirmed with specific CRISPR/Cas9 knockout of each before morphine administration, and similar enhancements to morphine potency were measured. KUNG65 showed a nanomolar affinity for Grp94 and significantly lower (73-fold or more) affinity for other Hsp90 isoforms. It also exhibited micromolar solubility and oral bioavailability. Importantly, when KUNG65 was delivered systemically, a similar enhancement of morphine potency was measured. After systemic administration, 1.9 fold shift was measured in the thermal nociception assay and a 2.2 fold shift was measured in the post-surgical model using KUNG65. After systemic

administration, KUNB106 exhibited similarly high affinity for Hsp90 $\beta$  over other isoforms, high distribution, and solubility and showed 3.3 and 2.5 fold shifts in the thermal nociception and post-surgical models of pain, respectively. Importantly, both systemic KUNG65 and KUNB106 rescued opioid tolerance and did not affect respiratory depression, despite the increased potency of morphine. To show that none of the small molecule compounds directly bind to the opioid receptors, competition radioligand binding assays were performed using human MOR, DOR, and KOR-expressing CHO cells. These experiments revealed that the compounds do not bind to the opioid receptors, at least up to 10 $\mu$ M concentrations. However, the question of how Hsp90 inhibition mechanistically leads to increased opioid potency remained in question.

### *GAT-2*

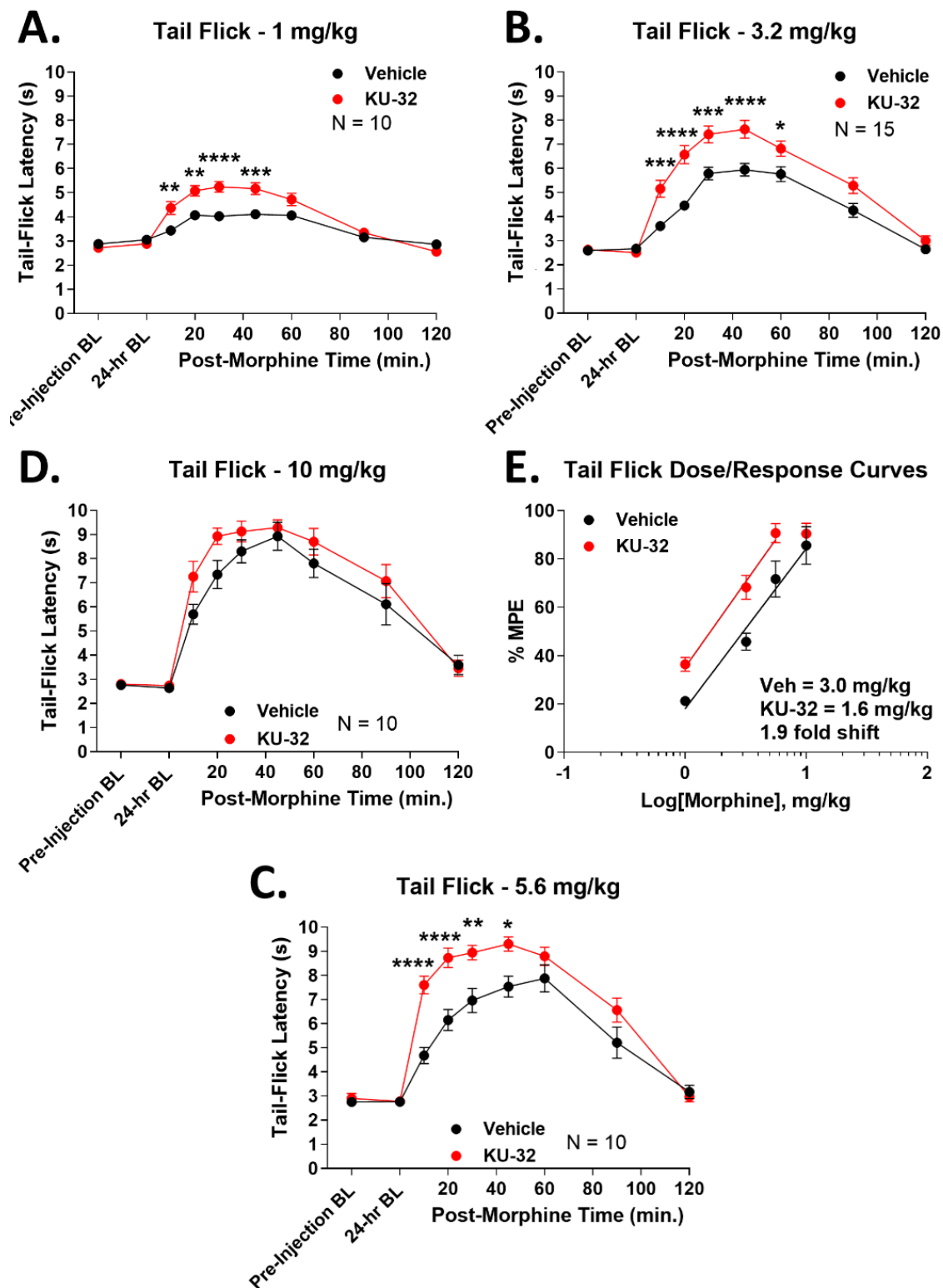
Our mechanistic investigation into Hsp90 inhibition first began with a proteomic analysis of spinal cord tissues treated with or without 17-AAG (a nonselective Hsp90 inhibitor). Mass spectrometry analyses revealed a 154-fold increase of GAT-2 in the 17-AAG condition compared to controls. This was a surprise, given that decreased GABA levels in the spinal cord are associated with hyperalgesia and allodynia. We hypothesized that, if GAT-2 was in the signaling pathway mediating the effect of 17-AAG, pharmacologically blocking GAT-2 in the spinal cord should prevent the increase in the potency of systemic morphine. We found just that. However, because of the lack of specificity of nipecotic acid, we decided to use a more specific approach and utilized a custom-designed CRISPR/Cas9 editing system to knockout GAT-2 in the spinal cord. After doing so, we treated the mice with 17-AAG and found that they resembled the control mice that were treated with a negative CRISPR control. This suggested that GAT-2 was

within the signaling pathway from Hsp90 to opioid potency. Since the GABA system is primarily comprised of GABA<sub>A</sub> and GABA<sub>B</sub> receptor subsystems, we attempted to distinguish between downstream receptor subtypes within this circuitry. To do this, we administered 17-AAG and subsequently added GABA<sub>A</sub> or GABA<sub>B</sub> agonists to block the effect of 17-AAG. We found sex-specific differences in the way opioid potency was modulated after 17-AAG by GABA receptor subtypes. While both GABA agonists prevented the increased opioid antinociception in males, only the GABA<sub>A</sub> agonist, Muscimol, prevented the effect in female mice. This led us to believe that perhaps the circuitry in naïve mice differs between the sexes, so we administered GABA<sub>A</sub> and GABA<sub>B</sub> antagonists along with morphine but no Hsp90 inhibitor and found that both antagonists enhanced the potency of morphine in the thermal nociception assay in male naïve mice, but neither did so in females. This suggested that the basic underlying circuitry involving GABA and opioid receptor systems differs at baseline between the sexes, and those effects extend into the context of Hsp90 inhibition. Further experiments elucidating the sex-dependent differences in GABA and opioid signaling in the spinal cord both at baseline and after Hsp90 inhibition remain to be performed. However, our work does show the involvement of GAT-2 in mediating Hsp90 inhibition-induced enhancement of opioid potency.

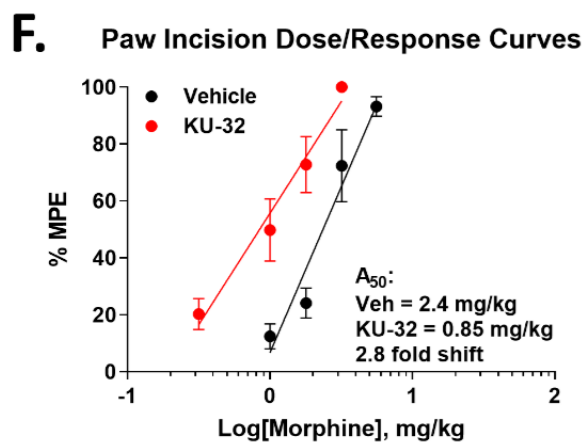
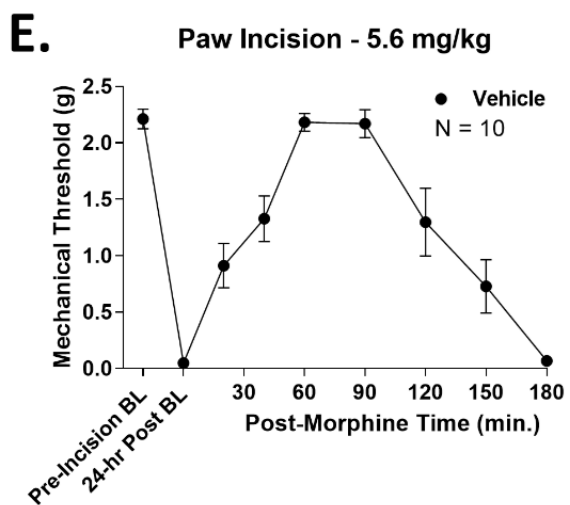
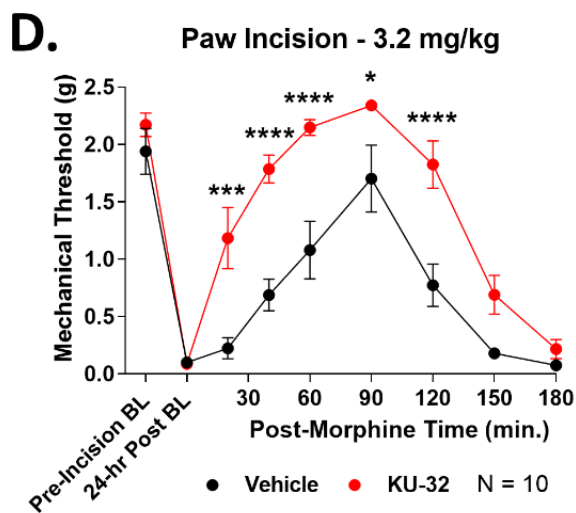
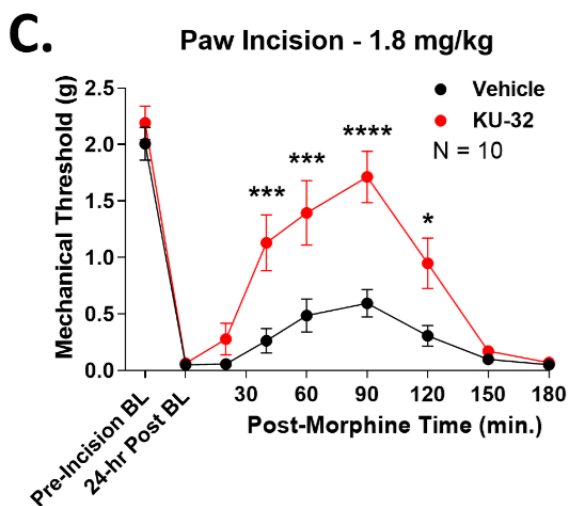
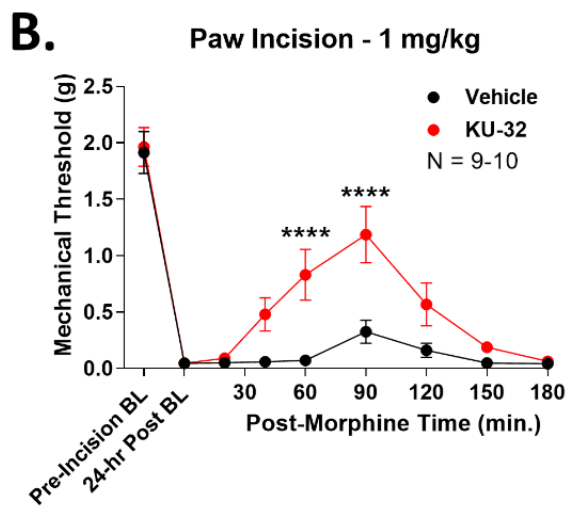
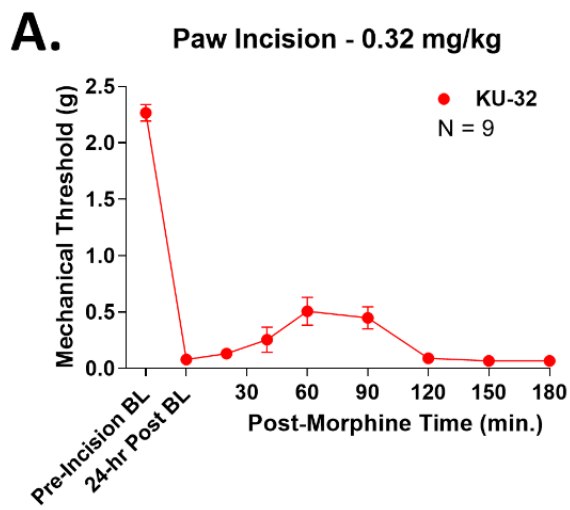
Yet, there is still more work to be done both at the translational and basic scientific levels. Understanding the toxicity of Hsp90 isoform inhibitors *in vivo* in dose-escalation experiments can be performed to determine effective dose ranges. *In vivo* experiments examining PD/PK will likely be performed in the near future to determine tolerability, tolerance, and toxicity. Furthermore, the molecular mechanisms of Hsp90 inhibition enhancing opioid analgesia need to be further characterized. In our lab, evidence continues to be produced that implicates

other molecules such as AKT, isoforms of PKC, and DUSP15. At the circuit level, the role of GABA and GAT-2 remain to be fully characterized. Experiments utilizing microdialysis, immunohistochemistry, and conditional CRISPR/Cas9 knockouts can greatly improve the resolution at which this circuitry is understood, and thus, provide greater insight into potential therapeutic targets for improving opioid therapy.

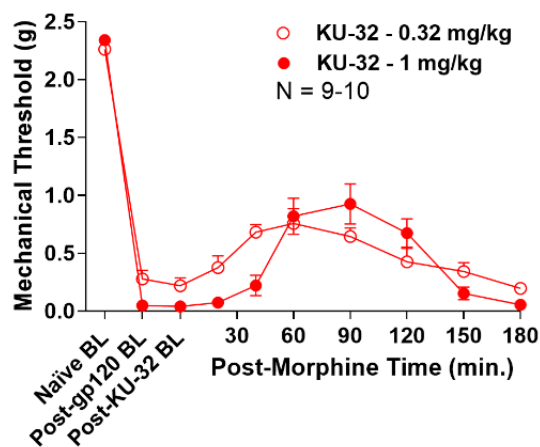
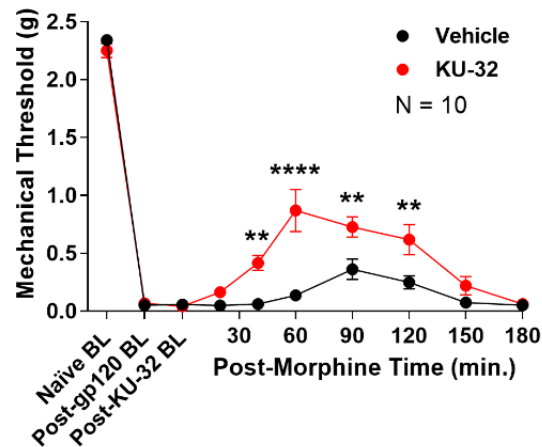
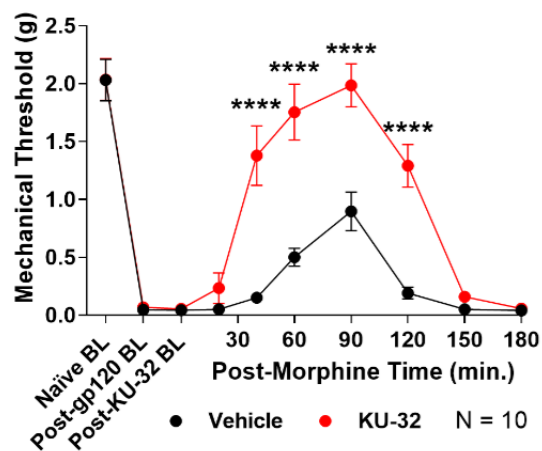
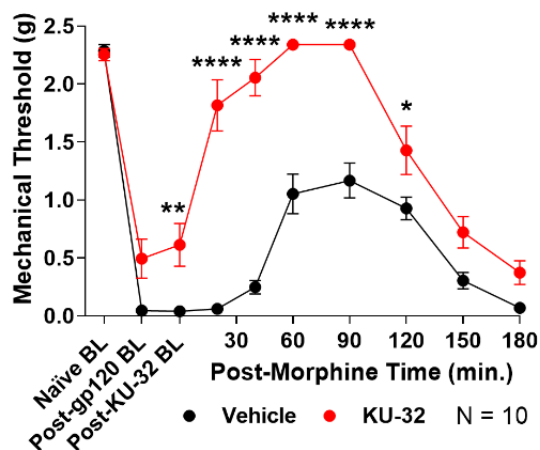
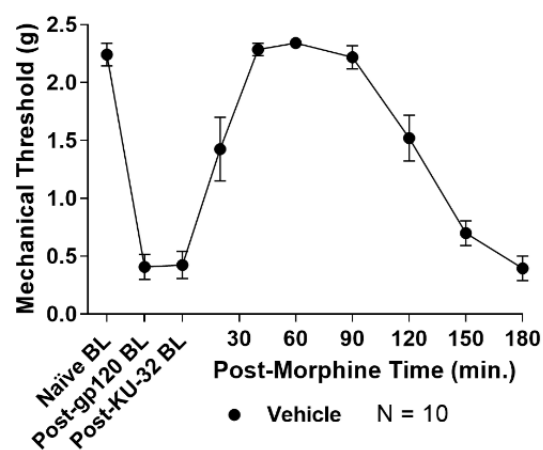
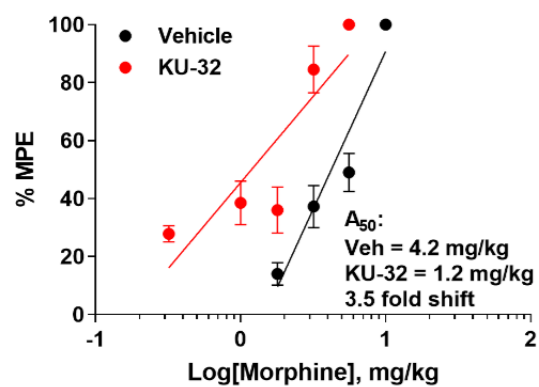
## Figures



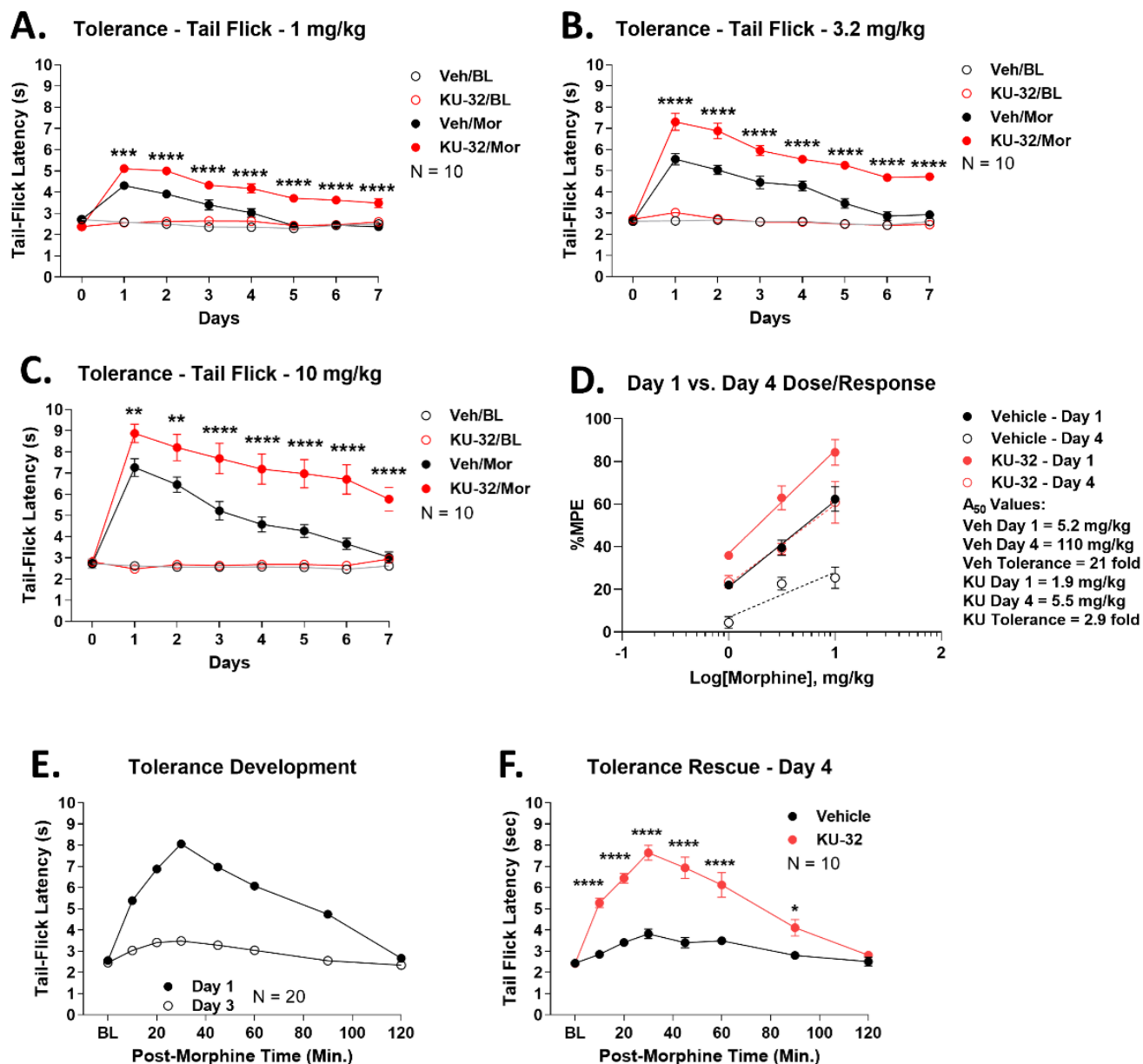
**Figure 1: Spinal Hsp90 inhibition increases morphine potency in acute heat-induced tail flick.** Male and female CD-1 mice were injected i.t. with 0.01 nmol KU-32 or Vehicle control, 24 hours, then 1-10 mg/kg morphine, s.c. Tail flick responses were recorded at 52°C with a 10 sec cutoff. Data reported as the mean  $\pm$  SEM, with sample sizes of mice/group noted in each graph. 2-3 technical replicates were performed per dose. \*, \*\*, \*\*\*, \*\*\*\* =  $p < 0.05, 0.01, 0.001, 0.0001$  vs. same time point Vehicle group by RM 2 Way ANOVA with Sidak's *post hoc* test. **A-D)** Individual dose curves shown as noted. Data not normalized. **E)** Dose/response analysis performed for individual curves, normalized as %MPE (baseline vs. 10 sec cutoff).  $A_{50}$ : Vehicle = 3.0 (2.5 – 3.7) mg/kg; KU-32 = 1.6 (1.3 – 2.0) mg/kg; 1.9 fold increase in potency (Data collected by KC, DD, PB).



**Figure 2: Spinal Hsp90 inhibition increases morphine potency in acute post-surgical paw incision pain.** Male and female CD-1 mice had the paw incision surgery performed, then were injected i.t. with 0.01 nmol KU-32 or Vehicle control, 24 hours, then 0.32-5.6 mg/kg morphine, s.c. Paw withdrawal responses recorded using von Frey filaments, including pre- and post-surgical baselines, validating the pain state. Data reported as the mean  $\pm$  SEM, with sample sizes of mice/group noted in each graph. 2 technical replicates were performed per dose. \*, \*\*\*, \*\*\*\* =  $p < 0.05$ , 0.001, 0.0001 vs. same time point Vehicle group by RM 2 Way ANOVA with Sidak's *post hoc* test. **A-E)** Individual dose curves shown as noted. Data not normalized. Vehicle at 0.32 mg/kg and KU-32 at 5.6 mg/kg were not measured since these would be too low (Vehicle) or hit the assay threshold (KU-32), meaning they would not fit the linear dose/response model used. **F)** Dose/response analysis performed for individual curves, normalized as %MPE (baseline vs. 2.34 g cutoff).  $A_{50}$ : Vehicle = 2.4 (2.0 – 2.8) mg/kg; KU-32 = 0.85 (0.64 – 1.1) mg/kg; 2.8 fold increase in potency (Data collected by KC, DD, PB).

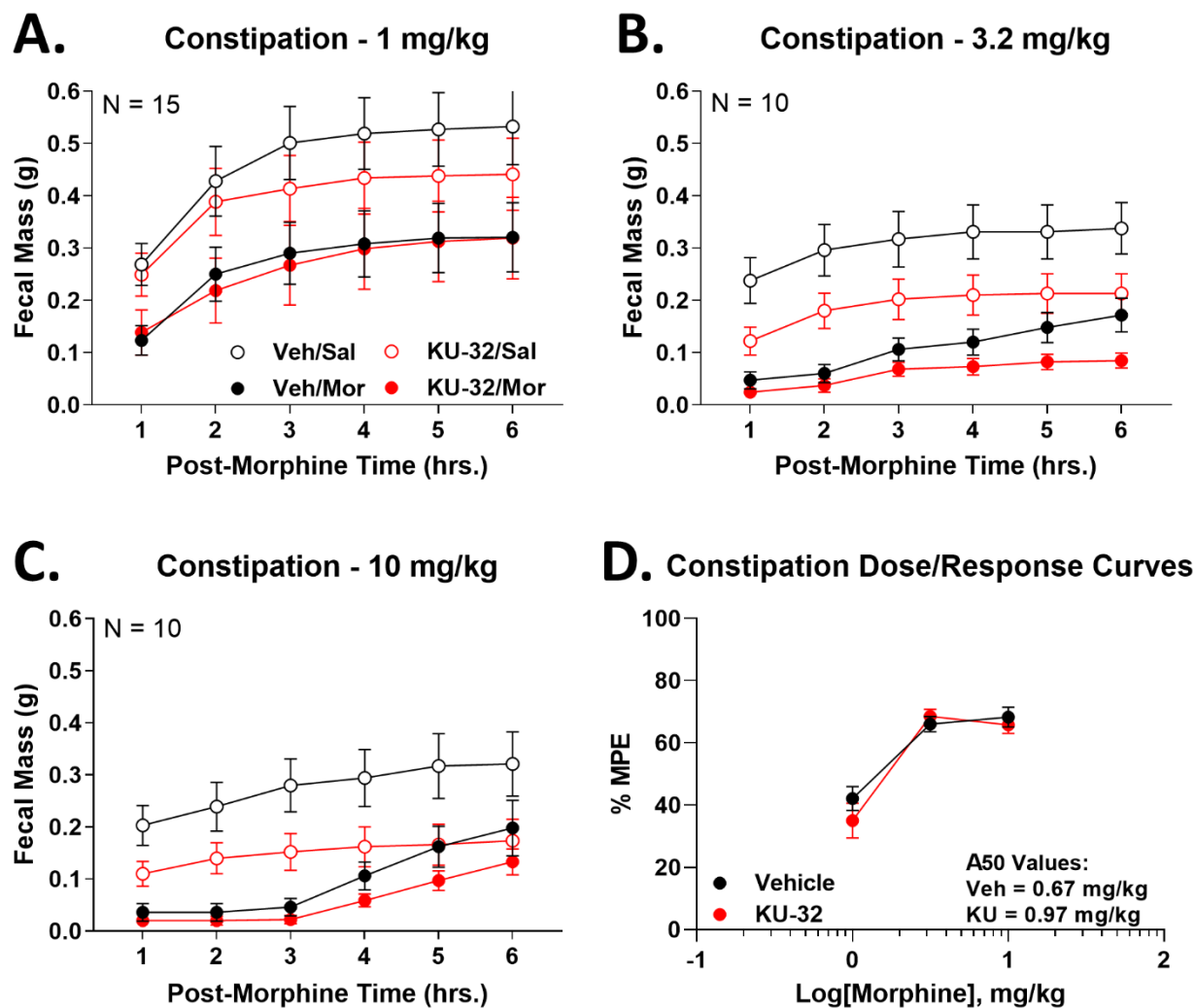
**A. HIV Neuropathy - 0.32 - 1 mg/kg****B. HIV Neuropathy - 1.8 mg/kg****C. HIV Neuropathy - 3.2 mg/kg****D. HIV Neuropathy - 5.6 mg/kg****E. HIV Neuropathy - 10 mg/kg****F. HIV Dose/Response Curves**

**Figure 3: Spinal Hsp90 inhibition increases morphine potency in chronic HIV neuropathy pain.** Male and female CD-1 mice were injected i.t. with gp120 protein on days 1, 3, and 5 (see Methods). On day 20, mice were injected i.t. with 0.01 nmol KU-32 or Vehicle control, 24 hours, then 0.32-10 mg/kg morphine, s.c. Paw withdrawal responses recorded using von Frey filaments, including pre- and post-treatment baselines, validating the pain state. Data reported as the mean  $\pm$  SEM, with sample sizes of mice/group noted in each graph. 2 technical replicates were performed per dose. \*, \*\*, \*\*\*\* =  $p < 0.05, 0.01, 0.0001$  vs. same time point Vehicle group by RM 2 Way ANOVA with Sidak's *post hoc* test. **A-E)** Individual dose curves shown as noted. Data not normalized. Vehicle at 0.32-1 mg/kg and KU-32 at 10 mg/kg were not measured since these would be too low (Vehicle) or hit the assay threshold (KU-32), meaning they would not fit the linear dose/response model used. **F)** Dose/response analysis performed for individual curves, normalized as %MPE (baseline vs. 2.34 g cutoff).  $A_{50}$ : Vehicle = 4.2 (3.7 – 4.8) mg/kg; KU-32 = 1.2 (0.87 – 1.5) mg/kg; 3.5 fold increase in potency (Data collected by KC, DD, PB).



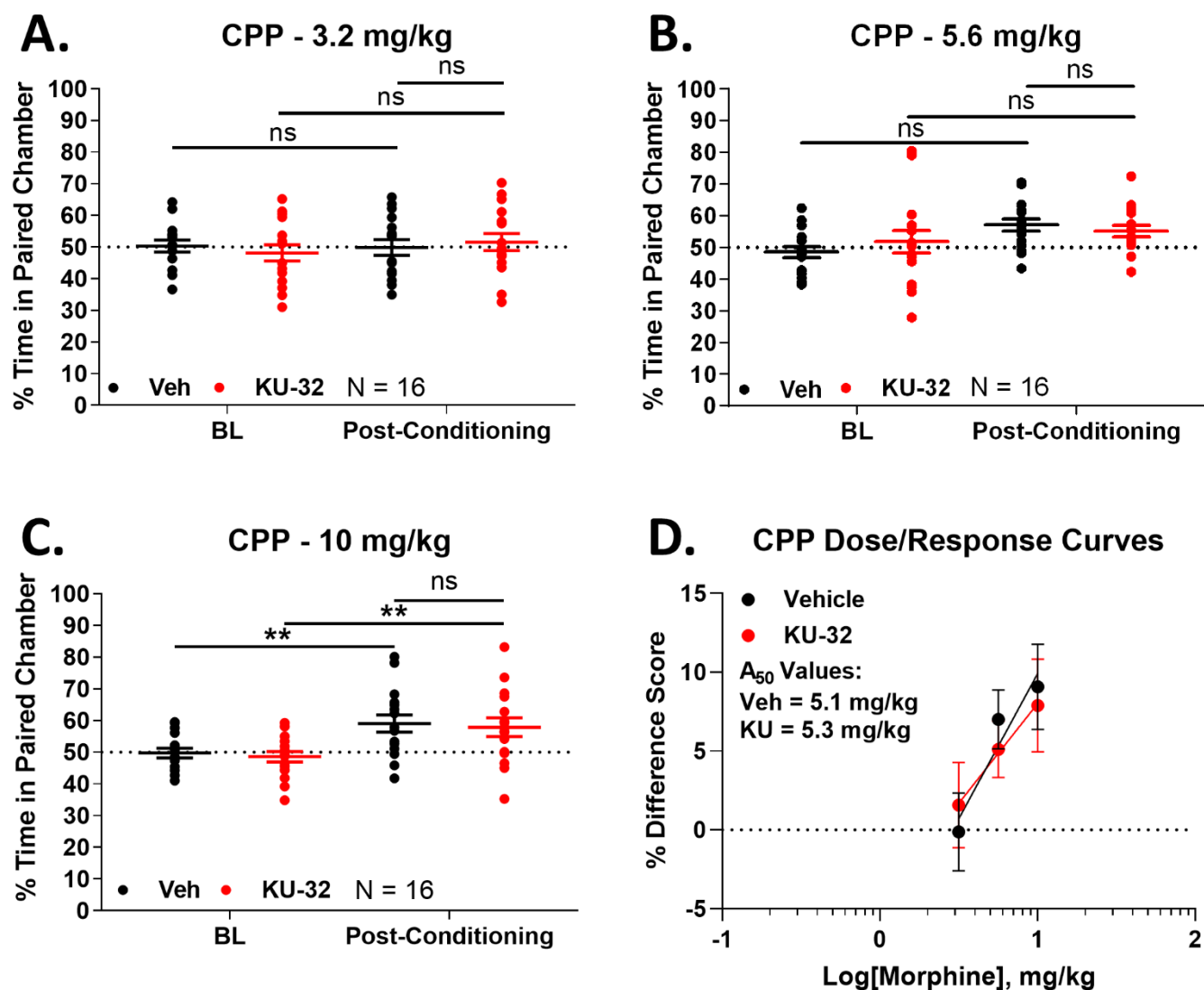
**Figure 4: Spinal Hsp90 inhibition reduces morphine anti-nociceptive tolerance and rescues established tolerance.** Data reported as the mean  $\pm$  SEM with sample sizes of mice/group noted in the graphs. A-C) Male and female CD-1 mice injected with 0.01 nmol KU-32 or Vehicle control i.t. beginning on day 0 and continuing daily until day 6. The mice were injected with 1-10 mg/kg morphine s.c. twice daily beginning on day 1 and continuing daily until day 7. Thermal

tail flick latencies (52°C, 10 sec cutoff) were recorded before treatment on day 0, daily before morphine injection (“BL”), and 30 minutes after each morning morphine injection on days 1-7. \*\*, \*\*\*, \*\*\*\* =  $p < 0.01, 0.001, 0.0001$  vs. same time point Veh/Mor group by RM 2 Way ANOVA with Tukey’s *post hoc* test. Individual dose/time curves shown as labeled. KU-32 treatment caused consistent elevation over Vehicle treatment over the 7 day period in all doses. Data not normalized. **D)** Day 1 vs. Day 4 dose/response analysis performed with the data from **A-C**. Data normalized to %MPE (baseline vs. 10 sec cutoff).  $A_{50}$ : Vehicle Day 1 = 5.2 (3.9 – 7.5) mg/kg, Vehicle Day 4 = 110 (30 – 6300) mg/kg, 21 fold shift; KU-32 Day 1 = 1.9 (1.3 – 2.5) mg/kg, KU-32 Day 4 = 5.5 (3.5 – 12) mg/kg, 2.9 fold shift. **E)** Male and female mice treated with twice daily morphine (10 mg/kg, s.c.) for 3 days to establish tolerance in all mice. Tail flick responses shown on day 1 (acute morphine) and day 3 (morphine-tolerant). **F)** On day 3, after measuring the tail flick time course, the mice were injected with 0.01 nmol KU-32 or Vehicle control, i.t., with a 24 hour recovery. On day 4, the mice were injected again with 10 mg/kg morphine, s.c., and a tail-flick time course performed. Experiment performed in 2 technical replicates. \*, \*\*\*\* =  $p < 0.05, 0.0001$  vs. same time point Vehicle group by RM 2 Way ANOVA with Sidak’s *post hoc* test. The KU-32 treated mice, previously tolerant on day 3, showed a statistically significant increase in morphine anti-nociception when compared to Vehicle (Data collected by KC, DD, PB).



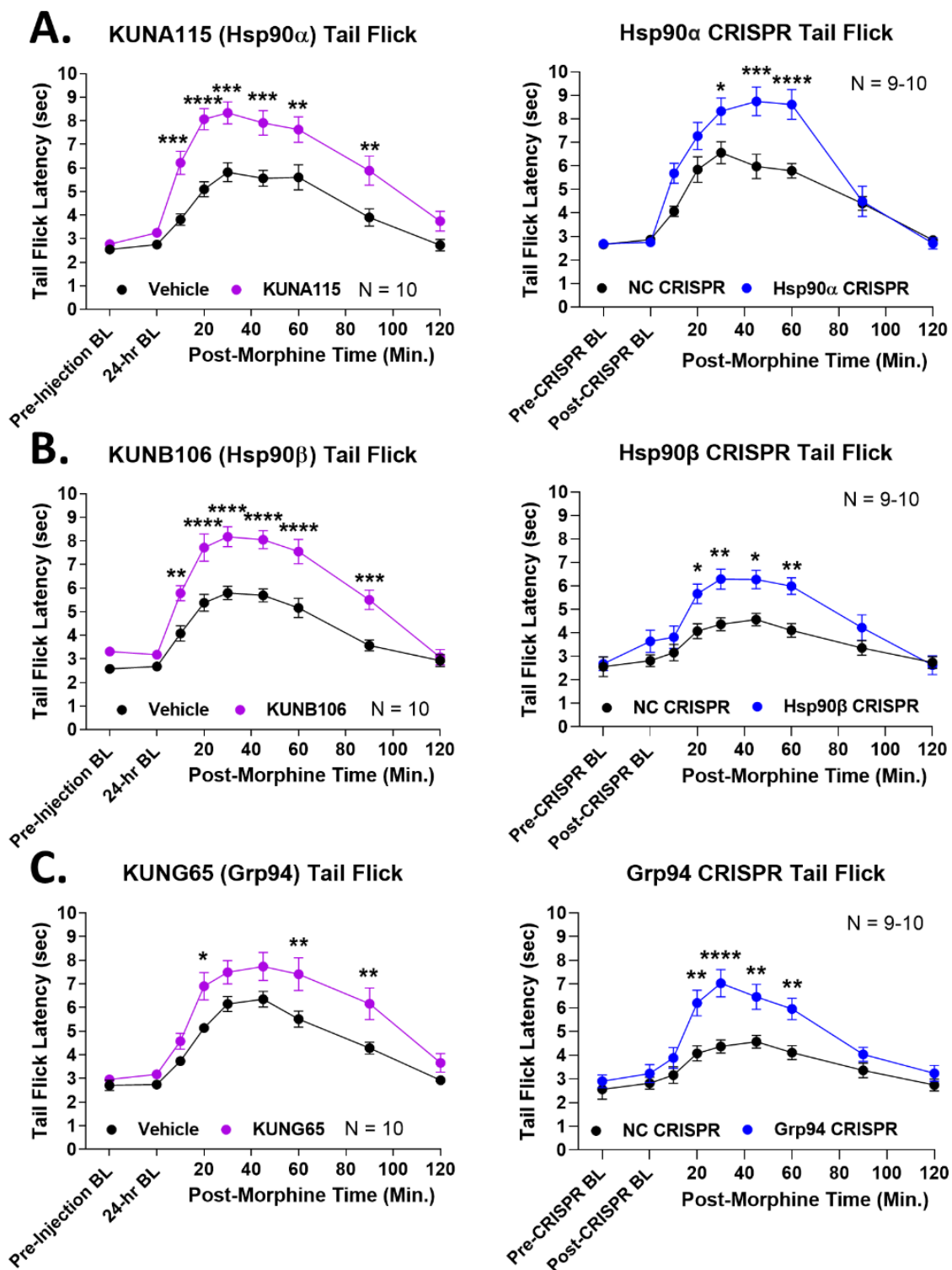
**Figure 5: Spinal Hsp90 inhibition does not alter morphine-induced constipation.** Male and female CD-1 mice treated with 0.01 nmol KU-32 or Vehicle control i.t., 24 hours, followed by 1-10 mg/kg morphine, s.c. Fecal mass was measured over 6 hours post-morphine, and used to construct cumulative plots. Curves for morphine as well as saline-injected controls shown. Data reported as the mean  $\pm$  SEM with the sample size of mice/group noted in the graphs. Experiments performed in 2-3 technical replicates. A-C) Individual dose curves reported, along with saline-injected controls. KU-32 treated saline or morphine groups were not statistically different from Vehicle saline or morphine injected groups, respectively, at any time point ( $p >$

0.05). **D)** Morphine injected animals were normalized to saline injected controls for each treatment group (Vehicle or KU-32) and used to construct dose/response curves. The 6 hour area under the curve (AUC) data from **A-C** was further normalized to %MPE (100% MPE = 0% fecal production/100% constipation). Only the 1 and 3.2 mg/kg dose curves were used to calculate the  $A_{50}$  since the dose response plateaus between 3.2-10 mg/kg.  $A_{50}$ : Vehicle = 0.67 (0.32 – 0.94) mg/kg; KU-32 = 0.97 (0.59 – 1.3) mg/kg (Data collected by KC, DD, PB).

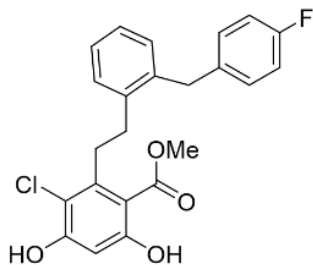


**Figure 6: Spinal Hsp90 inhibition does not alter reward learning.** Male and female mice were treated over 4 days with KU-32 or Vehicle treatment i.t., combined with 3.2-10 mg/kg morphine, s.c. as a conditioned place preference (CPP) stimulus (see Methods). On day 5, paired chamber preference was recorded. Data reported as the mean  $\pm$  SEM with the sample size of mice/group noted in the graphs. Each dose performed in 2 technical replicates. \*\* =  $p < 0.01$  vs. same treatment Baseline (BL) by RM 2 Way ANOVA with Tukey's *post hoc* test. A-C) The individual doses are shown. There was a trend to increasing preference with increasing dose that

reached significance over baseline at 10 mg/kg for both Vehicle and KU-32 treatment. There was no difference between Vehicle and KU-32 treatment ( $p > 0.05$ ). **D)** Dose/response analysis was performed, with the data reported as the % Difference Score (see Methods). For the purposes of  $A_{50}$  calculation, the response at 10 mg/kg in Vehicle-treated mice was considered to be a maximal response, since 100% preference is not possible in this assay.  $A_{50}$ : Vehicle = 5.1 (2.7 – 7.7) mg/kg; KU-32 = 5.3 ( $-\infty$  -  $+\infty$ ) mg/kg (Data collected by KC, DD, PB).



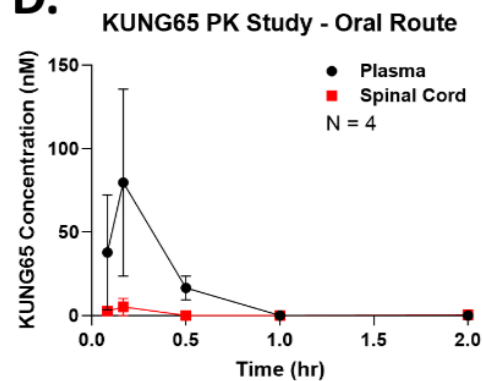
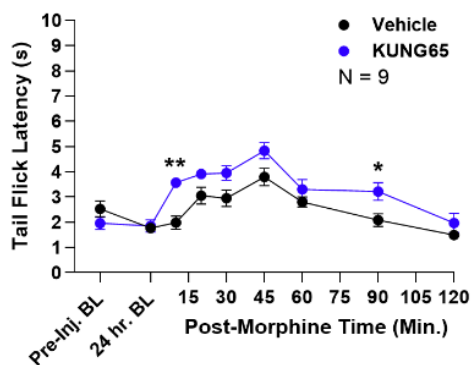
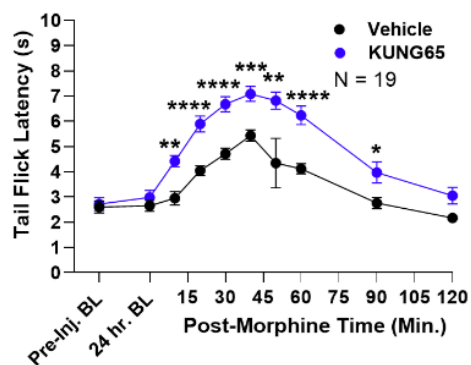
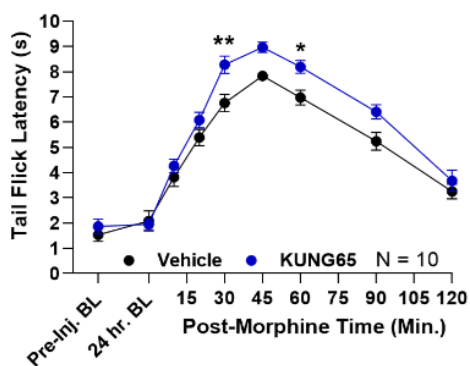
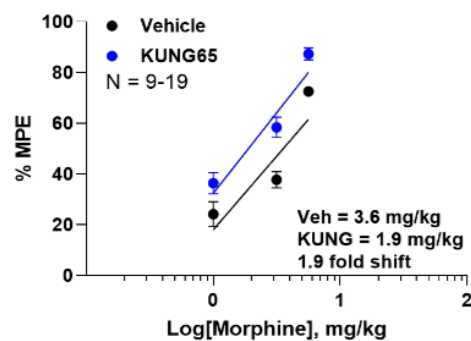
**Figure 7: Identification of spinal-cord specific Hsp90 isoforms that regulate opioid anti-nociception.** Male and female CD-1 mice were treated with 0.01 nmol of isoform-selective inhibitor or Vehicle control i.t. with a 24 hr treatment time; or with an isoform-selective CRISPR knockdown construct or universal negative control CRISPR construct (NC) with a 10 day treatment time (see Methods). Pre- and post-treatment baselines were recorded using the 52°C tail flick assay (as above), as well as tail flick timecourses in response to 3.2 mg/kg morphine s.c.. Data are presented as the mean  $\pm$  SEM with the sample size of mice/group noted in each graph. Each experiment was completed in 2 technical replicates. \*, \*\*, \*\*\*, \*\*\*\* =  $p < 0.05$ , 0.01, 0.001, 0.0001 vs. same time point Vehicle/NC group by 2 Way RM ANOVA with Sidak's *post hoc* test. **A)** The Hsp90 $\alpha$  isoform targeted with the selective inhibitor KUNA115 as well as selective CRISPR. **B)** The Hsp90 $\beta$  isoform targeted with the selective inhibitor KUNB106 as well as selective CRISPR. **C)** The Grp94 isoform targeted with the selective inhibitor KUNG65 as well as selective CRISPR. Both methods caused significant anti-nociceptive elevation for all 3 isoforms, confirming that all 3 isoforms regulate opioid anti-nociception in the spinal cord (Data collected by KC, DD, PB).

**A.****B.**

Isoform	KUNG65 $K_D$ (nM)
Grp94	540
Hsp90 $\alpha$	39,200 (73X)
Hsp90 $\beta$	>40,000
TRAP1	>40,000

**C.**

Property	KUNG65
LogD	3.30
Solubility ( $\mu$ M)	0.074
HLM $T_{1/2}$ (min.)	144
MLM $T_{1/2}$ (min.)	32

**D.****E. KUNG65 (IV) Tail Flick 1 mg/kg****KUNG65 (IV) Tail Flick 3.2 mg/kg****KUNG65 (IV) Tail Flick 5.6 mg/kg****F. KUNG65 Dose Response Curve**

**Figure 8: Systemic Grp94 inhibition enhances morphine anti-nociception.** **A)** Chemical structure of KUNG65. **B)** The affinity ( $K_D$ ) of KUNG65 for each Hsp90 isoform is shown; KUNG65 has a minimum selectivity of 73 fold vs. other isoforms (data taken from [49]). **C)** *In vitro* ADME parameters for KUNG65 are shown (see Methods). HLM/MLM = human/mouse liver microsomes;  $T_{1/2}$  = half-life. **D)** A pharmacokinetic (PK) study with KUNG65 was performed, dosed at 10 mg/kg by the oral (p.o.) route in male and female CD-1 mice (see Methods). Data presented as the mean  $\pm$  SEM, with the sample size of mice/group noted in the graphs, performed in one technical replicate. The KUNG65 is detectable in both plasma and spinal cord, with peak concentrations of 79.7 nM and 5.2 nM, respectively. The drug is undetectable past 30-60 minutes, so PK parameters could not be calculated (half-life, etc.) but the results are sufficient to show that the drug has systemic exposure and blood-brain barrier penetration with oral dosing. **E)** Male and female CD-1 mice treated with KUNG65 (1 mg/kg) or Vehicle injected i.v. with a 24 hr treatment time, followed by 1 – 5.6 mg/kg morphine, s.c., with tail flick time courses performed. Data presented as the mean  $\pm$  SEM, with the sample size of mice/group noted in the graphs, performed in 2 - 4 technical replicates. \*, \*\*, \*\*\*, \*\*\*\* =  $p < 0.05, 0.01, 0.001, 0.0001$  vs. same time point Vehicle group by 2 Way RM ANOVA with Sidak's *post hoc* test. Morphine anti-nociception is consistently elevated, similar to the results with direct spinal inhibition above in **Figure 1**. **F)** The data was transformed into %MPE and used to construct dose/response curves. Vehicle = 3.6 (2.9 – 4.6) mg/kg, KUNG65 = 1.9 (1.4 – 2.3) mg/kg; 1.9 fold improvement in morphine potency (Data collected by KC, DD, PB).

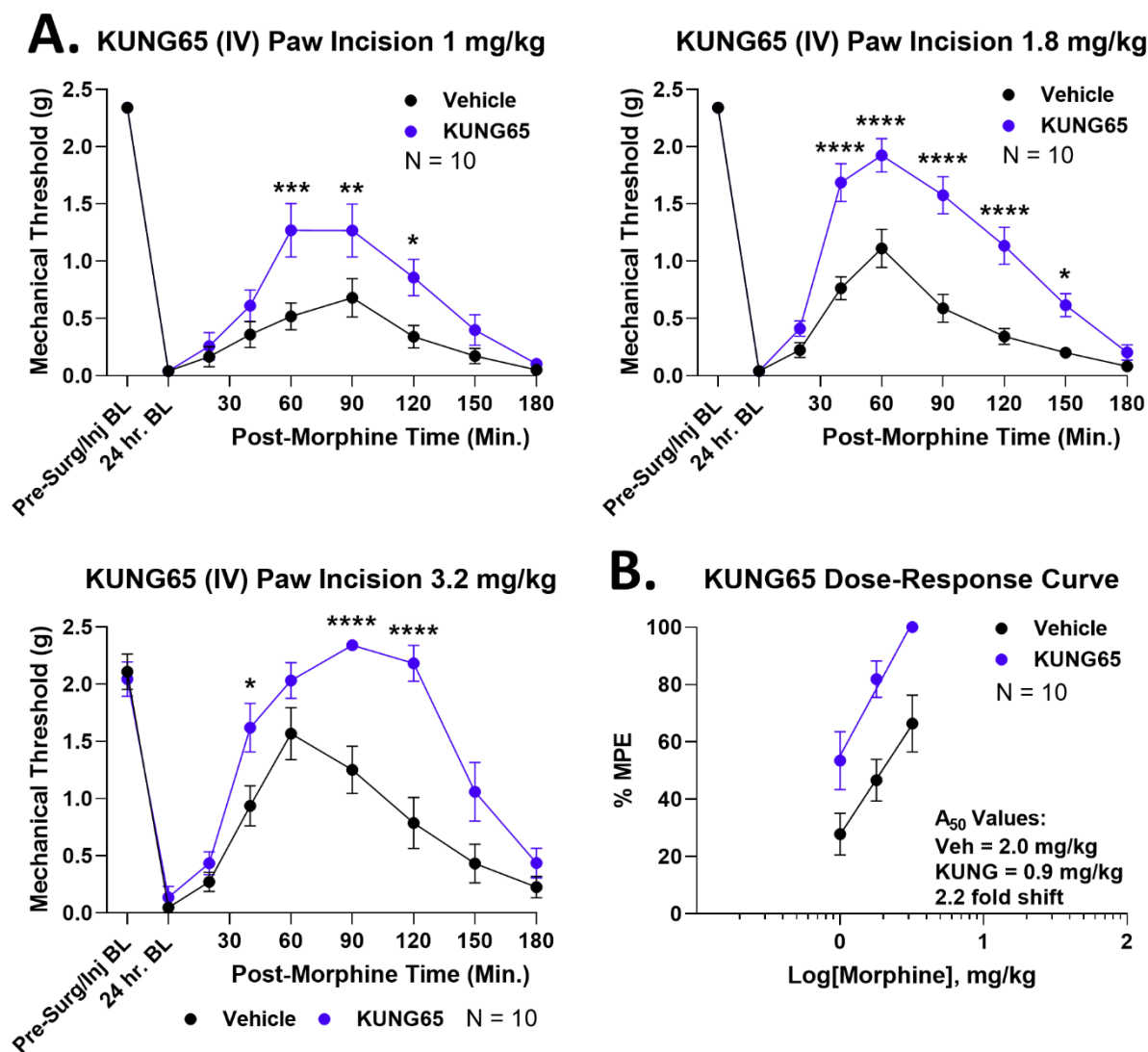
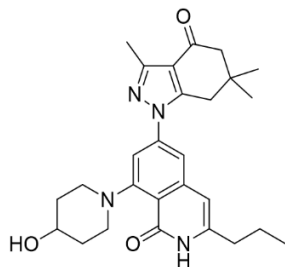


**Figure 9: Systemic Grp94 inhibition enhances morphine anti-nociception in paw incision pain.** Male and female CD-1 mice treated with paw incision surgery and 1 mg/kg KUNG65 or Vehicle control i.v., 24 hrs, followed by 1 – 3.2 mg/kg s.c. morphine and a Von Frey mechanical allodynia timecourse performed. Data presented as the mean  $\pm$  SEM, with sample sizes of mice/group noted in each graph; experiments performed in 2 technical replicates per dose. **A)** Individual dose curves shown (no transformation). \*, \*\*, \*\*\*, \*\*\*\* =  $p < 0.05$ , 0.01, 0.001, 0.0001 vs. same time point Vehicle group by 2 Way RM ANOVA with Sidak's *post hoc* test. KUNG65 treatment consistently elevated anti-nociception. **B)** Data transformed into %MPE and

used to construct dose/response curves.  $A_{50}$ : Vehicle = 2.0 (1.4 – 3.0) mg/kg, KUNG65 = 0.9 (0.5 – 1.2) mg/kg; 2.2 fold improvement in morphine potency (Data collected by KC, DD, PB).

A.



B.

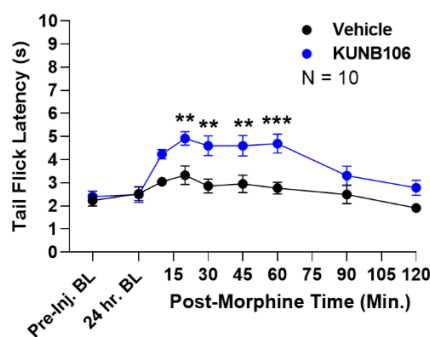
Isoform	KUNB106 K <sub>D</sub> (nM)
Hsp90β	91 ± 10
Hsp90α	38,000 ± 1,100
Grp94	>25,000
Trap1	>25,000

C.

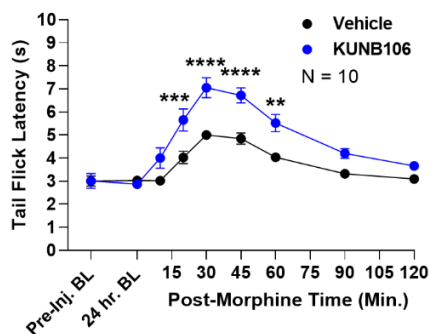
Property	KUNB106
LogD	2.26
Solubility (μM)	0.014
HLM T <sub>1/2</sub> (min.)	156
MLM T <sub>1/2</sub> (min.)	63

D.

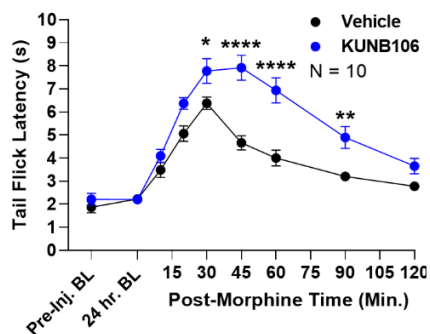
KUNB106 (IV) Tail Flick 1 mg/kg



KUNB106 (IV) Tail Flick 3.2 mg/kg



KUNB106 (IV) Tail Flick 5.6 mg/kg



E. KUNB106 Dose-Response Curve

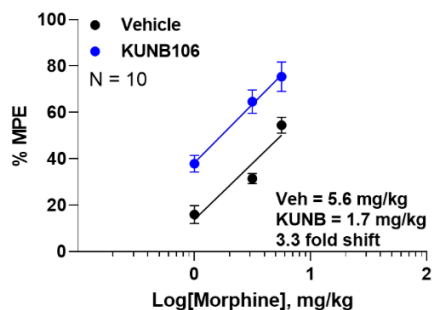


**Figure 10: Systemic Hsp90 $\beta$  inhibition enhances morphine anti-nociception.** **A)** Chemical structure of the Hsp90 $\beta$ -selective inhibitor KUNB106. **B)** Affinity ( $K_D$ ) of KUNB106 for each Hsp90 isoform, showing a minimum selectivity of 275 fold (data taken from [22]). **C)** *In vitro* ADME parameters for KUNB106 are shown (see Methods). HLM/MLM = human/mouse liver microsomes;  $T_{1/2}$  = half-life. **D)** Male and female CD-1 mice were treated with 1 mg/kg KUNB106 or Vehicle i.v., 24 hrs, followed by 1 – 5.6 mg/kg morphine s.c. and tail flick timecourses recorded. Data shown as the mean  $\pm$  SEM, with the sample size of mice per group noted in each graph, completed in 2 technical replicates. \*, \*\*, \*\*\*, \*\*\*\* =  $p < 0.05, 0.01, 0.001, 0.0001$  vs. same time point Vehicle group by 2 Way RM ANOVA with Sidak's *post hoc* test. KUNB106 caused increased anti-nociception over the whole morphine dose range. **E)** Dose-response curves generated from the data in **D**, after transformation to %MPE.  $A_{50}$ : Vehicle = 5.6 (4.4. -  $\infty$ ) mg/kg, KUNB106 = 1.7 (1.1 – 2.3) mg/kg; 3.3 fold increase in morphine potency (Data collected by KC, DD, PB).

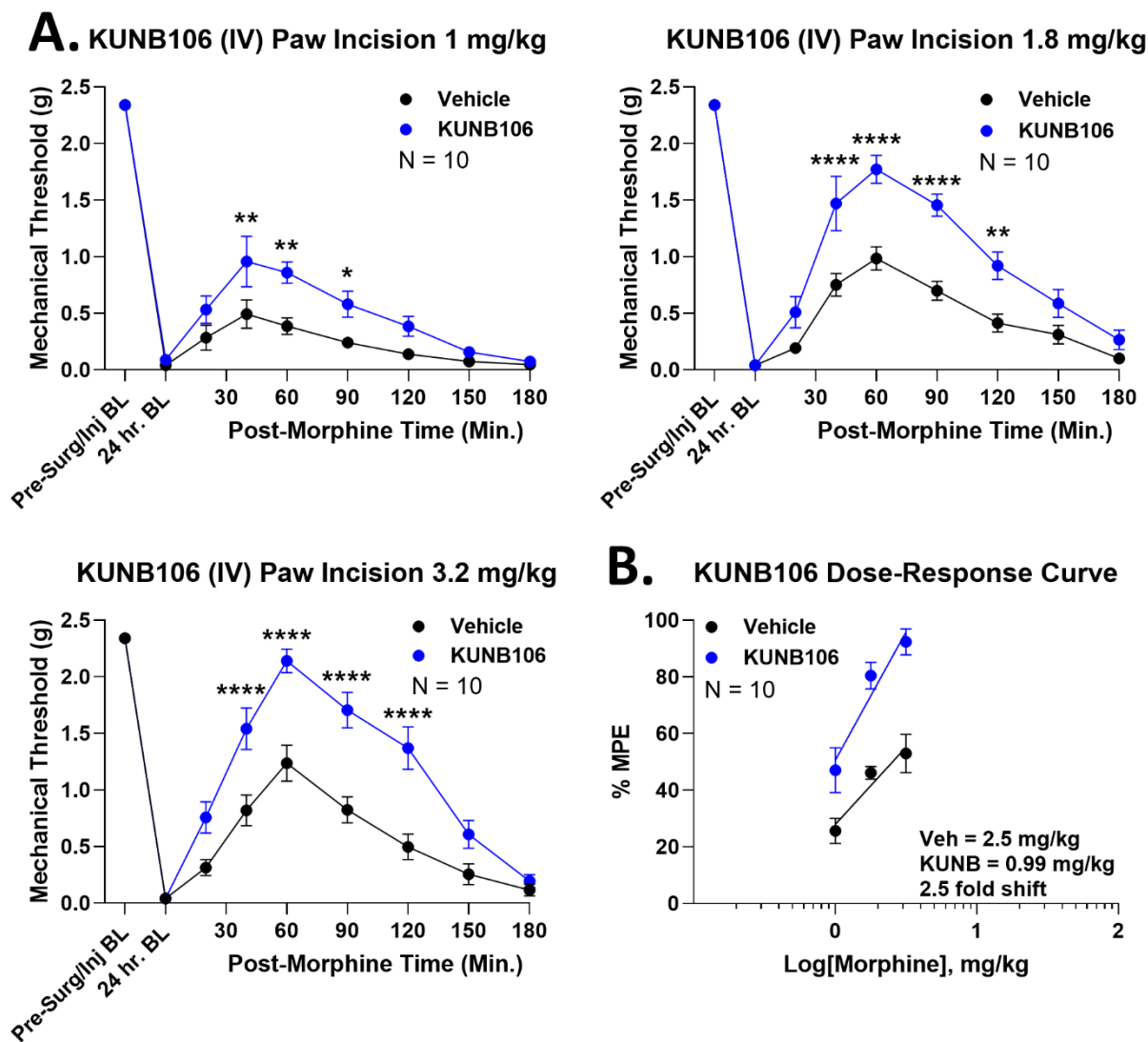


**Figure 11: Systemic Hsp90 $\beta$  inhibition enhances morphine anti-nociception in paw incision pain.** Male and female CD-1 mice treated with paw incision surgery and 1 mg/kg KUNB106 or Vehicle control i.v., 24 hrs, followed by 1 – 3.2 mg/kg s.c. morphine and a Von Frey mechanical allodynia timecourse performed. Data presented as the mean  $\pm$  SEM, with sample sizes of mice/group noted in each graph; experiments performed in 2 technical replicates per dose. **A)** Individual dose curves shown (no transformation). \*, \*\*, \*\*\*\* =  $p < 0.05, 0.01, 0.0001$  vs. same time point Vehicle group by 2 Way RM ANOVA with Sidak's *post hoc* test. KUNB106 treatment consistently elevated anti-nociception. **B)** Data transformed into %MPE and used to

construct dose/response curves.  $A_{50}$ : Vehicle = 2.5 (2.0 –  $\infty$ ) mg/kg, KUNB106 = 0.99 ( $\infty$  –  $\infty$ ) mg/kg; 2.5 fold improvement in morphine potency (Data collected by KC, DD, PB).

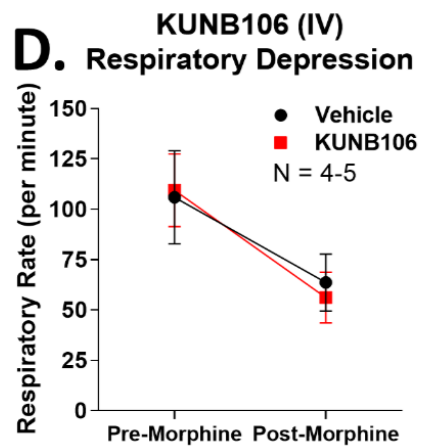
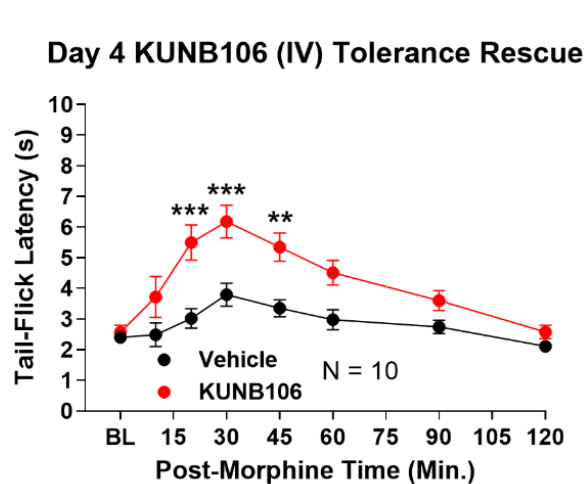
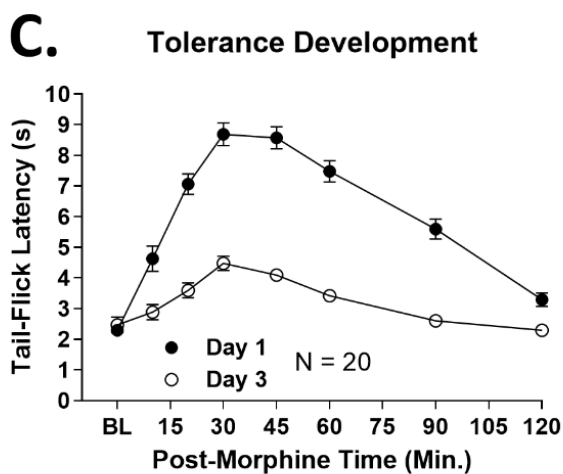
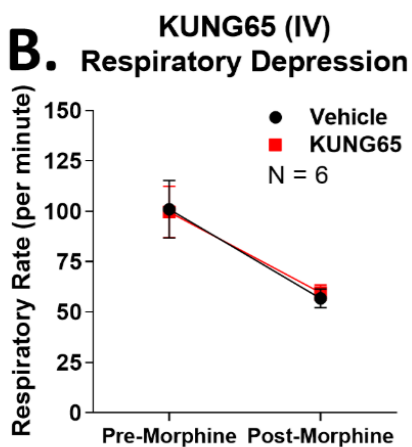
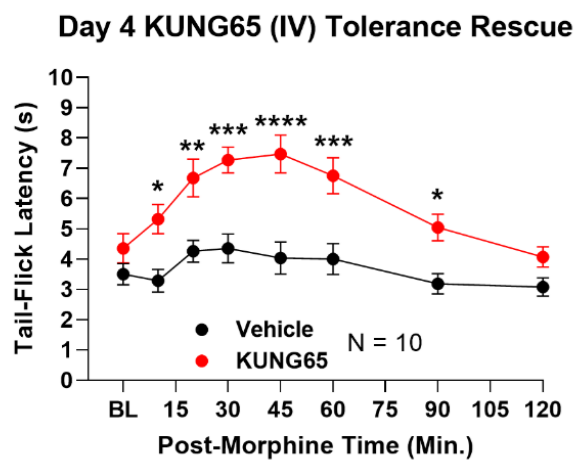
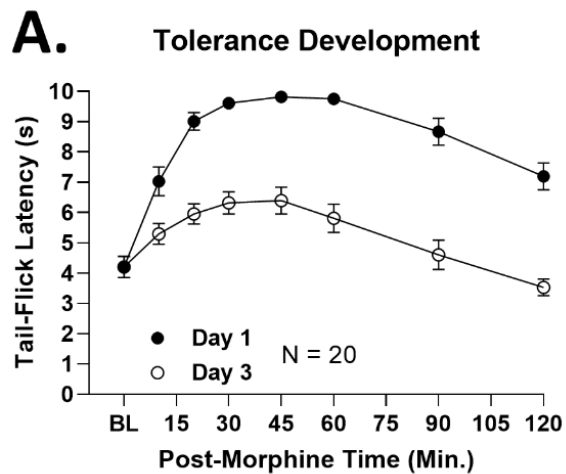


**Figure 12: Systemic Grp94 and Hsp90 $\beta$  inhibition rescues established tolerance without worsening opioid-induced respiratory depression.** Male and female CD-1 mice used for every experiment, with data presented as the mean  $\pm$  SEM and the sample size of mice/group noted in each graph. The tolerance experiments were performed in 2 technical replicates, and the respiratory depression experiments in 1 technical replicate. \*, \*\*, \*\*\*, \*\*\*\* =  $p < 0.05, 0.01, 0.001, 0.0001$  vs. same time point Vehicle group by 2 Way RM ANOVA with Sidak's *post hoc* test. **A)** Tolerance induced in all mice over 3 days with twice daily injection of 10 mg/kg morphine s.c. (as in **Figure 4**). On day 3, mice injected with 1 mg/kg KUNG65 or Vehicle i.v., 24 hrs, followed by 10 mg/kg morphine s.c. and another tail flick time course. KUNG65 rescued established tolerance much like intrathecal injection of KU-32 above. **B)** Mice injected with 1 mg/kg KUNG65 or Vehicle i.v., 24 hrs, then habituated and baselined in a whole body plethysmography chamber for 30 minutes (see Methods). All mice were then injected with 7.5 mg/kg morphine i.v., and respiratory activity recorded for another hour. KUNG65 had no effect on respiration before or after morphine injection ( $p > 0.05$ ). **C)** Tolerance induced as above, and on day 3, 1 mg/kg KUNB106 or Vehicle injected i.v., 24 hrs, followed by 10 mg/kg morphine s.c. and another tail flick timecourse. KUNB106 also rescued established tolerance like systemic KUNG65 or intrathecal KU-32. **D)** Mice injected with 1 mg/kg KUNB106 or Vehicle i.v., 24 hrs, then respiratory activity measured as above (including 7.5 mg/kg morphine i.v. challenge). KUNB106 had no impact on respiratory activity before or after morphine ( $p > 0.05$ ) (Data collected by KC, DD, PB).

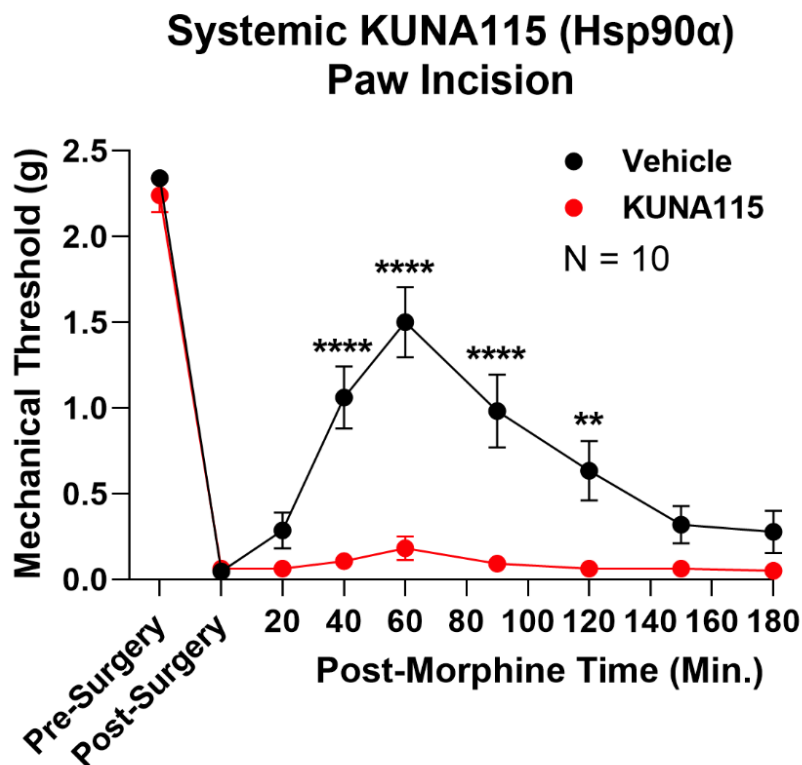


**Figure 13: Systemic Hsp90 $\alpha$  inhibition blocks opioid anti-nociception.** Male and female CD-1 mice had paw incision performed, then injected with 1 mg/kg KUNA115 or Vehicle i.v., 24 hrs, followed by 3.2 mg/kg morphine s.c. and a Von Frey mechanical allodynia timecourse performed. Data presented as the mean  $\pm$  SEM with the sample size of mice/group noted in the graph (performed in 2 technical replicates). \*\*, \*\*\*\* =  $p < 0.01, 0.0001$  vs. same time point Vehicle group by 2 Way RM ANOVA with Sidak's *post hoc* test. Unlike Hsp90 $\beta$  and Grp94 inhibition, systemic Hsp90 $\alpha$  inhibition via KUNA115 completely blocked opioid anti-nociception in this model (Data collected by KC, DD, PB).

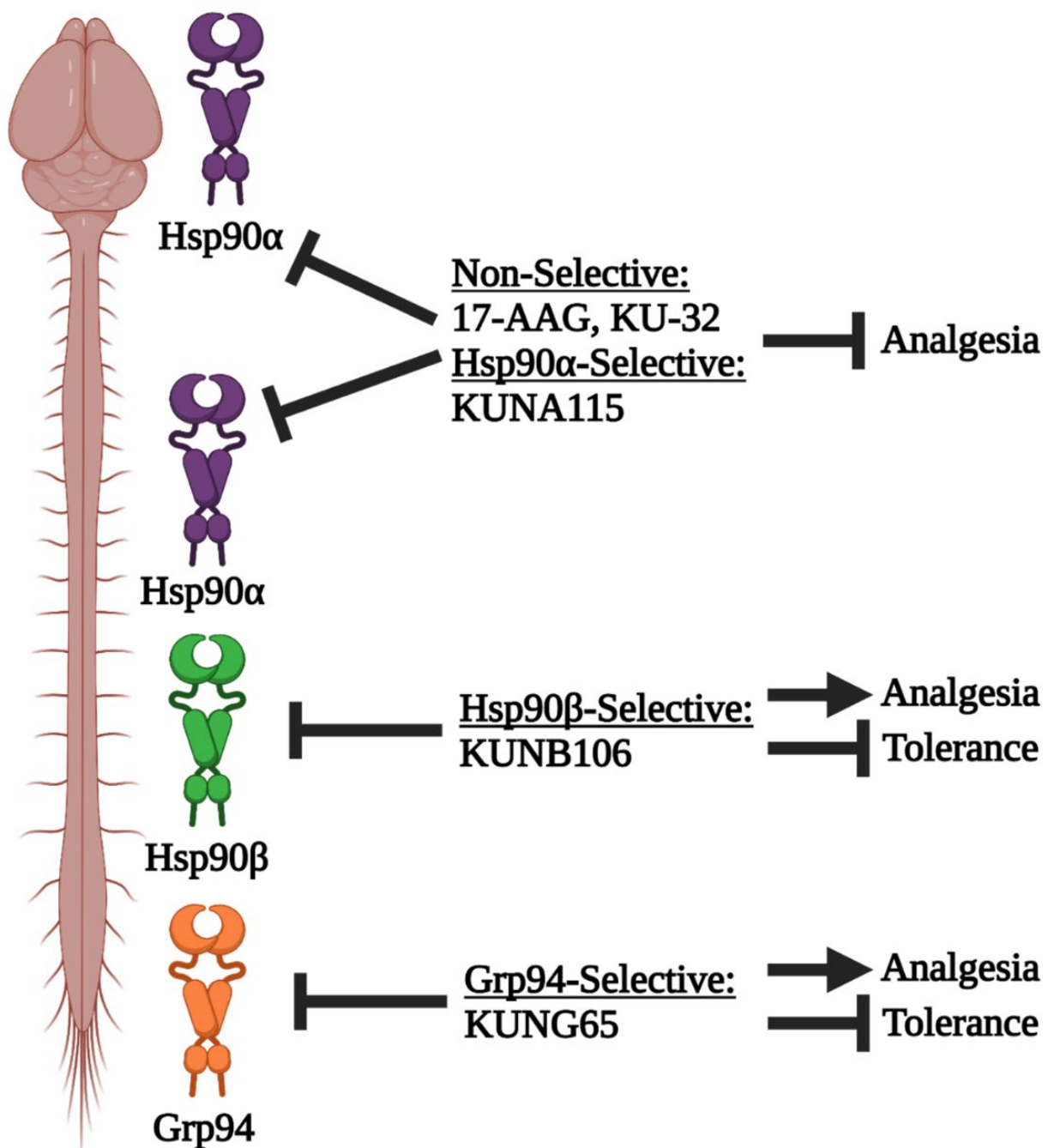


**Figure 14: Model of Hsp90 isoform inhibition in the brain vs. spinal cord.** In the brain, Hsp90 $\alpha$  alone regulates opioid signaling, while in the spinal cord, Hsp90 $\alpha$ , Hsp90 $\beta$ , and Grp94 all do so. When Hsp90 $\alpha$  is inhibited systemically with non-selective inhibitor or Hsp90 $\alpha$ -selective inhibitor, opioid anti-nociception is blocked, since brain Hsp90 is inhibited and a brain-

like response is evoked. In contrast, when Hsp90 $\beta$  or Grp94 are inhibited systemically with selective inhibitors, brain inhibition of Hsp90 $\alpha$  is avoided, and a spinal cord-like response is evoked – increased anti-nociception and decreased side effects. This model suggests that Hsp90 $\beta$  and Grp94 inhibitors could be given by translationally-relevant routes to improve the therapeutic index of opioids and enable a dose-reduction strategy. Figure created using biorender.com.

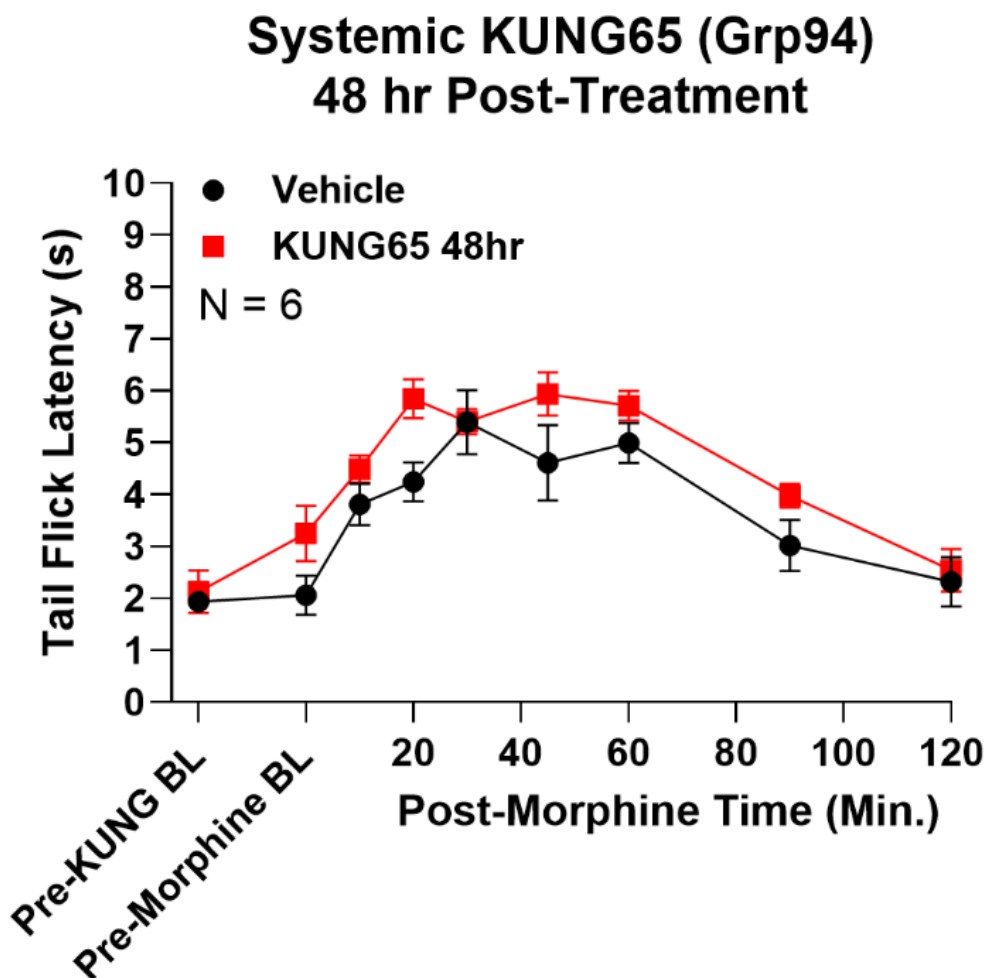
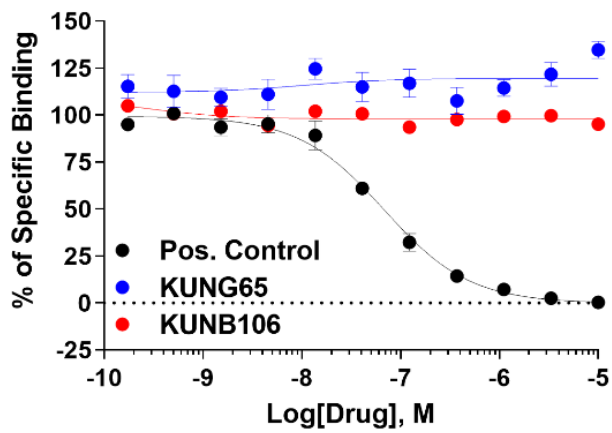
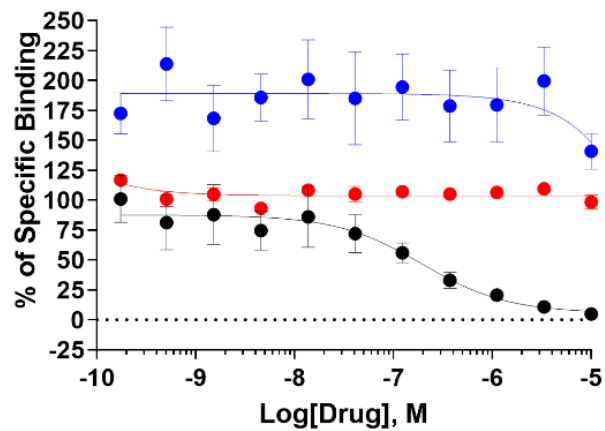


**Figure 15: Enhanced morphine anti-nociception after Grp94 inhibitor treatment dissipates by 48 hours post-treatment.** Male and female CD-1 mice were injected with 1 mg/kg KUNG65 or Vehicle control i.v., followed by 48 hrs of treatment, then 3.2 mg/kg morphine s.c. and a tail flick timecourse. Data displayed as the mean  $\pm$  SEM with the sample size of mice/group noted in the graph; the experiment was completed with 1 technical replicate. The anti-nociception after 48 hrs of KUNG65 treatment was not significantly different from control ( $p > 0.05$ ), suggesting that the benefits of the treatment wear off between 24 and 48 hrs post-treatment.

## Competition Binding - MOR



## Competition Binding - DOR



## Competition Binding - KOR

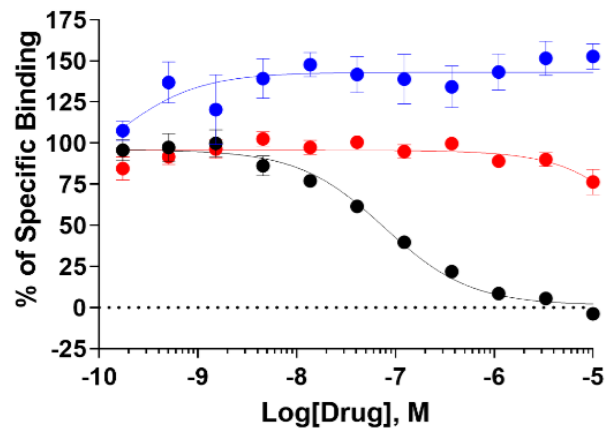


**Figure 16: The Grp94 and Hsp90 $\beta$  inhibitors KUNG65 and KUNB106 do not bind to the opioid receptors.** KUNG65, KUNB106, and positive control (naloxone for mu opioid receptor [MOR] and delta opioid receptor [DOR], U50,488 for kappa opioid receptor [KOR]) were competed against  $^3\text{H}$ -diprenorphine at all 3 human opioid receptors using competition radioligand binding (see Methods). Data shown as the mean  $\pm$  SEM of N = 3 independent experiments. Positive control compounds displayed competition as expected, validating the assay ( $K_I$  values: MOR =  $34 \pm 3$  nM; DOR =  $120 \pm 44$  nM; KOR =  $37 \pm 4$  nM). KUNG65 and KUNB106 did not display competition up to a 10  $\mu\text{M}$  concentration, ruling out opioid receptor binding as a potential confound for our findings (Data collected by CSC and PT).

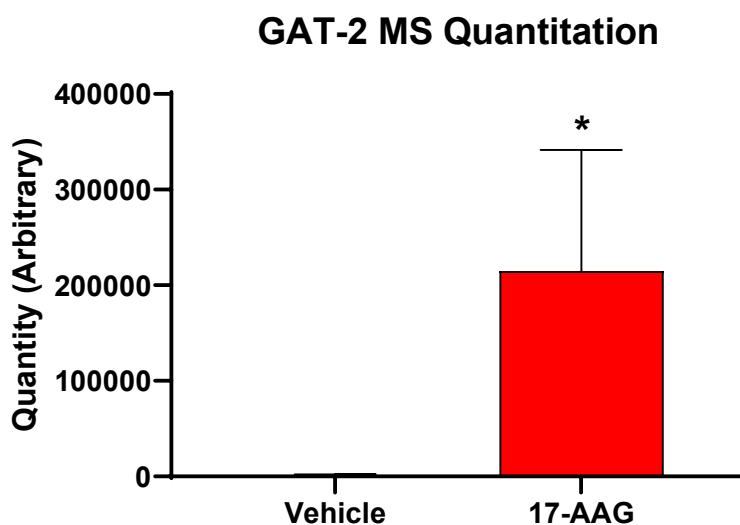


**Figure 17: Quantitative proteomic analysis of protein quantification following intrathecal 17-AAG administration.** Results revealed a 154-fold increase in GAT-2 expression levels 24 hours after intrathecal .5nmol 17-AAG administration in female CD-1 mice compared to vehicle controls. Spinal cords were analyzed using mass spectrometry reported in Duron et al, 2020. From this published data set, we extracted the raw mass spectrometry counts for GAT-2, shown here as the mean +/- SEM.  $P < .05$  by an Unpaired 2-Tailed  $t$  Test.

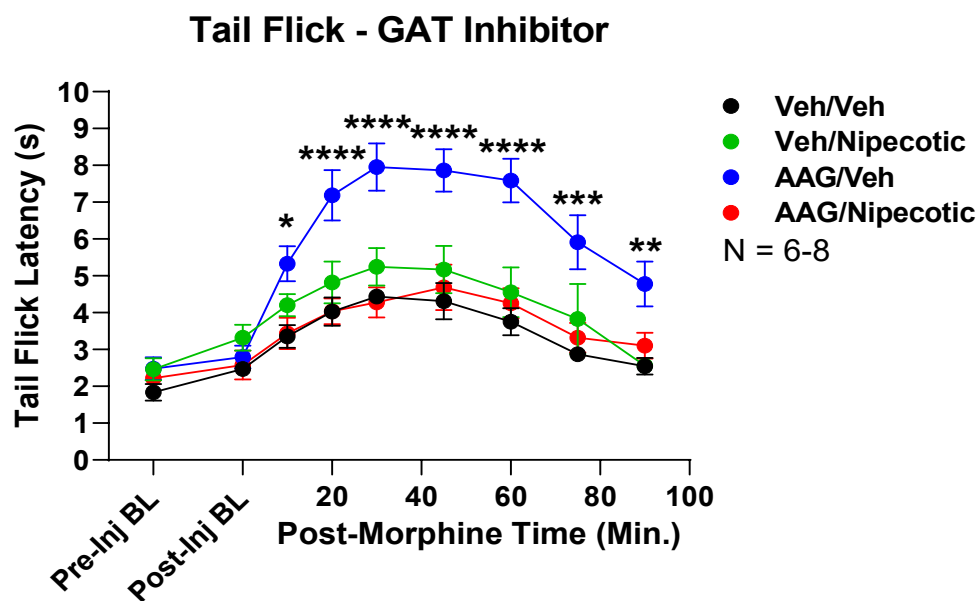
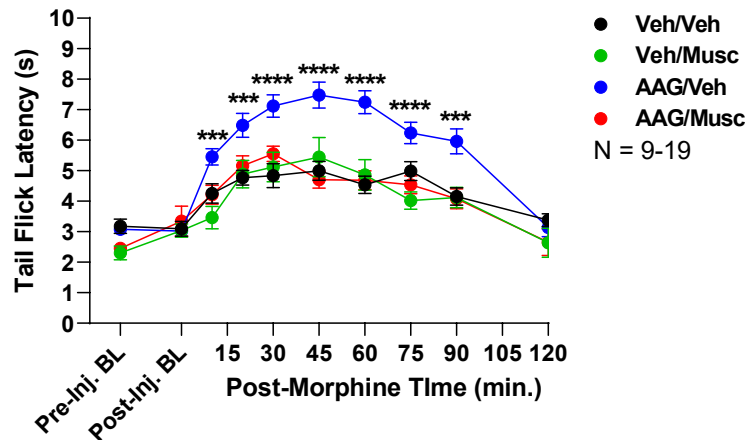
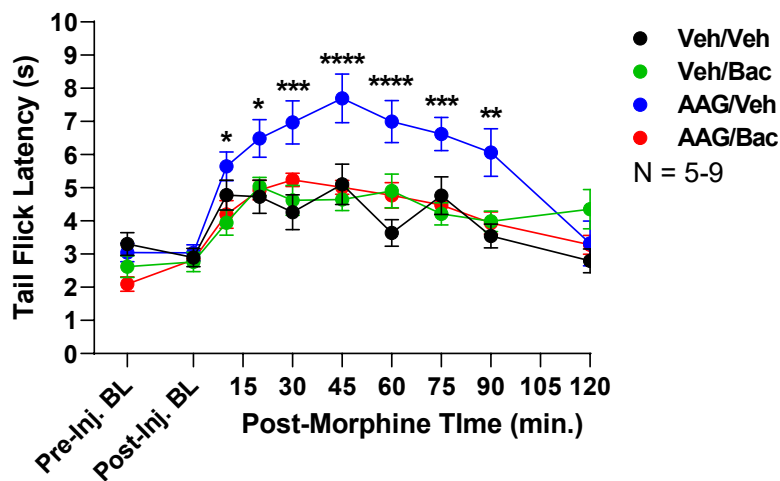


**Figure 18: Intrathecal Administration of Nipecotic Acid Blocks the Effect of 17-AAG on Morphine Analgesia.** Intrathecal administration of Nipecotic Acid, a nonspecific GAT-2 inhibitor, following 17-AAG treatment effectively blocked the 17-AAG induced enhancement of opioid analgesia in the hot water bath/tail-flick assay. The effect of the blockade remained significant throughout the entire time-course. Data reported as the mean  $\pm$  SEM, n=8 for the 17-AAG/NA group, n=8 mice for the 17-AAG/Veh group, n=8 for Veh/NA group, and n=6 for Veh/Veh group.

### Tail Flick - GABA Agonists Male & Female



### Tail Flick - GABA Agonists Male Only



### Tail Flick - GABA Agonists Female Only

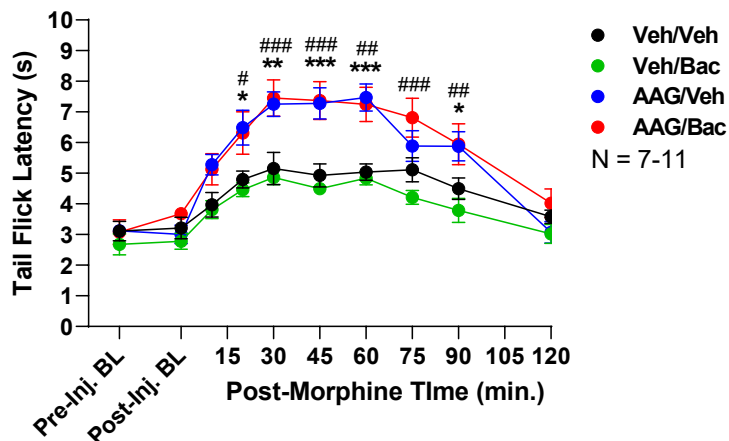


**Figure 19: Hsp90 inhibition mediates augmentation of opioid induced analgesia via GABA-A Receptor signaling in a sex-dependent manner.** Intrathecal administration of the GABA-A specific agonist Muscimol following 17-AAG administration similarly blocked the effects of 17-AAG on opioid analgesia, suggesting that the downstream effect of GAT-2 upregulation decreases GABA receptor signaling on post-synaptic targets involved in modulating opioid antinociception. Data reported as the mean  $\pm$  SEM, n=19 for the 17-AAG/Bac group, n=10 mice for the 17-AAG/Mus group, n=19 for 17-AAG/Veh group, n=14 for Veh/Veh group, n=16 for Veh/Bac group, and n=9 for Veh/Mus group. Intrathecal administration of the GABA-B selective agonist Baclofen revealed a sex-specific difference in blocking the effect of 17-AAG. The GABA-B agonist failed to block the effect of 17-AAG. Baclofen similarly blocked the effect of 17-AAG as the GABA-A agonist Muscimol. Data reported as the mean  $\pm$  SEM, n=11 for the 17-AAG/Bac group, n=5 mice for the 17-AAG/Mus group, n=11 for 17-AAG/Veh group, n=9 for Veh/Veh group, n=7 for Veh/Bac group, and n=2 for Veh/Mus group. Data reported as the mean  $\pm$  SEM, n=4 for the 17-AAG/Bac group, n=5 mice for the 17-AAG/Mus group, n=5 for 17-AAG/Veh group, n=2 for Veh/Veh group, n=5 for Veh/Bac group, and n=5 for Veh/Mus group.

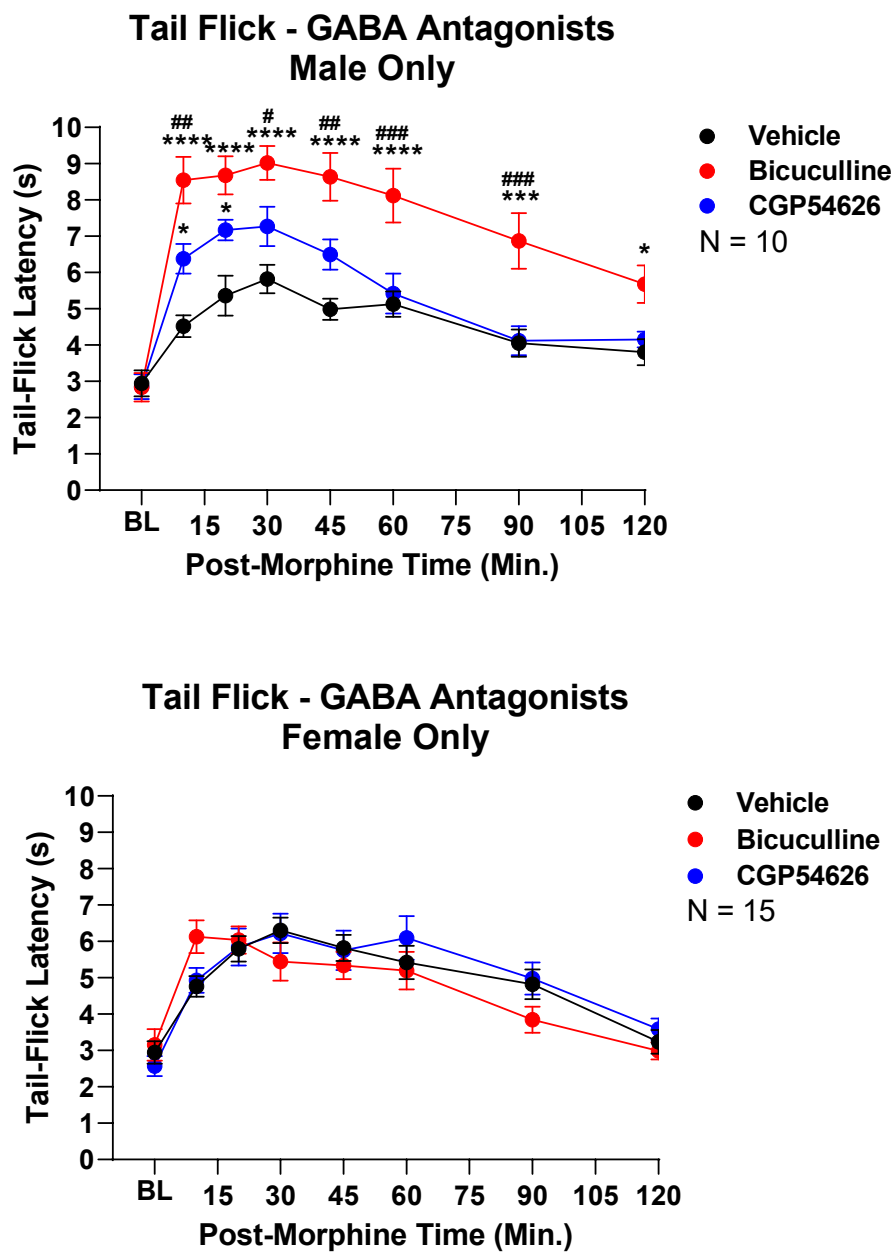


**Figure 20: Hsp90 inhibition mediates augmentation of opioid induced analgesia via GABA-B Receptor signaling in a sex-dependent manner.** Intrathecal administration of GABA-A, and to a lesser degree GABA-B specific antagonists in naïve (no 17-AAG) male mice produced potent increases in opioid antinociception, suggesting a GABAergic brake on opioid antinociceptive circuitry exists in the spinal cord. Intrathecal administration of GABA-A

(Bicuculline) or GABA-B (CGP54626) specific antagonists in naïve (no 17-AAG) female mice failed to produce any augmentation of opioid analgesia.

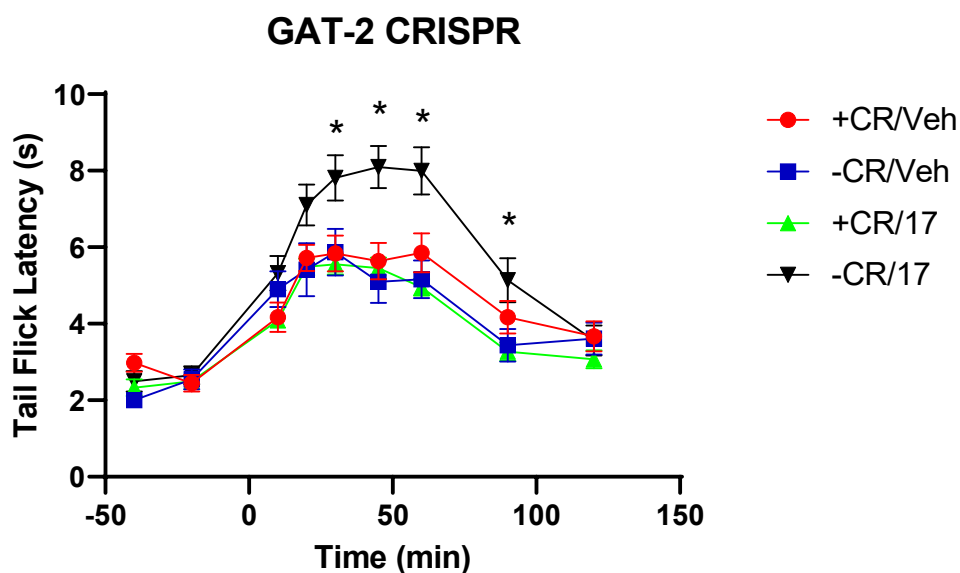


**Figure 21: CRISPR/Cas9 Slc6a13 Knockout in the spinal cord mimics the effects of intrathecal 17-AAG administration.**

Mice were given + or – CRISPR injections for three days intrathecally. On the 9<sup>th</sup> day, mice were given .5nmol 17-AAG or vehicle. On the 10<sup>th</sup> day, mice were given 3.2mg/kg morphine subcutaneously. Antinociception was measured over the course of two hours using the hot water bath/tail flick assay. All data reported as Mean +/- SEM. N= 8 per group.

## REFERENCES

1. International Association for the Study of Pain. IASP taxonomy. <http://www.iasp-pain.org/Taxonomy?&navItemNumber=576>. Updated October 20, 2014.
2. Reid KJ, Harker J, Bala MM, et al. Epidemiology of chronic noncancer pain in Europe: narrative review of prevalence, pain treatments and pain impact. *Curr Med Res Opin.* 2011;27(2):449-462.
3. Froud R, Patterson S, Eldridge S, et al. A systematic review and meta-synthesis of the impact of low back pain on people's lives. *BMC Musculoskelet Disord.* 2014;15:50.
4. Doth AH, Hansson PT, Jensen MP, Taylor RS. The burden of neuropathic pain: a systematic review and meta-analysis of health utilities. *Pain.* 2010;149(2):338-344.
5. Vos T, Flaxman AD, Naghavi M, et al. Years lived with disability (YLDs) for 1160 sequelae of 289 diseases and injuries 1990-2010: a systematic analysis for the Global Burden of Disease Study 2010. *Lancet.* 2012;380(9859):2163-2196.
6. McBeth J, Jones K. Epidemiology of chronic musculoskeletal pain. *Best Pract Res Clin Rheumatol.* 2007;21(3):403-425.
7. Thomas MJ, Roddy E, Zhang W, Menz HB, Hannan MT, Peat GM. The population prevalence of foot and ankle pain in middle and old age: a systematic review. *Pain.* 2011;152(12):2870-2880.
8. Macfarlane TV, Glenny AM, Worthington HV. Systematic review of population-based epidemiological studies of oro-facial pain. *J Dent.* 2001;29(7):451-467.
9. Unruh AM. Gender variations in clinical pain experience. *Pain.* 1996;65(2-3):123-167.
10. Abdulla A, Adams N, Bone M, et al; British Geriatric Society. Guidance on the management of pain in older people. *Age Ageing.* 2013;42(suppl 1):i1-i57.
11. Hoy D, Brooks P, Blyth F, Buchbinder R. The epidemiology of low back pain. *Best Pract Res Clin Rheumatol.* 2010;24(6):769-781.
12. Taylor JB, Goode AP, George SZ, Cook CE. Incidence and risk factors for first-time incident low back pain: a systematic review and meta-analysis. *Spine J.* 2014;14(10):2299-2319.

13. Côté P, van der Velde G, Cassidy JD, et al; Bone and Joint Decade 2000-2010 Task Force on Neck Pain and Its Associated Disorders. The burden and determinants of neck pain in workers: results of the Bone and Joint Decade 2000-2010 Task Force on Neck Pain and Its Associated Disorders. *Spine (Phila Pa 1976)*. 2008;33(4, suppl):S60-S74.
14. Sled M, Eccleston C, Beecham J, Knapp M, Jordan A. The economic impact of chronic pain in adolescence: methodological considerations and a preliminary costs-of-illness study. *Pain*. 2005;119(1-3):183-190.
15. Kronborg C, Handberg G, Axelsen F. Health care costs, work productivity and activity impairment in non-malignant chronic pain patients. *Eur J Health Econ*. 2009;10(1):5-13.
16. Schofield DJ, Shrestha RN, Passey ME, Earnest A, Fletcher SL. Chronic disease and labour force participation among older Australians. *Med J Aust*. 2008;189(8):447-450.
17. Freburger JK, Holmes GM, Agans RP, et al. The rising prevalence of chronic low back pain. *Arch Intern Med*. 2009;169(3):251-258.
18. Phillips CJ. Economic burden of chronic pain. *Expert Rev Pharmacoecon Outcomes Res*. 2006;6(5):591-601.
19. Access Economics Pty Limited. *The High Price of Pain: The Economic Impact of Persistent Pain in Australia*. Sydney, Australia: Access Economics Pty Limited; 2007.
20. Gaskin DJ, Richard P. The economic costs of pain in the United States. *J Pain*. 2012;13(8):715-724.
21. Clauw DJ, Essex MN, Pitman V, Jones KD. Reframing chronic pain as a disease, not a symptom: rationale and implications for pain management. *Postgrad Med* 2019; **131**: 185–98.
22. Daneshjou K, Jafarieh H, Raaeskarami SR. Congenital Insensitivity to Pain and Anhydrosis (CIPA) Syndrome; A Report of 4 Cases. *Iran J Pediatr*. 2012 Sep;22(3):412-6. PMID: 23400697; PMCID: PMC3564101.
22. Morasco BJ, Gritzner S, Lewis L, Oldham R, Turk DC, Dobscha SK. Systematic review of prevalence, correlates, and treatment outcomes for chronic non-cancer pain in patients with comorbid substance use disorder. *Pain* 2011; **152**: 488–97.

23. Treede RD, Rief W, Barke A, et al. Chronic pain as a symptom or a disease: the IASP Classification of Chronic Pain for the International Classification of Diseases (ICD-11). *Pain* 2019; **160**: 19–27.
24. Meints SM, Edwards RR. Evaluating psychosocial contributions to chronic pain outcomes. *Prog Neuropsychopharmacol Biol Psychiatry* 2018; **87**: 168–82.
25. Edwards RR, Dworkin RH, Sullivan MD, Turk DC, Wasan AD. The role of psychosocial processes in the development and maintenance of chronic pain. *J Pain* 2016; **17** (suppl): T70–92.
26. Samoborec S, Ruseckaite R, Ayton D, Evans S. Biopsychosocial factors associated with non-recovery after a minor transport-related injury: a systematic review. *PLoS One* 2018; **13**: e0198352.
27. DiBonaventura MD, Sadosky A, Concialdi K, et al. The prevalence of probable neuropathic pain in the US: results from a multimodal general-population health survey. *J Pain Res* 2017; **10**: 2525–38.
28. Cohen SP, Mao J. Neuropathic pain: mechanisms and their clinical implications. *BMJ* 2014; **348**: f7656.
29. Finnerup NB, Haroutounian S, Kamerman P, et al. Neuropathic pain: an updated grading system for research and clinical practice. *Pain* 2016; **157**: 1599–606.
30. Fitzcharles M, Cohen SP, Clauw DJ, et al. Nociceptive pain: towards an understanding of prevalent pain conditions. *Lancet* 2021; **397**: 2098–110.
31. Genc H, Nacir B, Duyur Cakit B, Saracoglu M, Erdem HR. The effects of coexisting fibromyalgia syndrome on pain intensity, disability, and treatment outcome in patients with chronic lateral epicondylitis. *Pain Med* 2012; **13**: 270–80.
32. Geneen LJ, Moore RA, Clarke C, Martin D, Colvin LA, Smith BH. Physical activity and exercise for chronic pain in adults: an overview of Cochrane reviews. *Cochrane Database Syst Rev* 2017; **4**: CD011279.
33. Williams AC, Fisher E, Hearn L, Eccleston C. Psychological therapies for the management of chronic pain (excluding headache) in adults. *Cochrane Database Syst Rev* 2020; **8**: CD007407.

34. Hilton L, Hempel S, Ewing BA, et al. Mindfulness meditation for chronic pain: systematic review and meta-analysis. *Ann Behav Med* 2017; **51**: 199–213.
35. Freynhagen R, Parada HA, Calderon-Ospina CA, et al. Current understanding of the mixed pain concept: a brief narrative review. *Curr Med Res Opin* 2019; **35**: 1011–18.
36. Ibor PJ, Sánchez-Magro I, Villoria J, Leal A, Esquivias A. Mixed pain can be discerned in the primary care and orthopedics settings in Spain: a large cross-sectional study. *Clin J Pain* 2017; **33**: 1100–08.
37. Cohen, S., Vase, L., Hooten, W. Chronic Pain: an update on burden, best practices, and new advances. *Lancet*, 2021; 397:2082-97.
38. Furlan AD, Giraldo M, Baskwill A, Irvin E, Imamura M. Massage for low-back pain. *Cochrane Database Syst Rev* 2015; **9**: CD001929.
39. Paley CA, Johnson MI. Acupuncture for the relief of chronic pain: a synthesis of systematic reviews. *Medicina (Kaunas)* 2019; **56**: 6.
40. Wieland LS, Skoetz N, Pilkington K, Vempati R, D'Adamo CR, Berman BM. Yoga treatment for chronic non-specific low back pain. *Cochrane Database Syst Rev* 2017; **1**: CD010671.
41. Hall A, Copsey B, Richmond H, et al. Effectiveness of Tai Chi for chronic musculoskeletal pain conditions: updated systematic review and meta-analysis. *Phys Ther* 2017; **97**: 227–38.
42. Coulter ID, Crawford C, Hurwitz EL, et al. Manipulation and mobilization for treating chronic low back pain: a systematic review and meta-analysis. *Spine J* 2018; **18**: 866–79.
43. Coulter ID, Crawford C, Vernon H, et al. Manipulation and mobilization for treating chronic nonspecific neck pain: a systematic review and meta-analysis for an appropriateness panel. *Pain Physician* 2019; **22**: E55–70.
44. Rosenow JM, Henderson JM. Anatomy and physiology of chronic pain. *Neurosurg Clin N Am* 2003; 14(3):445–62, vii.
45. Fishman S, Ballantyne J, Rathmell JP, et al. Bonica's management of pain. 4th edition. Baltimore (MD): Lippincott, Williams & Wilkins; 2010.

46. Hall JE, Guyton AC. Guyton and Hall textbook of medical physiology. 12th edition. Philadelphia: Saunders/Elsevier; 2011.
47. Cooper B, Ahlquist M, Friedman RM, et al. Properties of high-threshold mechanoreceptors in the goat oral mucosa. II. Dynamic and static reactivity in carrageenan-inflamed mucosa. *J Neurophysiol* 1991;66(4):1280–90.
48. Willis WD, Westlund KN. Neuroanatomy of the pain system and of the pathways that modulate pain. *J Clin Neurophysiol* 1997;14(1):2–31.
49. Neumann S, Doubell TP, Leslie T, et al. Inflammatory pain hypersensitivity mediated by phenotypic switch in myelinated primary sensory neurons. *Nature* 1996;384(6607):360–4.
50. Pitcher GM, Henry JL. Nociceptive response to innocuous mechanical stimulation is mediated via myelinated afferents and NK-1 receptor activation in a rat model of neuropathic pain. *Exp Neurol* 2004;186(2):173–97.
51. Devor M. Unexplained peculiarities of the dorsal root ganglion. *Pain* 1999;(Suppl 6):S27–35.
52. Amir R, Devor M. Chemically mediated crossexcitation in rat dorsal root ganglia. *J Neurosci* 1996;16(15):4733–41.
53. Applebaum ML, Clifton GL, Coggeshall RE, et al. Unmyelinated fibres in the sacral 3 and caudal 1 ventral roots of the cat. *J Physiol* 1976;256(3):557–72.
54. Coggeshall RE, Applebaum ML, Fazen M, et al. Unmyelinated axons in human ventral roots, a possible explanation for the failure of dorsal rhizotomy to relieve pain. *Brain* 1975;98(1):157–66.
55. Coggeshall RE, Maynard CW, Langford LA. Unmyelinated sensory and preganglionic fibers in rat L6 and S1 ventral spinal roots. *J Comp Neurol* 1980; 193(1):41–7.
56. Sykes MT, Coggeshall RE. Unmyelinated fibers in the human L4 and L5 ventral roots. *Brain Res* 1973;63:490–5.
57. Earle KM. The tract of Lissauer and its possible relation to the pain pathway. *J Comp Neurol* 1952;96(1): 93–111.
58. Benzel EC, Francis TB. Spine surgery: techniques, complication avoidance, and management. 3<sup>rd</sup> edition. Philadelphia: Elsevier/Saunders; 2012.

59. Gobel S. Golgi studies of the neurons in layer II of the dorsal horn of the medulla (trigeminal nucleus caudalis). *J Comp Neurol* 1978;180(2):395–413.
60. Mannion RJ, Doubell TP, Gill H, et al. Deafferentation is insufficient to induce sprouting of A-fibre central terminals in the rat dorsal horn. *J Comp Neurol* 1998;393(2):135–44.
61. Dostrovsky JO. Role of thalamus in pain. *Prog Brain Res* 2000;129:245–57.
62. Cameron AA, Khan IA, Westlund KN, et al. The efferent projections of the periaqueductal gray in the rat: a Phaseolus vulgaris-leucoagglutinin study. I. Ascending projections. *J Comp Neurol* 1995;351(4): 568–84.
63. Bowsher D. Role of the reticular formation in responses to noxious stimulation. *Pain* 1976;2(4):361–78.
64. Dado RJ, Katter JT, Giesler GJ Jr. Spinothalamic and spinothalamic tract neurons in the cervical enlargement of rats. II. Responses to innocuous and noxious mechanical and thermal stimuli. *J Neurophysiol* 1994;71(3):981–1002.
65. Lenz FA, Weiss N, Ohara S, et al. The role of the thalamus in pain. *Suppl Clin Neurophysiol* 2004;57: 50–61.
66. Ralston HJ 3rd. Pain and the primate thalamus. *Prog Brain Res* 2005;149:1–10.
67. Anderson WS, O'Hara S, Lawson HC, et al. Plasticity of pain-related neuronal activity in the human thalamus. *Prog Brain Res* 2006;157:353–64.
68. Lenz FA, Lee JJ, Garonzik IM, et al. Plasticity of pain related neuronal activity in the human thalamus. *Prog Brain Res* 2000;129:259–73.
69. Jones AK, Kulkarni B, Derbyshire SW. Pain mechanisms and their disorders. *Br Med Bull* 2003;65: 83–93.
70. Tran TD, Inui K, Hoshiyama M, et al. Cerebral activation by the signals ascending through unmyelinated C-fibers in humans: a magnetoencephalographic study. *Neuroscience* 2002;113(2):375–86.
71. Bourne, S., Machado, A., Nagel, S. *Basic Anatomy and Physiology of Pain Pathways*. *Neurosurg Clin N Am* 25 (2014) 629–638 <http://dx.doi.org/10.1016/j.nec.2014.06.001> .
72. Møller AR. *Textbook of tinnitus*. New York: Springer; 2011.

73. Ossipov, M. H., Dussor, G. O., & Porreca, F. (2010). Central modulation of pain. *The Journal of clinical investigation*, 120(11), 3779-3787.
74. Yeomans DC, Proudfit HK. Antinociception induced by microinjection of substance P into the A7 catecholamine cell group in the rat. *Neuroscience* 1992;49(3):681–91.
75. Kwon M, Altin M, Duenas H, et al. The role of descending inhibitory pathways on chronic pain modulation and clinical implications. *Pain Pract* 2013.
76. Al-Hasani R, Bruchas MR. 2011 Molecular mechanisms of opioid receptor-dependent signaling and behavior. *Anesthesiology* 115:1363–81 [PubMed: 22020140]
77. Kieffer BL, Evans CJ. 2009 Opioid receptors: from binding sites to visible molecules in vivo. *Neuropharmacology* 56(Suppl. 1):205–12 [PubMed: 18718480]
78. Toll L, Bruchas MR, Calo' G, Cox BM, Zaveri NT. 2016 Nociceptin/orphanin FQ receptor structure, signaling, ligands, functions, and interactions with opioid systems. *Pharmacol. Rev.* 68:419–57 [PubMed: 26956246]
79. Mansour A, Fox CA, Burke S, Meng F, Thompson RC, et al. 1994 Mu, delta, and kappa opioid receptor mRNA expression in the rat CNS: an in situ hybridization study. *J. Comp. Neurol.* 350:412–38 [PubMed: 7884049]
80. Neal CR, Mansour A, Reinscheid R, Nothacker HP, Civelli O, et al. 1999 Opioid receptor-like (ORL1) receptor distribution in the rat central nervous system: comparison of ORL1 receptor mRNA expression with 125I-[14Tyr]-orphanin FQ binding. *J. Comp. Neurol.* 412:563–605 [PubMed: 10464356]
81. Granier S, Manglik A, Kruse AC, Kobilka TS, Thian FS, et al. 2012 Structure of the  $\delta$ -opioid receptor bound to naltrindole. *Nature* 485:400–4 [PubMed: 22596164]
82. Manglik A, Kruse AC, Kobilka TS, Thian FS, Mathiesen JM, et al. 2012 Crystal structure of the  $\mu$ -opioid receptor bound to a morphinan antagonist. *Nature* 485:321–26 [PubMed: 22437502]
83. Thompson AA, Liu W, Chun E, Katritch V, Wu H, et al. 2012 Structure of the nociceptin/orphanin FQ receptor in complex with a peptide mimetic. *Nature* 485:395–99 [PubMed: 22596163]

84. Wu H, Wacker D, Mileni M, Katritch V, Han GW, et al. 2012 Structure of the human  $\kappa$ -opioid receptor in complex with JDTic. *Nature* 485:327–32
85. Manglik A, Lin H, Aryal DK, McCorvy JD, Dengler D, et al. 2016 Structure-based discovery of opioid analgesics with reduced side effects. *Nature* 537:185–90 [PubMed: 27533032]
86. Corder, G., Castro, D., Bruchas, M., Scherrer, G. Endogenous and Exogenous Opioids in Pain. *Ann Rev Neurosci.* 2018 July 08; 41: 4530473.
87. Banghart MR, Sabatini BL. 2012 Photoactivatable neuropeptides for spatiotemporally precise delivery of opioids in neural tissue. *Neuron* 73:249–59 [PubMed: 22284180]
88. Duggan AW. 2000 Neuropeptide spread in the brain and spinal cord. *Prog. Brain Res.* 125:369–80 [PubMed: 11098673]
89. Glass MJ, Vanyo L, Quimson L, Pickel VM. 2009 Ultrastructural relationship between N-methyl-D-aspartate-NR1 receptor subunit and mu-opioid receptor in the mouse central nucleus of the amygdala. *Neuroscience* 163:857–67 [PubMed: 19607886]
90. Mansour A, Khachaturian H, Lewis ME, Akil H, Watson SJ. 1988 Anatomy of CNS opioid receptors. *Trends Neurosci.* 11:308–14 [PubMed: 2465635]
91. Svingos AL, Moriwaki A, Wang JB, Uhl GR, Pickel VM. 1996 Ultrastructural immunocytochemical localization of  $\mu$ -opioid receptors in rat nucleus accumbens: extrasynaptic plasmalemmal distribution and association with Leu5-enkephalin. *J. Neurosci.* 16:4162–73 [PubMed: 8753878]
92. Bloom FE, Rossier J, Battenberg EL, Bayon A, French E, et al. 1978 beta-endorphin: cellular localization, electrophysiological and behavioral effects. *Adv. Biochem. Psychopharmacol.* 18:89–109 [PubMed: 77124]
93. Lazarus LH, Ling N, Guillemin R. 1976 beta-Lipotropin as a prohormone for the morphinomimetic peptides endorphins and enkephalins. *PNAS* 73:2156–59 [PubMed: 1064883]
94. Corder G, Doolen S, Donahue RR, Winter MK, Jutras BL, et al. 2013 Constitutive  $\mu$ -opioid receptor activity leads to long-term endogenous analgesia and dependence. *Science* 341:1394–99 [PubMed: 24052307]

95. Polter AM, Barcomb K, Chen RW, Dingess PM, Graziane NM, et al. 2017 Constitutive activation of kappa opioid receptors at ventral tegmental area inhibitory synapses following acute stress. *eLife* 6:e23785 [PubMed: 28402252]
96. Yao X-Q, Malik RU, Griggs NW, Skjaerven L, Traynor JR, et al. 2016 Dynamic coupling and allosteric networks in the  $\alpha$  subunit of heterotrimeric G proteins. *J. Biol. Chem.* 291:4742–53 [PubMed: 26703464]
97. Kenakin T 2001 Inverse, protean, and ligand-selective agonist: matters of receptor conformation. *FASEB J.* 3:593–611
98. Walwyn W, Evans CJ, Hales TG. 2007  $\beta$ -Arrestin2 and c-Src regulate the constitutive activity and recycling of  $\mu$  opioid receptors in dorsal root ganglion neurons. *J. Neurosci.* 27:5092–104 [PubMed: 17494695]
99. Rusin KI, Giovannucci DR, Stuenkel EL, Moises HC. 1997 K-Opioid receptor activation modulates  $Ca^{2+}$  currents and secretion in isolated neuroendocrine nerve terminals. *J. Neurosci.* 17:6565–74 [PubMed: 9254669]
100. Altier C, Khosravani H, Evans RM, Hameed S, Peloquin JB, et al. 2006 ORL1 receptor-mediated internalization of N-type calcium channels. *Nat. Neurosci.* 9:31–40 [PubMed: 16311589]
101. Torrecilla M, Marker CL, Cintora SC, Stoffel M, Williams JT, Wickman K. 2002 G-protein-gated potassium channels containing Kir3.2 and Kir3.3 subunits mediate the acute inhibitory effects of opioids on locus ceruleus neurons. *J. Neurosci.* 22:4328–34 [PubMed: 12040038]
102. Luján R, Marron Fernandez de Velasco E, Aguado C, Wickman K. 2014 New insights into the therapeutic potential of GIRK channels. *Trends Neurosci.* 37:20–29 [PubMed: 24268819]
103. Nagi K, Pineyro G. 2014 Kir3 channel signaling complexes: focus on opioid receptor signaling. *Front. Cell Neurosci.* 8:186 [PubMed: 25071446]
104. Eichel K, Jullie D, von Zastrow M. 2016  $\beta$ -Arrestin drives MAP kinase signalling from clathrin-coated structures after GPCR dissociation. *Nat. Cell Biol.* 18:303–10 [PubMed: 26829388]

105. Irannejad R, Tomshine JC, Tomshine JR, Chevalier M, Mahoney JP, et al. 2013 Conformational biosensors reveal GPCR signalling from endosomes. *Nature* 495:534–38 [PubMed: 23515162]
106. Arvidsson U, Dado RJ, Riedl M, Lee JH, Law PY, et al. 1995a delta-Opioid receptor immunoreactivity: distribution in brainstem and spinal cord, and relationship to biogenic amines and enkephalin. *J. Neurosci.* 15:1215–35 [PubMed: 7532700]
107. Arvidsson U, Riedl M, Chakrabarti S, Lee JH, Nakano AH, et al. 1995b Distribution and targeting of a mu-opioid receptor (MOR1) in brain and spinal cord. *J. Neurosci.* 15(5 Pt. 1):3328–41 [PubMed: 7751913]
108. Zhu Y, Hsu MS, Pintar JE. 1998 Developmental expression of the  $\mu$ ,  $\kappa$ , and  $\delta$  opioid receptor mRNAs in mouse. *J. Neurosci.* 18:2538–49
109. Chan HCS, McCarthy D, Li J, Palczewski K, Yuan S. 2017 Designing safer analgesics via  $\mu$ -opioid receptor pathways. *Trends Pharmacol. Sci.* 38:1016–37 [PubMed: 28935293]
110. Günther T, Dasgupta P, Mann A, Miess E, Kliewer A, et al. 2017 Targeting multiple opioid receptors— improved analgesics with reduced side effects? *Br. J. Pharmacol.* doi: 10.1111/bph.13809
111. Stein C, Clark JD, Oh U, Vasko MR, Wilcox GL, et al. 2009 Peripheral mechanisms of pain and analgesia. *Brain Res. Rev.* 60:90–113 [PubMed: 19150465]
112. Chen S-R, Pan H-L. 2008 Removing TRPV1-expressing primary afferent neurons potentiates the spinal analgesic effect of delta-opioid agonists on mechano-nociception. *Neuropharmacology* 55:215–22 [PubMed: 18579164]
113. Ueda H 2006 Molecular mechanisms of neuropathic pain-phenotypic switch and initiation mechanisms. *Pharmacol. Ther.* 109:57–77 [PubMed: 16023729]
114. Vetter I, Wyse BD, Monteith GR, Roberts-Thomson SJ, Cabot PJ. 2006 The  $\mu$  opioid agonist morphine modulates potentiation of capsaicin-evoked TRPV1 responses through a cyclic AMP-dependent protein kinase A pathway. *Mol. Pain* 2:22 [PubMed: 16842630]

115. Erbs E, Faget L, Scherrer G, Matifas A, Filliol D, et al. 2015 A mu-delta opioid receptor brain atlas reveals neuronal co-occurrence in subcortical networks. *Brain Struct. Funct.* 220:677–702 [PubMed: 24623156]
116. Scherrer G, Tryoen-Toth P, Filliol D, Matifas A, Laustriat D, et al. 2006 Knockin mice expressing fluorescent  $\delta$ -opioid receptors uncover G protein-coupled receptor dynamics in vivo. *PNAS* 103:9691–96 [PubMed: 16766653]
117. Usoskin D, Furlan A, Islam S, Abdo H, Lonnerberg P, et al. 2015 Unbiased classification of sensory neuron types by large-scale single-cell RNA sequencing. *Nat. Neurosci.* 18:145–53 [PubMed: 25420068]
118. Scherrer G, Imamachi N, Cao Y-Q, Contet C, Mennicken F, et al. 2009 Dissociation of the opioid receptor mechanisms that control mechanical and heat pain. *Cell* 137:1148–59 [PubMed: 19524516]
119. DeHaven-Hudkins DL, Dolle RE. 2004 Peripherally restricted opioid agonists as novel analgesic agents. *Curr. Pharm. Des.* 10:743–57 [PubMed: 15032700]
120. Vadivelu N, Mitra S, Hines RL. 2011 Peripheral opioid receptor agonists for analgesia: a comprehensive review. *J. Opioid Manag.* 7:55–68 [PubMed: 21434585]
121. Streicher JM, Bilsky EJ. 2017 Peripherally acting  $\mu$ -opioid receptor antagonists for the treatment of opioid-related side effects: mechanism of action and clinical implications. *J. Pharm. Pract.* doi: 10.1177/0897190017732263
122. Spahn V, Del Vecchio G, Labuz D, Rodriguez-Gaztelumendi A, Massaly N, et al. 2017 A nontoxic pain killer designed by modeling of pathological receptor conformations. *Science* 355:966–69 [PubMed: 28254944]
123. Weibel R, Reiss D, Karchewski L, Gardon O, Matifas A, et al. 2013 Mu opioid receptors on primary afferent nav1.8 neurons contribute to opiate-induced analgesia: insight from conditional knockout mice. *PLOS ONE* 8:e74706 [PubMed: 24069332]
124. Araldi D, Khomula EV, Ferrari LF, Levine JD. 2018 Fentanyl induces rapid onset hyperalgesic priming: type I at peripheral and type II at central nociceptor terminals. *J. Neurosci.* 38:2226–45 [PubMed: 29431655]

125. Aicher SA, Punnoose A, Goldberg A. 2000  $\mu$ -Opioid receptors often colocalize with the substance P receptor (NK1) in the trigeminal dorsal horn. *J. Neurosci.* 20:4345–54 [PubMed: 10818170]
126. Spike RC, Puskar Z, Sakamoto H, Stewart W, Watt C, Todd AJ. 2002 MOR-1-immunoreactive neurons in the dorsal horn of the rat spinal cord: evidence for nonsynaptic innervation by substance P-containing primary afferents and for selective activation by noxious thermal stimuli. *Eur. J. Neurosci.* 15:1306–16 [PubMed: 11994125]
127. Dado RJ, Law PY, Loh HH, Elde R. 1993 Immunofluorescent identification of a delta ( $\delta$ )-opioid receptor on primary afferent nerve terminals. *Neuroreport* 5:341–44 [PubMed: 8298100]
128. Wang D, Tawfik VL, Corder G, Low SA, Francois A, et al. 2018 Functional divergence of delta and mu opioid receptor organization in CNS pain circuits. *Neuron* 98(1):90–108.e5 [PubMed: 29576387]
129. Lai J, Luo M, Chen Q, Porreca F. 2008 Pronociceptive actions of dynorphin via bradykinin receptors. *Neurosci. Lett.* 437:175–79 [PubMed: 18450375]
130. Podvin S, Yaksh T, Hook V. 2016 The emerging role of spinal dynorphin in chronic pain: a therapeutic perspective. *Annu. Rev. Pharmacol. Toxicol.* 56:511–33 [PubMed: 26738478]
131. Xu M, Petraschka M, McLaughlin JP, Westenbroek RE, Caron MG, et al. 2004 Neuropathic pain activates the endogenous  $\kappa$  opioid system in mouse spinal cord and induces opioid receptor tolerance. *J. Neurosci.* 24:4576–84
132. Basbaum AI, Fields HL. 1984 Endogenous pain control systems: brainstem spinal pathways and endorphin circuitry. *Annu. Rev. Neurosci.* 7:309–38 [PubMed: 6143527]
133. al-Rodhan NR, Yaksh TL, Kelly PJ. 1992 Comparison of the neurochemistry of the endogenous opioid systems in two brainstem pain-processing centers. *Stereotact. Funct. Neurosurg.* 59:15–19 [PubMed: 1295034]
134. Rossi GC, Pasternak GW, Bodnar RJ. 1994  $\mu$  and  $\delta$  opioid synergy between the periaqueductal gray and the rostro-ventral medulla. *Brain Res.* 665:85–93 [PubMed: 7882023]

135. Cheng ZF, Fields HL, Heinricher MM. 1986 Morphine microinjected into the periaqueductal gray has differential effects on 3 classes of medullary neurons. *Brain Res.* 375:57–65 [PubMed: 3719359]
136. Fang FG, Haws CM, Drasner K, Williamson A, Fields HL. 1989 Opioid peptides (DAGO-enkephalin, dynorphin A(1–13), BAM 22P) microinjected into the rat brainstem: comparison of their antinociceptive effect and their effect on neuronal firing in the rostral ventromedial medulla. *Brain Res.* 501:116–28 [PubMed: 2572306]
137. Morgan MM, Heinricher MM, Fields HL. 1992 Circuitry linking opioid-sensitive nociceptive modulatory systems in periaqueductal gray and spinal cord with rostral ventromedial medulla. *Neuroscience* 47:863–71 [PubMed: 1579215]
138. Zhang Y, Zhao S, Rodriguez E, Takatoh J, Han B-X, et al. 2015 Identifying local and descending inputs for primary sensory neurons. *J. Clin. Investig.* 25:3782–94
139. François A, Low SA, Sypek EI, Christensen AJ, Sotoudeh C, et al. 2017 A brainstem-spinal cord inhibitory circuit for mechanical pain modulation by GABA and enkephalins. *Neuron* 93:822–839.e6 [PubMed: 28162807]
140. Price DD, Von der Gruen A, Miller J, Rafii A, Price C. 1985 A psychophysical analysis of morphine analgesia. *Pain* 22:261–69 [PubMed: 2993984]
141. Cobos EJ, Ghasemlou N, Araldi D, Segal D, Duong K, Woolf CJ. 2012 Inflammation-induced decrease in voluntary wheel running in mice: a nonreflexive test for evaluating inflammatory pain and analgesia. *Pain* 153:876–84 [PubMed: 22341563]
142. LaGraize SC, Borzan J, Peng YB, Fuchs PN. 2006 Selective regulation of pain affect following activation of the opioid anterior cingulate cortex system. *Exp. Neurol.* 197:22–30 [PubMed: 15996657]
143. Navratilova E, Xie JY, Meske D, Qu C, Morimura K, et al. 2015 Endogenous opioid activity in the anterior cingulate cortex is required for relief of pain. *J. Neurosci.* 35:7264–71 [PubMed: 25948274]
144. Borrás MC, Becerra L, Ploghaus A, Gostic JM, DaSilva A, et al. 2004 fMRI measurement of CNS responses to naloxone infusion and subsequent mild noxious thermal stimuli in healthy volunteers. *J. Neurophysiol.* 91:2723–33 [PubMed: 15136603]

145. Zubieta J-K, Bueller JA, Jackson LR, Scott DJ, Xu Y, et al. 2005 Placebo effects mediated by endogenous opioid activity on  $\mu$ -opioid receptors. *J. Neurosci.* 25:7754–62 [PubMed: 16120776]
146. Bingel U, Lorenz J, Schoell E, Weiller C, Büchel C. 2006 Mechanisms of placebo analgesia: rACC recruitment of a subcortical antinociceptive network. *Pain* 120:8–15 [PubMed: 16364549]
147. Wager TD, Scott DJ, Zubieta J-K. 2007 Placebo effects on human  $\mu$ -opioid activity during pain. *PNAS* 104:11056–61 [PubMed: 17578917]
148. LaGraize SC, Borzan J, Peng YB, Fuchs PN. 2006 Selective regulation of pain affect following activation of the opioid anterior cingulate cortex system. *Exp. Neurol.* 197:22–30 [PubMed: 15996657]
149. Navratilova E, Xie JY, Meske D, Qu C, Morimura K, et al. 2015 Endogenous opioid activity in the anterior cingulate cortex is required for relief of pain. *J. Neurosci.* 35:7264–71 [PubMed: 25948274]
150. Remeniuk B, Sukhtankar D, Okun A, Navratilova E, Xie JY, et al. 2015 Behavioral and neurochemical analysis of ongoing bone cancer pain in rats. *Pain* 156:1864–73 [PubMed: 25955964]
151. Navratilova E, Xie JY, Okun A, Qu C, Eyde N, et al. 2012 Pain relief produces negative reinforcement through activation of mesolimbic reward-valuation circuitry. *PNAS* 109:20709–13 [PubMed: 23184995]
152. Hipólito L, Wilson-Poe A, Campos-Jurado Y, Zhong E, Gonzalez-Romero J, et al. 2015 Inflammatory pain promotes increased opioid self-administration: role of dysregulated ventral tegmental area  $\mu$  opioid receptors. *J. Neurosci.* 35:12217–31 [PubMed: 26338332]
153. Narita M, Kishimoto Y, Ise Y, Yajima Y, Misawa K, Suzuki T. 2005 Direct evidence for the involvement of the mesolimbic  $\kappa$ -opioid system in the morphine-induced rewarding effect under an inflammatory pain-like state. *Neuropsychopharmacology* 30:111–18 [PubMed: 15257306]

154. Taylor AMW, Castonguay A, Taylor AJ, Murphy NP, Ghogha A, et al. 2015 Microglia disrupt mesolimbic reward circuitry in chronic pain. *J. Neurosci.* 35:8442–50 [PubMed: 26041913]
155. Winters BL, Gregoriou GC, Kissiwaa SA, Wells OA, Medagoda DI, et al. 2017 Endogenous opioids regulate moment-to-moment neuronal communication and excitability. *Nat. Commun.* 8:14611 [PubMed: 28327612]
156. Han S, Soleiman MT, Soden ME, Zweifel LS, Palmiter RD. 2015 Elucidating an affective pain circuit that creates a threat memory. *Cell* 162:363–74 [PubMed: 26186190]
157. Namburi P, Beyeler A, Yorozu S, Calhoon GG, Halbert SA, et al. 2015 A circuit mechanism for differentiating positive and negative associations. *Nature* 520:675–78 [PubMed: 25925480]
158. Crowley NA, Bloodgood DW, Hardaway JA, Kendra AM, McCall JG, et al. 2016 Dynorphin controls the gain of an amygdalar anxiety circuit. *Cell Rep.* 14:2774–83 [PubMed: 26997280]
159. McCall JG, Siuda ER, Bhatti DL, Lawson LA, McElligott ZA, et al. 2017 Locus coeruleus to basolateral amygdala noradrenergic projections promote anxiety-like behavior. *eLife* 6:e18247 [PubMed: 28708061]
160. Nygard SK, Hourguettes NJ, Sobczak GG, Carlezon WA, Bruchas MR. 2016 Stress-induced reinstatement of nicotine preference requires dynorphin/kappa opioid activity in the basolateral amygdala. *J. Neurosci.* 36:9937–48 [PubMed: 27656031]
161. Al-Hasani R, McCall JG, Shin G, Gomez AM, Schmitz GP, et al. 2015 Distinct subpopulations of nucleus accumbens dynorphin neurons drive aversion and reward. *Neuron* 87:1063–77 [PubMed: 26335648]
162. Castro DC, Berridge KC. 2014 Opioid hedonic hotspot in nucleus accumbens shell: mu, delta, and kappa maps for enhancement of sweetness “liking” and “wanting.” *J. Neurosci.* 34:4239–50 [PubMed: 24647944]
163. Negrete R, García Gutierrez MS, Manzanares J, Maldonado R. 2017 Involvement of the dynorphin/KOR system on the nociceptive, emotional and cognitive manifestations of joint pain in mice. *Neuropharmacology* 116:315–27 [PubMed: 27567942]

164. Park PE, Schlosburg JE, Vendruscolo LF, Schulteis G, Edwards S, Koob GF. 2015 Chronic CRF1 receptor blockade reduces heroin intake escalation and dependence-induced hyperalgesia. *Addict. Biol.* 20:275–84 [PubMed: 24330252]
165. Bruchas MR, Land BB, Chavkin C. 2010 The dynorphin/kappa opioid system as a modulator of stress-induced and pro-addictive behaviors. *Brain Res.* 1314:44–55 [PubMed: 19716811]
166. Land BB, Bruchas MR, Lemos JC, Xu M, Melief EJ, Chavkin C. 2008 The dysphoric component of stress is encoded by activation of the dynorphin K-opioid system. *J. Neurosci.* 28:407–14 [PubMed: 18184783]
167. Land BB, Bruchas MR, Schattauer S, Giardino WJ, Aita M, et al. 2009 Activation of the kappa opioid receptor in the dorsal raphe nucleus mediates the aversive effects of stress and reinstates drug seeking. *PNAS* 106:19168–73 [PubMed: 19864633]
168. Massaly N, Wilson-Poe A, Hipolito L, Markovic T, Bruchas MR, Moron J. 2017 Pain recruits accumbal kappa opioid system and alters opioid consumption. Presented at the International Narcotics Research Conference, Chicago, July 9–14
169. Kroenke, K., E.E. Krebs, and M.J. Bair, Pharmacotherapy of chronic pain: a synthesis of recommendations from systematic reviews. *Gen Hosp Psychiatry*, 2009. 31(3): p. 206-19.
170. Weiss, R.D. and V. Rao, The Prescription Opioid Addiction Treatment Study: What have we learned. *Drug Alcohol Depend*, 2017. 173 Suppl 1: p. S48-S54.
171. Varga, B., J.M. Streicher, and S. Majumdar, Strategies towards safer opioid analgesics - a review of old and upcoming targets. *Br J Pharmacol*, 2021.
172. Li, J. and J. Buchner, Structure, function and regulation of the hsp90 machinery. *Biomed J*, 2013. 36(3): p. 106-17.
173. Streicher, J.M., The Role of Heat Shock Proteins in Regulating Receptor Signal Transduction. *Mol Pharmacol*, 2019. 95(5): p. 468-474.
174. Hutchinson, M.R., K.M. Ramos, L.C. Loram, J. Wieseler, P.W. Sholar, J.J. Kearney, M.T. Lewis, N.Y. Crysedale, Y. Zhang, J.A. Harrison, et al., Evidence for a role of heat shock protein-90 in toll like receptor 4 mediated pain enhancement in rats. *Neuroscience*, 2009. 164(4): p. 1821-32. 2783248.

175. Lewis, S.S., M.R. Hutchinson, N. Rezvani, L.C. Loram, Y. Zhang, S.F. Maier, K.C. Rice, and L.R. Watkins, Evidence that intrathecal morphine-3-glucuronide may cause pain enhancement via toll-like receptor 4/MD-2 and interleukin-1beta. *Neuroscience*, 2010. 165(2): p. 569-83. PMC2795035.
176. Grace, P.M., K.A. Strand, E.L. Galer, K.C. Rice, S.F. Maier, and L.R. Watkins, Protraction of neuropathic pain by morphine is mediated by spinal damage associated molecular patterns (DAMPs) in male rats. *Brain Behav Immun*, 2017.
177. Abul-Husn, N.S., S.P. Annangudi, A. Ma'ayan, D.L. Ramos-Ortolaza, S.D. Stockton, Jr., I. Gomes, J.V. Sweedler, and L.A. Devi, Chronic morphine alters the presynaptic protein profile: identification of novel molecular targets using proteomics and network analysis. *PLoS One*, 2011. 6(10): p. e25535. 3197197.
178. Koshimizu, T.A., H. Tsuchiya, H. Tsuda, Y. Fujiwara, K. Shibata, A. Hirasawa, G. Tsujimoto, and A. Fujimura, Inhibition of heat shock protein 90 attenuates adenylate cyclase sensitization after chronic morphine treatment. *Biochem Biophys Res Commun*, 2010. 392(4): p. 603-7.
179. Zhang, Y., P. Zhou, Z. Wang, M. Chen, F. Fu, and R. Su, Hsp90beta positively regulates mu-opioid receptor function. *Life Sci*, 2020. 252: p. 117676.
180. Streicher, J.M., The role of heat shock protein 90 in regulating pain, opioid signaling, and opioid antinociception. *Vitam Horm*, 2019. 111: p. 91-103.
181. Lei, W., N. Mullen, S. McCarthy, C. Brann, P. Richard, J. Cormier, K. Edwards, E.J. Bilsky, and J.M. Streicher, Heat shock protein 90 (Hsp90) promotes opioid-induced antinociception by an ERK Mitogen Activated Protein Kinase (MAPK) mechanism in mouse brain. *J Biol Chem*, 2017.
182. Lei, W., D.I. Duron, C. Stine, S. Mishra, B.S.J. Blagg, and J.M. Streicher, The Alpha Isoform of Heat Shock Protein 90 and the Co-chaperones p23 and Cdc37 Promote Opioid Anti-nociception in the Brain. *Front Mol Neurosci*, 2019. 12: p. 294. PMC6895903.
183. Stine, C., D.L. Coleman, A.T. Flohrschutz, A.L. Thompson, S. Mishra, B.S. Blagg, T.M. Largent-Milnes, W. Lei, and J.M. Streicher, Heat shock protein 90 inhibitors block the

- anti-nociceptive effects of opioids in mouse chemotherapy-induced neuropathy and cancer bone pain models. *Pain*, 2020.
184. Duron, D.I., W. Lei, N.K. Barker, C. Stine, S. Mishra, B.S.J. Blagg, P.R. Langlais, and J.M. Streicher, Inhibition of Hsp90 in the spinal cord enhances the antinociceptive effects of morphine by activating an ERK-RSK pathway. *Sci Signal*, 2020. 13(630).
  185. Sandweiss, A.J., M.I. McIntosh, A. Moutal, R. Davidson-Knapp, J. Hu, A.K. Giri, T. Yamamoto, V.J. Hruby, R. Khanna, T.M. Largent-Milnes, et al., Genetic and pharmacological antagonism of NK1 receptor prevents opiate abuse potential. *Mol Psychiatry*, 2017.
  186. Streicher, J.M. and E.J. Bilsky, Peripherally Acting micro-Opioid Receptor Antagonists for the Treatment of Opioid-Related Side Effects: Mechanism of Action and Clinical Implications. *J Pharm Pract*, 2017: p. 897190017732263. PMC6291905.
  187. Grenald, S.A., M.A. Young, Y. Wang, M.H. Ossipov, M.M. Ibrahim, T.M. Largent-Milnes, and T.W. Vanderah, Synergistic attenuation of chronic pain using mu opioid and cannabinoid receptor 2 agonists. *Neuropharmacology*, 2017. 116: p. 59-70. PMC5385155.
  188. Burlison, J.A., L. Neckers, A.B. Smith, A. Maxwell, and B.S. Blagg, Novobiocin: redesigning a DNA gyrase inhibitor for selective inhibition of hsp90. *J Am Chem Soc*, 2006. 128(48): p. 15529-36.
  189. Mishra, S.J., A. Khandelwal, M. Banerjee, M. Balch, S. Peng, R.E. Davis, T. Merfeld, V. Munthali, J. Deng, R.L. Matts, et al., Selective Inhibition of the Hsp90alpha Isoform. *Angew Chem Int Ed Engl*, 2021. 60(19): p. 10547-10551. PMC8086817.
  190. Mishra, S.J., W. Liu, K. Beebe, M. Banerjee, C.N. Kent, V. Munthali, J. Koren, 3rd, J.A. Taylor, 3rd, L.M. Neckers, J. Holzbeierlein, et al., The Development of Hsp90beta-Selective Inhibitors to Overcome Detriments Associated with pan-Hsp90 Inhibition. *J Med Chem*, 2021. 64(3): p. 1545-1557. PMC8996186.
  191. Duerfeldt, A.S., L.B. Peterson, J.C. Maynard, C.L. Ng, D. Eletto, O. Ostrovsky, H.E. Shinogle, D.S. Moore, Y. Argon, C.V. Nicchitta, et al., Development of a Grp94 inhibitor. *J Am Chem Soc*, 2012. 134(23): p. 9796-804. PMC3414055.

192. Ananthan, S., S.K. Saini, C.M. Dersch, H. Xu, N. McGlinchey, D. Giuvelis, E.J. Bilsky, and R.B. Rothman, 14-Alkoxy- and 14-acyloxy pyridomorphinans: mu agonist/delta antagonist opioid analgesics with diminished tolerance and dependence side effects. *J Med Chem*, 2012. 55(19): p. 8350-63. PMC3499949.
193. Lei, W., N. Mullen, S. McCarthy, C. Brann, P. Richard, J. Cormier, K. Edwards, E.J. Bilsky, and J.M. Streicher, Heat-shock protein 90 (Hsp90) promotes opioid-induced anti-nociception by an ERK mitogen-activated protein kinase (MAPK) mechanism in mouse brain. *J Biol Chem*, 2017. 292(25): p. 10414-10428. PMC5481554.
194. Duron, D.I., F. Hanak, and J.M. Streicher, Daily intermittent fasting in mice enhances morphine-induced anti-nociception while mitigating reward, tolerance, and constipation. *Pain*, 2020.
195. Chaplan, S.R., F.W. Bach, J.W. Pogrel, J.M. Chung, and T.L. Yaksh, Quantitative assessment of tactile allodynia in the rat paw. *J Neurosci Methods*, 1994. 53(1): p. 55-63.
196. Lei, W., R.H. Vekariya, S. Ananthan, and J.M. Streicher, A Novel Mu-Delta Opioid Agonist Demonstrates Enhanced Efficacy with Reduced Tolerance and Dependence in Mouse Neuropathic Pain Models. *J Pain*, 2019.
197. Wilson, D.M., X. Wang, E. Walsh, and R.A. Rourick, High throughput log D determination using liquid chromatography-mass spectrometry. *Comb Chem High Throughput Screen*, 2001. 4(6): p. 511-9.
198. Zhou, L., L. Yang, S. Tilton, and J. Wang, Development of a high throughput equilibrium solubility assay using miniaturized shake-flask method in early drug discovery. *J Pharm Sci*, 2007. 96(11): p. 3052-71.
199. Di, L., E.H. Kerns, S.Q. Li, and S.L. Petusky, High throughput microsomal stability assay for insoluble compounds. *Int J Pharm*, 2006. 317(1): p. 54-60.
200. Lei, W., R.H. Vekariya, S. Ananthan, and J.M. Streicher, A Novel Mu-Delta Opioid Agonist Demonstrates Enhanced Efficacy With Reduced Tolerance and Dependence in Mouse Neuropathic Pain Models. *J Pain*, 2020. 21(1-2): p. 146-160. PMC6906261.
201. Stefanucci, A., M.P. Dimmito, G. Macedonio, L. Ciarlo, S. Pieretti, E. Novellino, W. Lei, D. Barlow, K.L. Houseknecht, J.M. Streicher, et al., Potent, Efficacious, and Stable

- Cyclic Opioid Peptides with Long Lasting Antinociceptive Effect after Peripheral Administration. *J Med Chem*, 2020. 63(5): p. 2673-2687.
202. Vekariya, R.H., W. Lei, A. Ray, S.K. Saini, S. Zhang, G. Molnar, D. Barlow, K.L. Karlage, E.J. Bilsky, K.L. Houseknecht, et al., Synthesis and Structure-Activity Relationships of 5'-Aryl-14-alkoxy-pyridomorphinans: Identification of a mu Opioid Receptor Agonist/delta Opioid Receptor Antagonist Ligand with Systemic Antinociceptive Activity and Diminished Opioid Side Effects. *J Med Chem*, 2020. 63(14): p. 7663-7694.
203. LaVigne, J.E., R. Hecksel, A. Keresztes, and J.M. Streicher, Cannabis sativa terpenes are cannabimimetic and selectively enhance cannabinoid activity. *Sci Rep*, 2021. 11(1): p. 8232. PMC8050080.
204. Tanguturi, P., V. Pathak, S. Zhang, O. Moukha-Chafiq, C.E. Augelli-Szafran, and J.M. Streicher, Discovery of Novel Delta Opioid Receptor (DOR) Inverse Agonist and Irreversible (Non-Competitive) Antagonists. *Molecules*, 2021. 26(21). PMC8587863.
205. Berge, O.G., Predictive validity of behavioural animal models for chronic pain. *Br J Pharmacol*, 2011. 164(4): p. 1195-206. 3229757.
206. Yuan, S.B., Y. Shi, J. Chen, X. Zhou, G. Li, B.B. Gelman, J.G. Lisinicchia, S.M. Carlton, M.R. Ferguson, A. Tan, et al., Gp120 in the pathogenesis of human immunodeficiency virus-associated pain. *Ann Neurol*, 2014. 75(6): p. 837-50. PMC4077969.
207. Warner, M., J.P. Trinidad, B.A. Bastian, A.M. Minino, and H. Hedegaard, Drugs Most Frequently Involved in Drug Overdose Deaths: United States, 2010-2014. *Natl Vital Stat Rep*, 2016. 65(10): p. 1-15.
208. Hoot, M.R., E.I. Sypek, K.J. Reilley, A.N. Carey, J.M. Bidlack, and J.P. McLaughlin, Inhibition of Gbetagamma-subunit signaling potentiates morphine-induced antinociception but not respiratory depression, constipation, locomotion, and reward. *Behav Pharmacol*, 2013. 24(2): p. 144-52.
209. Stone, L.S., J.P. German, K.F. Kitto, C.A. Fairbanks, and G.L. Wilcox, Morphine and clonidine combination therapy improves therapeutic window in mice: synergy in

- antinociceptive but not in sedative or cardiovascular effects. *PLoS One*, 2014. 9(10): p. e109903. PMC4192360.
210. Eisenstein, T.K., X. Chen, S. Inan, J.J. Meissler, C.S. Tallarida, E.B. Geller, S.M. Rawls, A. Cowan, and M.W. Adler, Chemokine Receptor Antagonists in Combination with Morphine as a Novel Strategy for Opioid Dose Reduction in Pain Management. *Mil Med*, 2020. 185(Suppl 1): p. 130-135.
  211. Sidera, K. and E. Patsavoudi, HSP90 inhibitors: current development and potential in cancer therapy. *Recent Pat Anticancer Drug Discov*, 2014. 9(1): p. 1-20.
  212. Wu, Y., X. Zheng, Y. Ding, M. Zhou, Z. Wei, T. Liu, and K. Liao, The molecular chaperone Hsp90alpha deficiency causes retinal degeneration by disrupting Golgi organization and vesicle transportation in photoreceptors. *J Mol Cell Biol*, 2020. 12(3): p. 216-229. PMC7181719.
  213. Xu, J.T., J.Y. Zhao, X. Zhao, D. Ligons, V. Tiwari, F.E. Atianjoh, C.Y. Lee, L. Liang, W. Zang, D. Njoku, et al., Opioid receptor-triggered spinal mTORC1 activation contributes to morphine tolerance and hyperalgesia. *J Clin Invest*, 2014.
  214. Zhai, M.L., Y. Chen, C. Liu, J.B. Wang, and Y.H. Yu, Spinal glucocorticoid receptor regulated chronic morphine tolerance may be through extracellular signal regulated kinase 1/2. *Mol Med Rep*, 2018. 18(1): p. 1074-1080.
  215. Pan, Y., X. Sun, L. Jiang, L. Hu, H. Kong, Y. Han, C. Qian, C. Song, Y. Qian, and W. Liu, Metformin reduces morphine tolerance by inhibiting microglial-mediated neuroinflammation. *J Neuroinflammation*, 2016. 13(1): p. 294. PMC5114746.
  216. Pawar, M., P. Kumar, S. Sunkaraneni, S. Sirohi, E.A. Walker, and B.C. Yoburn, Opioid agonist efficacy predicts the magnitude of tolerance and the regulation of mu-opioid receptors and dynamin-2. *Eur J Pharmacol*, 2007. 563(1-3): p. 92-101. PMC1995431.
  217. Crowley, V.M., D.J.E. Huard, R.L. Lieberman, and B.S.J. Blagg, Second Generation Grp94-Selective Inhibitors Provide Opportunities for the Inhibition of Metastatic Cancer. *Chemistry*, 2017. 23(62): p. 15775-15782. PMC5722212.

218. Gilron I, Bailey JM, Tu D, Holden RR, Weaver DF, Houlden RL. Morphine, gabapentin, or their combination for neuropathic pain. *N Engl J Med*. 2005;352(13):1324-1334. doi:10.1056/NEJMoa042580
219. Coussens NP, Sittampalam GS, Jonson SG, Hall MD, Gorby HE, Tamiz AP, McManus OB, Felder CC, Rasmussen K. The Opioid Crisis and the Future of Addiction and Pain Therapeutics. *J Pharmacol Exp Ther*. 2019 Nov;371(2):396-408. doi: 10.1124/jpet.119.259408. Epub 2019 Sep 3. PMID: 31481516; PMCID: PMC6863454.
220. Duron DI, Lei W, Barker NK, Stine C, Mishra S, Blagg BSJ, Langlais PR, Streicher JM. Inhibition of Hsp90 in the spinal cord enhances the antinociceptive effects of morphine by activating an ERK-RSK pathway. *Sci Signal*. 2020 May 5;13(630):eaaz1854. doi: 10.1126/scisignal.aaz1854. PMID: 32371496.
221. Abul-Husn, N. S., Annangudi, S. P., Ma'ayan, A., Ramos-Ortolaza, D. L., Stockton, S. D., Jr., Gomes, I., et al. (2011). Chronic morphine alters the presynaptic protein profile: Identification of novel molecular targets using proteomics and network analysis. *PLoS One*, 6(10), e25535. <https://doi.org/10.1371/journal.pone.0025535>.
222. Yashpal, K., Pitcher, G., Henry, J. (1994). *Noxious peripheral stimulation produces antinociception mediated via substance P and opioid mechanisms in the rat tail-flick test*. *Brain Research* 674:97-103.
223. Cridland, R.A., Henry, J.L. Intrathecal administration of substance P in the rat: spinal transection or morphine blocks the behavioral responses, but not of the tail flick reflex. *Neuroscience Letters* 84:2, 203-208.
224. Todd, A. Neuronal Circuitry for pain processing in the dorsal horn. *Nat Rev Neurosci* 11(12): 823-836.
225. Chen SR, Pan HL. Blocking mu opioid receptors in the spinal cord prevents the analgesic action by subsequent systemic opioids. *Brain Res*. 2006 Apr 7;1081(1):119-25. doi: 10.1016/j.brainres.2006.01.053. Epub 2006 Feb 24. PMID: 16499888.
226. Kemp T, Spike RC, Watt C, Todd AJ. The mu-opioid receptor (MOR1) is mainly restricted to neurons that do not contain GABA or glycine in the superficial dorsal horn

- of the rat spinal cord. *Neuroscience*. 1996 Dec;75(4):1231-8. doi: 10.1016/0306-4522(96)00333-8. PMID: 8938756.
227. Chang H. M., Berde C. B., Holz G. G., Steward G. F. and Kream R. M. (1989) Sufentanil, morphine, met-enkephalin, and kappa-agonist (U-50,488H) inhibit substance P release from primary sensory neurons: a model for presynaptic spinal opioid actions. *Anesthesiology* 70,672–677.
  228. Jessel T. M. and Iversen L. L. (1977) Opiate analgesics inhibit substance P release from rat trigeminal nucleus. *Nature* 268,549–551.
  229. Yaksh T. L., Jessel T. M., Gamse R., Mudge A. W. and Leeman S. E. (1980) Intrathecal morphine inhibits substance P release from mammalian spinal cord in vivo. *Nature* 286,155–157.
  230. Glaum S. R., Miller R. J. and Hammond D. L. (1994) Inhibitory actions of  $\delta$ -,  $\kappa$ -, and  $\mu$ -opioid receptor agonists on excitatory transmission in lamina II neurons of adult rat spinal cord. *J. Neurosci.* 14,4965–4971.
  231. Grudt T. J. and Williams J. T. (1994)  $\mu$ -Opioid agonists inhibit spinal trigeminal substantia gelatinosa neurons in guinea pig and rat. *J. Neurosci.* 14,1646–1654.
  232. Jeftinija S. (1988) Enkephalins modulate excitatory synaptic transmission in the superficial dorsal horn by acting at  $\mu$ -opioid receptor sites. *Brain Res.* 460,260–268.
  233. Contet C, Kieffer BL, Befort K. Mu opioid receptor: a gateway to drug addiction. *Curr Opin Neurobiol.* 2004 Jun;14(3):370-8. doi: 10.1016/j.conb.2004.05.005. PMID: 15194118.
  234. Minami, M., & Satoh, M. (1995). Molecular biology of the opioid receptors: structures, functions and distributions. *Neuroscience research*, 23(2), 121-145.
  235. Olsen RW, DeLorey TM. GABA Receptor Physiology and Pharmacology. In: Siegel GJ, Agranoff BW, Albers RW, et al., editors. *Basic Neurochemistry: Molecular, Cellular and Medical Aspects*. 6th edition. Philadelphia: Lippincott-Raven; 1999.
  236. Kaupmann K, Huggel K, Heid J, et al. Expression cloning of GABA<sub>B</sub> receptors uncovers similarity to metabotropic glutamate receptors. *Nature*. 1997;386:239–246.

237. Punnakal, P., von Schoultz, C., Haenraets, K., Wildner, H., & Zeilhofer, H. U. (2014). Morphological, biophysical and synaptic properties of glutamatergic neurons of the mouse spinal dorsal horn. *The Journal of physiology*, 592(4), 759–776. <https://doi.org/10.1113/jphysiol.2013.264937>
238. Vos T., Allen C., Arora M. Global, regional, and national incidence, prevalence, and years lived with disability for 328 diseases and injuries for 195 countries, 1990–2016: a systematic analysis for the Global Burden of Disease Study 016. *Lancet*. 2017;390:1211–1259.
239. Chen, J., Lin, Y., Huang, J., Wang, W., Wei, Y., Li, Y., Kaneko, T., Wu, S. Mammal retinal distribution of Enkergetic amacrine cells and their neurochemical features: Evidence from the PPE-GFP transgenic mice. *Neuroscience Letters*. 2013; 548:223-238.
240. Brewer, C., Li, J., O’Conor, K., Serafin, E., Baccei, M. Neonatal injury evokes persistent deficits in dynorphin inhibitory circuits within the adult mouse superficial dorsal horn. *The Journal of Neuroscience*. 2020; 40:3882-3895.
241. Takigawa, T., & Alzheimer, C. (1999). G protein-activated inwardly rectifying K<sup>+</sup> (GIRK) currents in dendrites of rat neocortical pyramidal cells. *The Journal of physiology*, 517 ( Pt 2)(Pt 2), 385–390. <https://doi.org/10.1111/j.1469-7793.1999.0385t.x>
242. NIH fact sheets – pain management. National Institutes of Health website. [Report.nih.gov/nihfactsheets/ViewFactSheet.aspx?csid=57](https://report.nih.gov/nihfactsheets/ViewFactSheet.aspx?csid=57). Updated March 29, 2013. Accessed September 20, 2022.
243. Basbaum AI, Fields HL: Endogenous pain control systems: brainstem spinal pathways and endorphin circuitry. *Annu Rev Neurosci* 1984, 7:309-338.
244. Watkins LR, Mayer DJ: Organization of endogenous opiate and nonopiate pain control systems. *Science* 1982, 216:1185-1192.
245. Hohmann AG, Suplita RL, Bolton NM, Neely MH, Fegley D, Mangieri R, Krey JF, Walker JM, Holmes PV, Crystal JD et al.: An endocannabinoid mechanism for stress-induced analgesia. *Nature* 2005, 435:1108-1112.
246. Moreau JL, Fields HL: Evidence for GABA involvement in midbrain control of medullary neurons that modulate nociceptive transmission. *Brain Res* 1986, 397:37-46.

247. Behhehani MM, Fields HL: Evidence that an excitatory connection between the periaqueductal gray and the nucleus raphe magnus mediates stimulation produced analgesia. *Brain Res* 1979, 170:85-93.
248. Yeung JC, Yaksh TL, Rudy TA: Concurrent mapping of brain sites for sensitivity to the direct application of morphine and focal electrical stimulation in the production of antinociception in the rat. *Pain* 1977, 4:23-40.
249. Tsou K, Jang CS: Studies on the site of analgesic action of morphine by intracerebral micro-injection. *Sci Sin* 1964, 13:1099-1109.
250. Meng ID, Manning BH, Martin WJ, Fields HL: An analgesia circuit activated by cannabinoids. *Nature* 1998, 395:381-383.
251. Fields HL, Bry J, Hentall I, Zorman G: The activity of neurons in the rostral medulla of the rat during withdrawal from noxious heat. *J Neurosci* 1983, 3:2545-2552.
252. Gao K, Chen DO, Genzen JR, Mason P: Activation of serotonergic neurons in the raphe magnus is not necessary for morphine analgesia. *J Neurosci* 1998, 18:1860-1868.
253. Heinricher MM, Morgan MM, Fields HL: Direct and indirect actions of morphine on medullary neurons that modulate nociception. *Neuroscience* 1992, 48:533-543.
254. Heinricher MM, Morgan MM, Tortorici V, Fields HL: Disinhibition of off-cells and antinociception produced by an opioid action within the rostral ventromedial medulla. *Neuroscience* 1994, 63:279-288.
255. Tortorici V, Morgan MM: Comparison of morphine and kainic acid microinjections into identical PAG sites on the activity of RVM neurons. *J Neurophysiol* 2002, 88:1707-1715.
256. Vanegas H, Barbaro NM, Fields HL: Tail-flick related activity in medullospinal neurons. *Brain Res* 1984, 321:135-141.
257. Heinricher MM, Cheng ZF, Fields HL: Evidence for two classes of nociceptive modulating neurons in the periaqueductal gray. *J Neurosci* 1987, 7:271-278.
258. Pan ZZ, Williams JT, Osborne PB: Opioid actions on single nucleus raphe magnus neurons from rat and guinea-pig in vitro. *J Physiol* 1990, 427:519-532.

259. Vaughan CW, Connor M, Bagley EE, Christie MJ: Actions of cannabinoids on membrane properties and synaptic transmission in rat periaqueductal gray neurons in vitro. *Mol Pharmacol* 2000, 57:288-295.
260. Vaughan CW, McGregor IS, Christie MJ: Cannabinoid receptor activation inhibits GABAergic neurotransmission in rostral ventromedial medulla neurons in vitro. *Br J Pharmacol* 1999, 127:935-940.
261. Chieng B, Christie MJ: Inhibition by opioids acting on mu-receptors of GABAergic and glutamatergic postsynaptic potentials in single rat periaqueductal gray neurones in vitro. *Br J Pharmacol* 1994, 113:303-309.
262. Chiou LC, Huang LY: Mechanism underlying increased neuronal activity in the rat ventrolateral periaqueductal grey by a mu-opioid. *J Physiol* 1999, 518(Pt. 2):551-559.
263. Vaughan CW, Christie MJ: Presynaptic inhibitory action of opioids on synaptic transmission in the rat periaqueductal grey in vitro. *J Physiol* 1997, 498(Pt. 2):463-472.
264. Vaughan CW, Ingram SL, Christie MJ: How opioids inhibit GABA-mediated neurotransmission. *Nature* 1997, 390:611-614.
265. Manchikanti L, Atluri S, Hansen H, et al. Opioids in chronic noncancer pain: have we reached a boiling point yet? *Pain Physician*. 2014;17(1):e1-e10.
266. Portenoy RK, Foley KM. Chronic use of opioid analgesics in non-malignant pain: report of 38 cases. *Pain*. 1986;25(2):171-186.
267. America's addiction to opioids: heroin and prescription drug abuse. National Institute of Drug Abuse website. [drugabuse.gov/about-nida/legislative-activities/testimony-to-congress/2016/americas-addiction-to-opioids-heroin-prescription-drug-abuse](http://drugabuse.gov/about-nida/legislative-activities/testimony-to-congress/2016/americas-addiction-to-opioids-heroin-prescription-drug-abuse). Updated May 14, 2014. Accessed September 20, 2022.
268. Bonnie RJ, Ford MA, Phillips JK, et al. *Pain Management and the Opioid Epidemic: Balancing Societal and Individual Benefits and Risks of Prescription Opioid Use*. Washington, DC: National Academies Press (US); 2017. doi: 10.17226/24781.
269. Federation of State Medical Boards of the United States, Inc. Model policy for the use of controlled substances for the treatment of pain. 2004. Indian Health Service website.

- [www.ihs.gov/painmanagement/includes/themes/newihstheme/display\\_objects/documents/modelpolicytreatmentpain.pdf](http://www.ihs.gov/painmanagement/includes/themes/newihstheme/display_objects/documents/modelpolicytreatmentpain.pdf). Accessed September 20, 2022.
270. Department of Veterans Affairs. Pain as the 5th vital sign toolkit. VA website. [www.va.gov/PAINMANAGEMENT/docs/Pain\\_As\\_the\\_5th\\_Vital\\_Sign\\_Toolkit.pdf](http://www.va.gov/PAINMANAGEMENT/docs/Pain_As_the_5th_Vital_Sign_Toolkit.pdf). Published October 2000. Accessed September 28, 2022.
271. Phillips DM. JCAHO pain management standards are unveiled. Joint Commission on Accreditation of Healthcare Organizations. *JAMA*. 2000;284(4):428-429.
272. America's addiction to opioids: heroin and prescription drug abuse. National Institute of Drug Abuse website. [drugabuse.gov/about-nida/legislative-activities/testimony-to-congress/2016/americas-addiction-to-opioids-heroin-prescription-drug-abuse](http://drugabuse.gov/about-nida/legislative-activities/testimony-to-congress/2016/americas-addiction-to-opioids-heroin-prescription-drug-abuse). Updated May 14, 2014. Accessed August 20, 2022.
273. Felter C. The US opioid epidemic. Council on Foreign Relations website. [www.cfr.org/backgrounders/us-opioid-epidemic](http://www.cfr.org/backgrounders/us-opioid-epidemic). Updated December 26, 2017. Accessed August 28, 2022.
274. CDC. Annual surveillance report of drug-related risks and outcomes. Washington, DC: CDC National Center for Injury Prevention and Control; 2017. [cdc.gov/drugoverdose/pdf/pubs/2017-cdc-drug-surveillance-report.pdf](http://cdc.gov/drugoverdose/pdf/pubs/2017-cdc-drug-surveillance-report.pdf). Accessed August 28, 2022.
275. Opioid overdose: prescribing data. CDC website. [cdc.gov/drugoverdose/data/prescribing.html](http://cdc.gov/drugoverdose/data/prescribing.html). Updated August 30, 2017. Accessed September 28, 2022.
276. McDonald DC, Carlson K, Izrael D. Geographic variation in opioid prescribing in the U.S. *J Pain*. 2012;13(10):988-996. doi: 10.1016/j.jpain.2012.07.007.
277. The opioid epidemic by the numbers. Department of Health and Human Services website. [hhs.gov/opioids/sites/default/files/2018-01/opioids-infographic.pdf](http://hhs.gov/opioids/sites/default/files/2018-01/opioids-infographic.pdf). Updated January 2018. Accessed August 28, 2022.
278. HHS acting secretary declares public health emergency to address national opioid crisis [news release]. Washington, DC: US Department of Health and Human Services;

- October 26, 2017. [hhs.gov/about/news/2017/10/26/hhs-acting-secretary-declares-public-health-emergency-address-national-opioid-crisis.html](https://www.hhs.gov/about/news/2017/10/26/hhs-acting-secretary-declares-public-health-emergency-address-national-opioid-crisis.html). Accessed August 28, 2022.
279. American Psychiatric Association. *Diagnostic and Statistical Manual of Mental Disorders, Fifth Edition*. Washington, DC: American Psychiatric Association; 2013.
280. Substance use disorders. Substance Abuse and Mental Health Services Administration website. [samhsa.gov/disorders/substance-use](https://www.samhsa.gov/disorders/substance-use). Updated October 27, 2015. Accessed September 10, 2022.
281. Rudd RA, Seth P, David F, Scholl L. Increases in drug and opioid-involved overdose deaths—United States, 2010–2015. *MMWR Morb Mortal Wkly Rep*. 2016;65(5051):1445-1452. doi: 10.15585/mmwr.mm655051e1.
282. Opioid overdose: understanding the epidemic. CDC website. [cdc.gov/drugoverdose/epidemic/index.html](https://www.cdc.gov/drugoverdose/epidemic/index.html). Updated August 30, 2017. Accessed August 28, 2022.
283. Overdose death rates. National Institute on Drug Abuse website. [drugabuse.gov/related-topics/trends-statistics/overdose-death-rates](https://www.drugabuse.gov/related-topics/trends-statistics/overdose-death-rates). Updated September 2017. Accessed August 28, 2022.
284. CDC. Vital signs: overdoses of prescription opioid pain relievers—United States, 1999–2008. *MMWR Morb Mortal Wkly Rep*. 2011;60(43):1487-1492.
285. Council of Economic Advisers (CEA). The underestimated cost of the opioid crisis: executive summary. Washington, DC: Council of Economic Advisers (CEA); 2017. [whitehouse.gov/sites/whitehouse.gov/files/images/The Underestimated Cost of the Opioid Crisis.pdf](https://www.whitehouse.gov/sites/whitehouse.gov/files/images/The_Underestimated_Cost_of_the_Opioid_Crisis.pdf). Accessed August 28, 2022.
286. Varga BR, Streicher JM, Majumdar S. Strategies towards safer opioid analgesics-A review of old and upcoming targets. *Br J Pharmacol*. 2021 Nov 26;111:15760. doi: 10.1111/bph.15760. Epub ahead of print.
287. Haji, A., & Takeda, R. (2001). Effects of a kappa-receptor agonist U-50488 on bulbar respiratory neurons and its antagonistic action against the mu receptor-induced respiratory depression in decerebrate cats. *Japanese Journal of Pharmacology*, 87, 333–337. <https://doi.org/10.1254/jjp.87.333>

288. Bohn, L. M., Lefkowitz, R. J., Gainetdinov, R. R., Peppel, K., Caron, M. G., & Lin, F. T. (1999). Enhanced morphine analgesia in mice lacking  $\beta$ -arrestin 2. *Science*, 286, 2495–2498.
289. Bohn, L. M., Gainetdinov, R. R., Lin, F. T., Lefkowitz, R. J., & Caron, M. G. (2000).  $\mu$ -Opioid receptor desensitization by  $\beta$ -arrestin-2 determines morphine tolerance but not dependence. *Nature*, 408, 720–723.
290. Bohn, L. M., Gainetdinov, R. R., Sotnikova, T. D., Medvedev, I. O., Lefkowitz, R. J., Dykstra, L. A., & Caron, M. G. (2003). Enhanced rewarding properties of morphine, but not cocaine, in  $\beta$ arrestin-2 knock-out mice. *The Journal of Neuroscience*, 23, 10265–10273. <https://doi.org/10.1523/JNEUROSCI.23-32-10265.2003>
291. Lewis, S. S., Hutchinson, M. R., Rezvani, N., Loram, L. C., Zhang, Y., Maier, S. F., Rice, K. C., & Watkins, L. R. (2010). Evidence that intrathecal morphine-3-glucuronide may cause pain enhancement via toll-like receptor 4/MD-2 and interleukin-1 $\beta$ . *Neuroscience*, 165, 569–583.
292. Abul-Husn, N. S., Annangudi, S. P., Ma'ayan, A., Ramos-Ortolaza, D. L., Stockton, S. D. Jr., Gomes, I., Sweedler, J. V., & Devi, L. A. (2011). Chronic morphine alters the presynaptic protein profile: Identification of novel molecular targets using proteomics and network analysis. *PLoS ONE*, 6, e25535.
293. Koshimizu, T. A., Tsuchiya, H., Tsuda, H., Fujiwara, Y., Shibata, K., Hirasawa, A., Tsujimoto, G., & Fujimura, A. (2010). Inhibition of heat shock protein 90 attenuates adenylate cyclase sensitization after chronic morphine treatment. *Biochemical and Biophysical Research Communications*, 392, 603–607.
294. Lei, W., Mullen, N., McCarthy, S., Brann, C., Richard, P., Cormier, J., Edwards, K., Bilsky, E. J., & Streicher, J. M. (2017). Heat-shock protein 90 (Hsp90) promotes opioid-induced anti-nociception by an ERK mitogen-activated protein kinase (MAPK) mechanism in mouse brain. *The Journal of Biological Chemistry*, 292, 10414–10428. <https://doi.org/10.1074/jbc.M116.769489>
295. Stine, C., Coleman, D. L., Flohrschutz, A. T., Thompson, A. L., Mishra, S., Blagg, B. S., Largent-Milnes, T. M., Lei, W., & Streicher, J. M. (2020). Heat shock protein 90

- inhibitors block the antinociceptive effects of opioids in mouse chemotherapy-induced neuropathy and cancer bone pain models. *Pain*, 161, 1798–1807.
296. Duron, D. I., Lei, W., Barker, N. K., Stine, C., Mishra, S., Blagg, B. S. J., Langlais, P. R., & Streicher, J. M. (2020). Inhibition of Hsp90 in the spinal cord enhances the antinociceptive effects of morphine by activating an ERK-RSK pathway. *Science Signaling*, 13(630), eaaz1854.
297. Chen, N. H., Reith, M. E., and Quick, M. W. (2004) Synaptic uptake and beyond. The sodium- and chloride-dependent neurotransmitter transporter family SLC6. *Pflugers Arch.* 447, 519–531.
298. Hahn, M. K., and Blakely, R. D. (2007) The functional impact of SLC6 transporter genetic variation. *Annu. Rev. Pharmacol. Toxicol.* 47, 401–441.
299. Madsen, K. K., White, H. S., and Schousboe, A. (2010) Neuronal and non-neuronal GABA transporters as targets for antiepileptic drugs. *Pharmacol. Ther.* 125, 394–401.
300. Erdö, S. L., and Wolff, J. R. (1990) gamma-Aminobutyric acid outside the mammalian brain. *J. Neurochem.* 54, 363–372.
301. Nakashita, M., Sasaki, K., Sakai, N., and Saito, N. (1997) Effects of tricyclic and tetracyclic antidepressants on the three subtypes of GABA transporter. *Neurosci. Res.* 29, 87–91.
302. Zhou Y, Holmseth S, Guo C, Hassel B, Höfner G, Huitfeldt HS, Wanner KT, Danbolt NC. Deletion of the  $\gamma$ -aminobutyric acid transporter 2 (GAT2 and SLC6A13) gene in mice leads to changes in liver and brain taurine contents. *J Biol Chem.* 2012 Oct 12;287(42):35733-35746. doi: 10.1074/jbc.M112.368175. Epub 2012 Aug 15. PMID: 22896705; PMCID: PMC3471754.
303. Kuroda, E., Watanabe, M., Tamayama, T., and Shimada, M. (2000) Autoradiographic distribution of radioactivity from GABA in the mouse. *Microsc. Res. Tech.* 48, 116–126.
304. Hespe, W., Roberts, E., and Prins, H. (1969) Autoradiographic investigation of the distribution of GABA in tissues of normal and aminooxyacetic acid-treated mice. *Brain Res.* 14, 663–671.

305. Minuk, G. Y., Vergalla, J., Ferenci, P., and Jones, E. A. (1984) Identification of an acceptor system for gamma-aminobutyric acid on isolated rat hepatocytes. *Hepatology* 4, 180–185.
306. Goodyer, P. R., Rozen, R., and Scriver, C. R. (1985) A  $\gamma$ -aminobutyric acid-specific transport mechanism in mammalian kidney. *Biochim. Biophys. Acta* 818, 45–54.
307. Liu, Q. R., López-Corcuera, B., Nelson, H., Mandiyan, S., and Nelson, N. (1992) Cloning and expression of a cDNA encoding the transporter of taurine and  $\alpha$ -alanine in mouse brain. *Proc. Natl. Acad. Sci. U.S.A.* 89, 12145–12149.
308. Smith, K. E., Borden, L. A., Wang, C. H., Hartig, P. R., Branchek, T. A., and Weinshank, R. L. (1992) Cloning and expression of a high affinity taurine transporter from rat brain. *Mol. Pharmacol.* 42, 563–569.
309. Hari K, Lucas-Osma AM, Metz K, Lin S, Pardell N, Roszko DA, Black S, Minarik A, Singla R, Stephens MJ, Pearce RA, Fouad K, Jones KE, Gorassini MA, Fenrich KK, Li Y, Bennett DJ. GABA facilitates spike propagation through branch points of sensory axons in the spinal cord. *Nat Neurosci.* 2022 Oct;25(10):1288-1299. doi: 10.1038/s41593-022-01162-x. Epub 2022 Sep 26. PMID: 36163283.